

FUZZY MONITORING OF INTRAVENOUS PROPOFOL
INFUSION ANESTHESIA IN DOGS

By

BRENT D. EILERTS

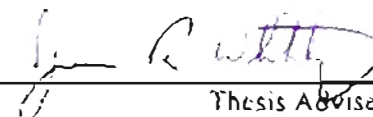
Bachelor of Science
Cellular Biology
University of Kansas
Lawrence, Kansas
1989

Bachelor of Science
Chemical Engineering
University of Kansas
Lawrence, Kansas
1994

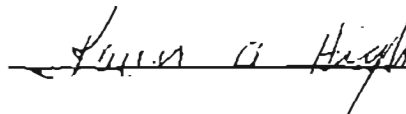
Submitted to the Faculty of the
Graduate College of the
Oklahoma State University
in partial fulfillment of
the requirements for
the Degree of
MASTER OF SCIENCE
July, 1997

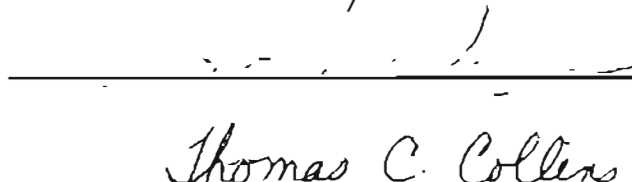
FLUZZY MONITORING OF INTRAVENOUS PROPOFOL
INFUSION ANESTHESIA IN DOGS

Thesis Approved:



Thesis Adviser





Dean of the Graduate College

ACKNOWLEDGMENTS

I would like to express my gratitude to my faculty adviser, Dr. Robert Whiteley, and to Dr. Ron Mandsager for their instruction and assistance during all phases of this project. I would also like to thank Dr. Cyril Clarke and Dr. David Bourne for their constructive input into the conduct of this project. I would also like to thank my other committee members, Dr. Karen High and Dr. Jan Wagner, and the other faculty of the School of Chemical Engineering from whom I have received superior instruction.

In addition to those who provided intellectual support, I would like to recognize and express my gratitude to those who have provided financial support. My thanks go to the family of Dr. Lyman Yarborough, from whom I have received support through a Distinguished Graduate Fellowship in his name. I also would like to thank the National Institutes of Health and the School of Chemical Engineering for their financial assistance.

I would like to thank the staff of the Boren Veterinary Medical Teaching Hospital for their support of our research activities. I would also like to thank our experimental subjects, Sleepy, Stinky, Squirmy, Timid, Squealy, Stubborn, Squat, Stenchy, Crusty, Sniffy, Squealy, Speedy, Different, and especially my dog Elmo, who gallantly sacrificed his reproductive capability in the name of science.

No acknowledgment of academic and financial support could be complete without mentioning my wife, Nancy, and my parents, without whom none of this would have been possible. I would also like to thank my sister for her support and entertainment.

TABLE OF CONTENTS

Chapter	Page
1.0 INTRODUCTION	1
1.1 INFERENCE OF DEPTH OF ANESTHESIA	1
1.2 APPLICATION OF FUZZY LOGIC	3
1.3 PROPOSED MODEL	5
1.4 ORGANIZATION OF THESIS	6
2.0 MOTIVATION	7
2.1 PROPOFOL ANESTHESIA	8
2.2 ASSESSMENT OF ANESTHETIC DEPTH	9
2.3 FUZZY LOGIC	13
2.4 SIGNIFICANCE OF CURRENT WORK	17
3.0 METHOD	20
3.1 DATA COLLECTION	20
3.2 DATA ANALYSIS	28
3.3 MODEL DEVELOPMENT	33
4.0 RESULTS	39
4.1 ANALYSIS FROM PHYSIOLOGICAL PRINCIPLES ALONE ..	39
4.2 ANALYSIS FROM CLINICAL ASSESSMENT	51
4.3 PULSE EXPERIMENT	95
4.4 SURGICAL EXPERIMENT	98
5.0 DISCUSSION OF RESULTS	103
5.1 EVALUATION OF MODEL	104
5.2 IMPLEMENTATION ISSUES	108
6.0 CONCLUSIONS AND RECOMMENDATIONS	110
6.1 CONCLUSIONS	110
6.2 RECOMMENDATIONS	111
REFERENCES	113

APPENDICES	117
APPENDIX A: FUZZY INFERENCE AND DEFUZZIFICATION ..	117
APPENDIX B: EXPERIMENTAL SUBJECTS	123
APPENDIX C: SAMPLE CLINICAL ASSESSMENT WORKSHEET ..	125
APPENDIX D: SUMMARY OF SERUM PROPOFOL DATA	127
APPENDIX E: EXAMPLE EXPERIMENT PLOTS	128
APPENDIX F: FUZZY RULEBASE	162
APPENDIX G: TILSHELL PROJECT INFORMATION	164

LIST OF TABLES

Table	Page
3.1 EEG data acquired	25
3.2 ECG data acquired	27
3.3 Infusion pump data acquired	27
3.4 Scaling methodology for ABETA, TOTPOW, and EMGLO	30
3.5 Model input variables	31
3.6 Calculation of ABETArate and EMGrate	34
4.1 Physiological consistency of model input and output variables for initial experiments	43
4.2 Physiological consistency of model input and output variables for verification experiments	49
4.3 Comparison of model with overall clinical assessment for experiment 1 .	55
4.4 Comparison of model with overall clinical assessment for experiment 2 .	59
4.5 Comparison of model with overall clinical assessment for experiment 3 .	61
4.6 Comparison of model with overall clinical assessment for experiment 4 .	64
4.7 Comparison of model with overall clinical assessment for experiment 5 .	67
4.8 Comparison of model with overall clinical assessment for experiment 6 .	71
4.9 Comparison of model with overall clinical assessment for experiment 7 .	75
4.10 Comparison of model with overall clinical assessment for experiment 8 .	78
4.11 Comparison of model with overall clinical assessment for experiment 9 .	81
4.12 Comparison of model with overall clinical assessment for experiment 10 .	84

4.13	Comparison of model with overall clinical assessment for experiment 11 .	88
4.14	Comparison of model with overall clinical assessment for experiment 12 .	91
4.15	Comparison of model with overall clinical assessment for initial experiments	93
4.16	Comparison of model with overall clinical assessment for verification experiments	94
4.17	Event list for surgical experiment	99

LIST OF FIGURES

Figure	Page
2.1 Propofol (2,6-diisopropylphenol)	8
2.2 Relation of time domain to frequency domain via fast Fourier transform	11
2.3 Determination of burst suppression	11
2.4 Spectral edge and median frequency as determined from EEG power spectrum	12
2.5 Venn diagram	15
2.6 Hot temperature membership function	15
2.7 Fuzzy temperature spectrum	16
3.1 EEG electrode montage	22
3.2 Experimental schematic diagram	24
3.3 Input and output variable membership functions	35
3.4 Comparison of raw and smoothed values of relative Beta power (Experiment 1)	37
4.1 Dimensionless absolute power in Beta frequency band (Experiment 1)	40
4.2 Dimensionless total absolute power in 0 -30 Hz frequency band (Experiment 1)	41
4.3 Dimensionless absolute power in EMG low frequency band (Experiment 1)	41
4.4 Model output (Experiment 1)	41
4.5 Relative power in Beta frequency band (Experiment 1)	44
4.6 Dimensionless absolute power in Beta frequency band (Experiment 2)	45

4.7	Dimensionless total absolute power in 0 -30 Hz frequency band (Experiment 2)	45
4.8	Dimensionless absolute power in EMG low frequency band (Experiment 2)	45
4.9	Model output (Experiment 2)	46
4.10	Dimensionless absolute power in Beta frequency band (Experiment 3) . .	46
4.11	Dimensionless total absolute power in 0 -30 Hz frequency band (Experiment 3)	46
4.12	Model output (Experiment 3)	47
4.13	Model output (Experiment 1)	53
4.14	Rescaled clinical assessment (Experiment 1)	53
4.15	Model deviation from clinical assessment (Experiment 1)	54
4.16	Rate of change in absolute Beta power over five minutes (Experiment 1) .	54
4.17	Rate of change in absolute EMG power over five minutes (Experiment 1)	54
4.18	Model output (Experiment 2)	56
4.19	Rescaled clinical assessment (Experiment 2)	56
4.20	Model deviation from clinical assessment (Experiment 2)	57
4.21	Dimensionless absolute power in Beta frequency band (Experiment 2) . .	57
4.22	Dimensionless total absolute power in 0-30 Hz frequency band (Experiment 2)	57
4.23	Dimensionless total absolute power in EMG low frequency band (Experiment 2)	58
4.24	Rate of change in absolute Beta power over five minutes (Experiment 2) .	58
4.25	Rate of change in absolute EMG power over five minutes (Experiment 2)	58
4.26	Model output (Experiment 3)	60
4.27	Rescaled clinical assessment (Experiment 3)	60
4.28	Model deviation from clinical assessment (Experiment 3)	60

4.29	Dimensionless total absolute power in 0-30 Hz frequency band (Experiment 3)	61
4.30	Model output (Experiment 4)	62
4.31	Rescaled clinical assessment (Experiment 4)	62
4.32	Model deviation from clinical assessment (Experiment 4)	63
4.33	Dimensionless total absolute power in 0-30 Hz frequency band (Experiment 4)	63
4.34	Model output (Experiment 5)	65
4.35	Rescaled clinical assessment (Experiment 5)	65
4.36	Model deviation from clinical assessment (Experiment 5)	65
4.37	Dimensionless absolute power in Beta frequency band (Experiment 5)	66
4.38	Dimensionless total absolute power in 0-30 Hz frequency band (Experiment 5)	66
4.39	Dimensionless total absolute power in EMG low frequency band (Experiment 5)	66
4.40	Model output (Experiment 6)	68
4.41	Rescaled clinical assessment (Experiment 6)	68
4.42	Model deviation from clinical assessment (Experiment 6)	69
4.43	Suppression Ratio (Experiment 6)	69
4.44	Dimensionless absolute power in Beta frequency band (Experiment 6)	69
4.45	Dimensionless total absolute power in 0-30 Hz frequency band (Experiment 6)	70
4.46	Dimensionless total absolute power in EMG low frequency band (Experiment 6)	70
4.47	Model output (Experiment 7)	73
4.48	Rescaled clinical assessment (Experiment 7)	73
4.49	Model deviation from clinical assessment (Experiment 7)	73

4.50	Dimensionless absolute power in Beta frequency band (Experiment 7) . .	74
4.51	Dimensionless total absolute power in 0-30 Hz frequency band (Experiment 7)	74
4.52	Dimensionless total absolute power in EMG low frequency band (Experiment 7)	74
4.53	Suppression Ratio (Experiment 7)	75
4.54	Model output (Experiment 8)	76
4.55	Rescaled clinical assessment (Experiment 8)	76
4.56	Model deviation from clinical assessment (Experiment 8)	77
4.57	Dimensionless absolute power in Beta frequency band (Experiment 8) . .	77
4.58	Dimensionless total absolute power in 0-30 Hz frequency band (Experiment 8)	77
4.59	Dimensionless total absolute power in EMG low frequency band (Experiment 8)	78
4.60	Model output (Experiment 9)	79
4.61	Rescaled clinical assessment (Experiment 9)	79
4.62	Model deviation from clinical assessment (Experiment 9)	79
4.63	Dimensionless absolute power in Beta frequency band (Experiment 9) . .	80
4.64	Dimensionless total absolute power in 0-30 Hz frequency band (Experiment 9)	80
4.65	Dimensionless total absolute power in EMG low frequency band (Experiment 9)	80
4.66	Model output (Experiment 10)	82
4.67	Rescaled clinical assessment (Experiment 10)	82
4.68	Model deviation from clinical assessment (Experiment 10)	83
4.69	Dimensionless absolute power in Beta frequency band (Experiment 10) .	83
4.70	Dimensionless total absolute power in 0-30 Hz frequency band (Experiment 10)	83

4.71	Dimensionless total absolute power in EMG low frequency band (Experiment 10)	84
4.72	Model output (Experiment 11)	85
4.73	Rescaled clinical assessment (Experiment 11)	86
4.74	Model deviation from clinical assessment (Experiment 11)	86
4.75	Dimensionless absolute power in Beta frequency band (Experiment 11)	86
4.76	Dimensionless total absolute power in 0-30 Hz frequency band (Experiment 11)	87
4.77	Dimensionless total absolute power in EMG low frequency band (Experiment 11)	87
4.78	Model output (Experiment 12)	89
4.79	Rescaled clinical assessment (Experiment 12)	89
4.80	Model deviation from clinical assessment (Experiment 12)	90
4.81	Dimensionless absolute power in Beta frequency band (Experiment 12)	90
4.82	Dimensionless total absolute power in 0-30 Hz frequency band (Experiment 12)	90
4.83	Dimensionless total absolute power in EMG low frequency band (Experiment 12)	91
4.84	Model output (Pulse experiment)	95
4.85	Rescaled clinical assessment (Pulse experiment)	96
4.86	Model deviation from clinical assessment (Pulse experiment)	96
4.87	Dimensionless absolute power in Beta frequency band (Pulse experiment)	96
4.88	Dimensionless total absolute power in 0-30 Hz frequency band (Pulse experiment)	97
4.89	Dimensionless total absolute power in EMG low frequency band (Pulse experiment)	97
4.90	Suppression Ratio (Pulse experiment)	97
4.91	Model output (Surgical experiment)	100

4.92	Rescaled clinical assessment (Surgical experiment)	100
4.93	Model deviation from clinical assessment (Surgical experiment)	100
4.94	Dimensionless absolute power in Beta frequency band (Surgical experiment)	101
4.95	Dimensionless total absolute power in 0-30 Hz frequency band (Surgical experiment)	101
4.96	Dimensionless total absolute power in EMG low frequency band (Surgical experiment)	101
4.97	Suppression Ratio (Surgical experiment)	102

GLOSSARY

ABETA	A measure of absolute power in the EEG Beta frequency band.
ABETArate	Rate of change of ABETA over 5 minute period.
Alpha frequency band	Band of EEG power spectrum between 8 and 13 Hz
AWARE	Output variable of model developed in this thesis: Proposed index of anesthetic depth.
Beta frequency band	Band of EEG power spectrum between 13 and 30 Hz.
Bolus	A dosage of a drug given at once.
Burst suppression	EEG phenomenon occurring when EEG voltage is continuously $0 \pm 5\mu\text{V}$ for at least 240 ms. This phenomenon corresponds to CNS inactivity.
Corneal reflex	Response of cornea to digital stimulation.
Crisp	Not ambiguous; having fuzzy set membership of 1.
Delta frequency band	Band of EEG power spectrum between 0 and 4 Hz.
Defuzzification	Conversion of a fuzzy quantity to a crisp value using one of many conventional methods.
EEG	Electroencephalogram: relating to electrical activity of brain.
Electroencephalography	Recording of electrical activity of the brain.
Electromyography	Recording of electrical activity of muscles.
EMG frequency band	Band of EEG power spectrum between 70 and 300 Hz.
EMGrate	Rate of change of EMGLO over 5 minute period.

EMGLO	Absolute power in the EMG low frequency band (70 - 110 Hz).
Fuzzification	Conversion of a crisp input to a fuzzy value via a membership function.
Fuzzy logic	Formal methodology for performing logical operations with fuzzy sets.
Fuzzy set	A set in which an element can belong to some degree rather than be limited to complete inclusion or exclusion.
Hypotension	Low blood pressure.
Median frequency	Frequency below which 50% of power in the EEG power spectrum is expressed.
Membership function	A function that relates a crisp quantity to degree of membership in a fuzzy set.
Palpebral reflex	Response of eyelid to digital stimulation.
Propofol	Anesthetic agent (2,6-diisopropylphenol). Also known by trade name, Diprivan.
RBETA	Fraction of EEG total power expressed in the Beta frequency band.
Spectral edge frequency	Frequency below which some specified fraction of power in the EEG power spectrum is expressed.
Suppression ratio	Fraction of time during a sampling period that EEG signal is considered suppressed. See burst suppression.
Theta frequency band	Band of EEG power spectrum between 4 and 8 Hz
TOTPOW	A measure of total absolute power in the 0 - 30 Hz EEG frequency band.
Vasodilator	Drug that dilates blood vessels
Vasopressor	Drug that constricts blood vessels

1.0

INTRODUCTION

Anesthesia has made possible many of the surgical advances in modern medicine. Complicated surgical techniques cannot be used humanely in a non-compliant patient who feels pain. Anesthesia is also used in critical care environments where the alternative is to administer strong, addictive pain relieving agents which may prevent a patient from feeling much pain, but would probably also prevent the patient from feeling much else. Whether anesthesia is required for pain relief, muscle relaxation, or general unconsciousness in a patient, it may be administered for a lengthy period which can be fatiguing for the personnel involved. The purpose of this work is to propose a means for quantification of the assessment of anesthetic depth. The model described in this thesis uses multiple-variable input obtained from both electroencephalographic and cardiovascular data to yield a numerical output representing an index of anesthetic depth. This approach of assessing depth of anesthesia has not been attempted previously. The resulting assessment could be used as a tool for the anesthesiologist or it could be used as a controlled variable in a closed loop control system. Although inhalant anesthesia and multiple agent anesthetic regimens are clinically more common, the experimentation required for model development has been purposely limited to infusion anesthesia using propofol only.

1.1 INFERENCE OF DEPTH OF ANESTHESIA

Whether an anesthesiologist is attending a human or a canine patient, he relies on his evaluation of a set of clinical observables to make an inference of anesthetic depth. A veterinary anesthesiologist infers anesthetic depth of a dog by monitoring jaw tone,

palpebral reflex, corneal reflex, heart rate, and blood pressure. Jaw tone is the perceived stiffness of the jaw muscles. Palpebral and corneal reflexes are the responses of the eyelid and eyeball to touch. As the plane of anesthesia deepens, jaw tone decreases, and the palpebral and corneal reflexes become slower. Depending on the anesthetic used, heart rate and blood pressure decrease as the anesthetic plane deepens. From evaluating these variables, the anesthesiologist synthesizes an assessment of anesthetic depth based on training and experience and adjusts the rate of administration accordingly. This methodology is applicable for humans as well as dogs. An anesthesiologist working with a human patient will evaluate a similar set of clinical observables to make an assessment of anesthetic depth. Therefore a model designed to automate the inference of anesthetic depth would have broad application within human medicine as well as veterinary medicine.

The methods used by an anesthesiologist to assess depth of anesthesia are difficult to replicate using an automated system. Meters or other devices to determine the quality of jaw tone, palpebral reflex, and corneal reflex do not exist, therefore alternative clinical observables are necessary to automate the assessment of anesthetic depth. Ideally, these clinical observables should be easily acquired and also provide information from which the quality of central nervous system activity can be inferred.

Alternative sets of easily acquired clinical observables are available and have been used in anesthesia monitoring and control. Previous efforts to monitor anesthetic depth have involved blood pressure and electroencephalography (EEG), the analysis of electrical activity of the brain. These studies have primarily evaluated individual variables for their suitability as overall indicators of anesthetic depth. Previous efforts to control anesthesia have focused primarily on the control of blood pressure or an EEG variable, therefore

implying that adequate control of depth of anesthesia could be inferred from adequate control of one variable.

Although most monitoring and control strategies rely on a single monitoring or control variable, an accurate assessment requires a multivariable analysis; no single observable is sufficient for determination of anesthetic depth. Our efforts have been aimed at developing a model which describes anesthetic depth given cardiovascular and EEG input: a multivariable approach similar to that used by the anesthesiologist.

1.2 APPLICATION OF FUZZY LOGIC

Two traditional approaches to creating a model to infer depth of anesthesia would be the regression approach and the expert system approach. The regression approach would require a precise numerical assessment of anesthetic depth to be correlated to tissue concentrations of anesthetic agent and determination of mathematical correlations between EEG data, cardiovascular data, and tissue concentrations. The assessment of anesthetic depth could then be related parametrically to EEG data and cardiovascular data. The expert system approach would be to assemble a database of IF-THEN rules that relate EEG and cardiovascular data with their corresponding numerical assessments of anesthetic depth to be incorporated into a vast matrix, or look-up table.

There are methodological problems with both of these methods. The regression method requires a precise numerical assessment of anesthetic depth. A subjective assessment rendered by an anesthesiologist may be clinically sufficient, but could not be reasonably described as precise, however. The expert system approach requires a set of IF-THEN rules appropriately chained together that satisfy all reasonable clinical scenarios. The resulting problem in this application is that the IF-THEN rules are difficult to

implement due to the clinical necessity for flexibility. A second problem with the expert system approach is that it is computationally inefficient.

Our depth-of-anesthesia model was not developed using either the regression approach or the traditional expert system approach, but was developed using fuzzy set theory implemented in a fuzzy expert system. Fuzzy logic provides a rigorous and consistent means of mathematically interpreting uncertainty. Fuzzy logic has been used to control cement kilns, steam engines, and commuter trains and has been employed in a wide variety of consumer products. These consumer products include washing machines that can adjust cycles depending on the weight and relative dirtiness of a load of laundry, video cameras which can negate the wiggling of images caused by hand-held operation, and automatic transmissions in automobiles that shift in a manner more similar to human drivers.

Fuzzy logic makes it possible for a machine to recognize not only "True" and "False," but also the continuum of ambiguity in between. Fuzzy logic does not make machines "think" or "reason" like humans, but provides a mathematical framework which allows for machine interpretation of multi-valued logic in a manner that accommodates ambiguity. A classic example of ambiguity is the paradox of the heap of sand. One can remove an individual grain from a heap of sand and the remainder is still a heap. Continue removing individual grains and eventually the remainder is no longer a heap. If a machine were to recognize whether sand constituted a heap, binary logic would require the designation of an arbitrary breakpoint; i.e., N grains constitute "heap," whereas $N-1$ grains constitute "not a heap." A machine using fuzzy logic can determine that a heap of N grains of sand is "more of a heap," while a heap of $N-1$ grains is "less of a heap." Humans recognize that the quality of being a heap is determined by a continuum of numbers of

grains of sand. The fuzzy system accommodates this continuum; the binary system does not.

The accommodation of ambiguity is what makes fuzzy logic useful for model development and control applications. Fuzzy logic allows for the solution of some control problems without the development of a rigorous mathematical model of the process, and allows for the development of models where the processes to be described are complicated or difficult to quantify. Control or modeling problems that are strong candidates for a fuzzy solution are those which are mastered by human control and perception. The determination and control of anesthetic depth falls into that category. Fuzzy logic control can be applied in other contexts, but the application of fuzzy logic to control of mathematically well-defined systems, such as control of a DC motor, is less practical and probably has value only as an academic exercise.

1.3 PROPOSED MODEL

When the anesthesiologist synthesizes an assessment of anesthetic depth he relies on his experience, training, and common sense. He assesses input values, assigns weights to the input values, notes changes in these input values over time, and reflects on training and experience. He then makes a sensible assessment. The model that has been developed here has been synthesized similarly. Based on basic physiological tenets and observation of several anesthetized patients, several processed EEG variables were selected as algorithm input. During a battery of experiments, these variables were identified as possibly correlating to the subjective assessment of anesthetic depth provided by our anesthesiologist. The general trends were noted and a set of rules that linguistically described these trends in relation to anesthetic depth was developed. Experimental data

were imported into a fuzzy logic software package and processed using the set of rules via fuzzy logic to provide our model which assesses anesthetic depth. The model was validated using experimental data obtained from another battery of experiments.

This model has several potential uses. The resulting assessment of anesthetic depth could be used in a real-time anesthesia monitoring scheme by an anesthesiologist, either for monitoring or open-loop control. The assessment variable could also be used in real-time as a variable to be controlled in a closed-loop control scheme. This application would be analogous to a “cruise control” system for anesthesia delivery. The anesthesiologist could induce and monitor induction, only initiating the automatic control once he is satisfied with the observed depth of anesthesia in the patient.

1.4 ORGANIZATION OF THESIS

Chapter 1 provides an overview of the study that was undertaken. Chapter 2 details the motivation for this work and the development of technology used to create the computer model which is the end product of this endeavor. Chapter 3 provides a discussion of the methods used to develop the model. Chapter 4 is an experiment-by-experiment summary of results and analysis. Chapter 5 provides an evaluation of the model and a discussion of model limitations. Conclusions and recommendations are presented in Chapter 6.

MOTIVATION

The clinical use of anesthesia serves to accomplish three purposes for a patient: maintenance of an unconscious state, pain suppression, and muscle relaxation. For these goals to be satisfied, the administration of anesthesia must be properly monitored by a trained anesthesiologist. Monitoring is necessary to ensure that the patient is maintained in an anesthetic plane deep enough such that he is both compliant and unaware of noxious stimuli yet not so deep as to be comatose. Typically, the assessment of anesthetic depth is determined by evaluating a combination of clinical observables, such as reflex actions, muscle tone, and patient movement, cardiovascular observables, such as blood pressure and heart rate, and occasionally electroencephalographic (EEG) observables. Electroencephalography is used to assess central nervous system activity as a means of inferring anesthetic depth.

The clinical observables are the source of most information to the anesthesiologist. Unfortunately, the clinical observables may be obscured when multiple agents such as vasodilators, vasopressors, beta blockers, calcium channel blockers, and neuromuscular blockers are employed (Nayak 1994). An alternative means to determine and monitor depth of anesthesia would therefore be useful to the anesthesiologist.

Certain clinical environments require long-duration administration of anesthesia. These might include long surgical procedures and long-term relief of pain in an intensive care environment. A long surgical procedure can be fatiguing for an anesthesiologist and intensive care monitoring by anesthesiologists would be costly. The introduction of an automated means of assessment of anesthetic depth would be beneficial in both scenarios.

A system analogous to an automobile “cruise control” would relieve some tedium for the attending anesthesiologist. An automated system could improve patient safety and reduce healthcare costs.

2.1 PROPOFOL ANESTHESIA

Propofol (2,6-diisopropylphenol, Figure 2.1) is used exclusively in this study. Slightly soluble in water, propofol is formulated as an emulsion for clinical use. This anesthetic agent is a sedative-hypnotic which produces dose-dependent depression of the central nervous system. The pharmacokinetics of propofol make it suitable for continuous intravenous infusion. Patients recover rapidly and experience few adverse side effects other than occasional pain on injection (Larijani 1989).

Propofol is typically used in combination with narcotics (e.g. fentanyl) and inhalation anesthetics (e.g. nitrous oxide). In this study, propofol is used alone to ensure pharmacological simplicity for a pilot investigation of anesthesia monitoring. Exclusive use of propofol also provides a reference case for the interpretation of future results involving combinations of anesthetic agents. The broader intent of the project is to prepare a methodology for studying other anesthetic agents alone and in combination.

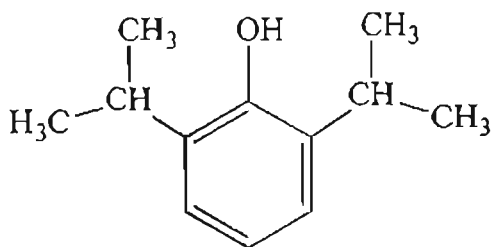


Figure 2.1: Propofol (2,6-diisopropylphenol)

2.2 ASSESSMENT OF ANESTHETIC DEPTH

The clinician relies primarily on evaluation of clinical observables, such as reflexes, muscle tone, and patient movement, to infer depth of anesthesia. Cardiovascular data are almost always available. EEG data are not routinely available but can be if utility is demonstrated.

2.2.1 Clinical Observables

Jaw tone is a means of determining “sufficiency” of propofol anesthesia in a dog (Watkins 1987; Weaver 1990; Robertson 1992). Intraocular pressure as determined by evaluation of corneal reflex is also useful as an indicator of anesthetic depth with propofol (Larijani 1989). Palpebral reflex, the reflex of the eyelid in response to digital stimulation, has also been used as an indicator of anesthetic depth in dogs (Zoran 1993). All three have been used in our work.

2.2.2 Cardiovascular Observables

Attempts have been made to infer adequacy of anesthesia from blood pressure (Smith 1972) and heart rate (Suppan 1972). Different anesthetic agents affect these cardiovascular parameters differently. Intravenous induction of anesthesia with propofol has been seen to decrease blood pressure 20-30 percent in humans (Larijani 1989). One study involving dogs indicated that blood pressure variations during prolonged propofol infusion were minor and transient (Robertson 1992). This study also specified a lowest permissible limit of mean arterial pressure in a dog of 65 mmHg and suggested that anesthetic depth during propofol infusion may not be a strong function of blood pressure, although mean arterial pressure should be maintained above a threshold value. Another

study has reported no clear link between depth of propofol anesthesia and heart rate (Watkins 1987).

2.2.3 EEG Observables

The electroencephalogram provides insight into central nervous system activity in real-time and has been shown to have utility in monitoring of anesthesia (Donegan 1990; Stanski 1992). Raw EEG waveforms record summed field potentials resulting from depolarization of nerve cells (Donegan 1990) and are difficult to interpret without applying sophisticated signal processing methods. Two broad categories of algorithms, time domain and frequency domain, are typically used to process the raw EEG signals. Time domain algorithms analyze data acquired within the period of a sampling window, or epoch, as a function of time. Frequency domain algorithms require Fourier transform analysis to analyze waveform amplitude, or power, as a function of frequency (Figure 2.2). The result is a power spectrum, analogous to a light spectrum separated by a glass prism.

2.2.3.1 EEG Time Domain Variables

An important processed EEG variable calculated in the time domain is the burst suppression ratio. This value indicates the fraction of an EEG signal being suppressed and is a useful indicator of metabolic depression with drugs such as thiopental, isoflurane (Donegan 1990), and propofol (Kanto 1989). A sampling epoch would be considered suppressed if the value of the measured potential is between $\pm 0.05 \mu\text{V}$ for at least 240 ms (Donegan 1990). An example illustration is provided in Figure 2.3. The suppression ratio as calculated by the EEG monitor in this work is the fraction of epochs considered suppressed within the last 123 sampled (Aspect Medical Systems 1996).

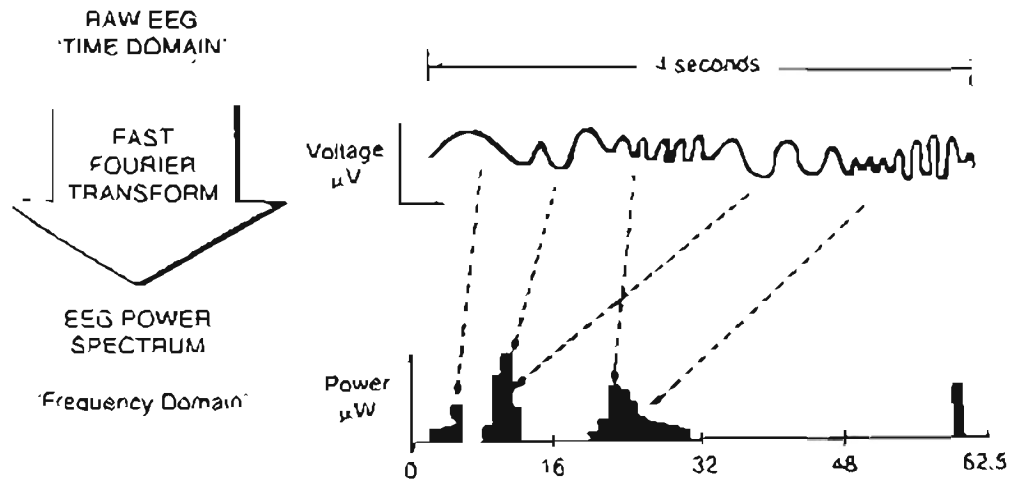


Figure 2.2: Relation of time domain to frequency domain via fast Fourier transform. (Donegan 1990)

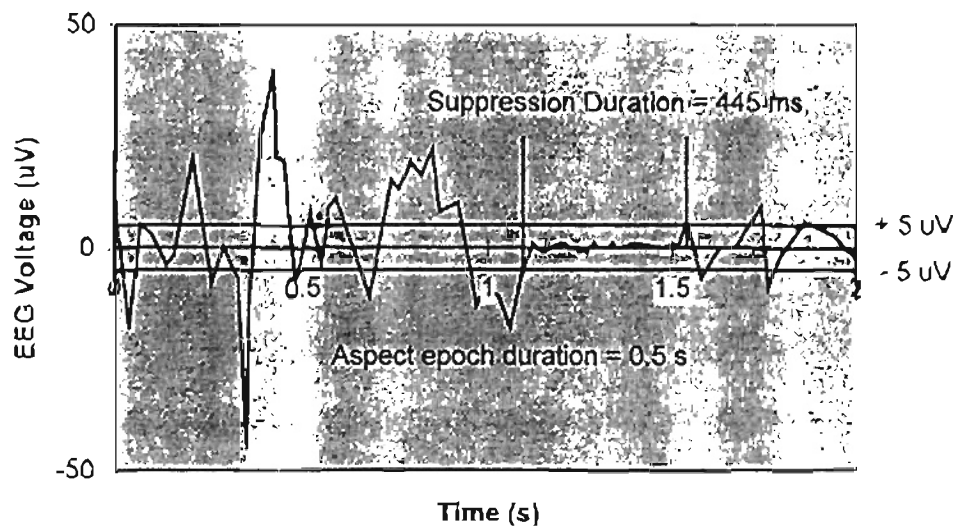


Figure 2.3: Determination of burst suppression. The EEG signal is considered suppressed if the EEG signal is $0 \pm 5 \mu V$ for at least 240 ms (Donegan 1990). The suppression ratio calculated by the Aspect EEG monitor is the fraction of suppressed epochs within the last 124 sampled epochs. An Aspect epoch is approximately 0.5 s in duration (Aspect Medical Systems 1996).

2.2.3.2 EEG Frequency Domain Variables

Variables that are determined in the frequency domain are the variables that relate power (waveform amplitude) to frequency. These variables include spectral edge frequency, median frequency, total power, and power in specific frequency bands.

Spectral edge frequency (SEF) is the frequency below which some fraction of the total power is expressed: e.g. the 95% SEF, or SEF95, is the frequency below which 95 percent of the total power is expressed. The median frequency is the 50% SEF (SEF50). Figure 2.4 provides an example of both 95% SEF and median frequency. Both the SEF and the median frequency have been used as univariate measures of EEG anesthesia effect (Stanski 1992). In general, deepening of the anesthetic plane will correspond to a decrease in spectral edge frequency. Reduced central nervous system activity is reflected in a shift to a lower spectral edge frequency.

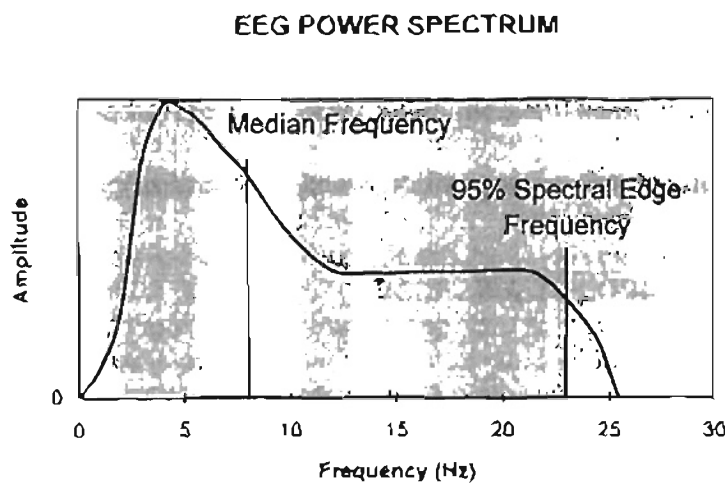


Figure 2.4: Spectral edge and median frequency as determined from EEG power spectrum. (Donegan 1990)

The adequacy of SEF values as indicators of anesthetic depth has been the source of some debate, however. Some researchers have found the SEF to be a useful indicator of anesthetic depth (Otto 1991; Gurman 1994; Arndt 1995; Gaitini 1995). Other researchers are more skeptical of the utility of SEF for anesthesia monitoring (Ghouri 1993; Dwyer 1994; Koch 1994; Nayak 1994; Sebel 1995).

Power distribution within frequency bands of the EEG power spectrum is another source of information regarding depth of anesthesia. For ease of categorization, the EEG spectrum from 0 to 30 Hz has been divided into four frequency bands, delta (0-4 Hz), theta (4-8Hz), alpha (8-13 Hz), and beta (13-30 Hz) by convention (Donegan 1990). While a patient is alert or lightly anesthetized, power is expressed predominantly in the higher frequency beta and alpha bands. As the anesthetic plane deepens, the distribution of power shifts to the lower frequency bands. Power distribution during propofol anesthesia in humans has been shown to shift according to this rule of thumb (Kanto 1989). Other studies have suggested that variations on this method of analysis in dogs (Nayak 1994) and horses (Otto 1991) are useful for determination of anesthetic depth. Our proposed methodology utilizes these known shifts in power distribution.

2.3 FUZZY LOGIC

One of the goals of this project is to synthesize an assessment of anesthetic depth from a multivariable set of input as an anesthesiologist would. Rather than using the traditional expert system approach of employing crisp, "either-or" type rules and database searches or the traditional mathematical modeling approach requiring correlation studies and multiple-parameter regression, the approach used in this study is to use fuzzy logic to synthesize an assessment of anesthetic depth. The anesthesiologist in a clinical

environment is required to make decisions based on quantitatively vague, ambiguous input data. Fuzzy logic is a rigorous mathematical means to make quantitative decisions given similarly vague, ambiguous quantitative input data.

Humans process information much differently than digital computers. Humans communicate in words and make decisions linguistically. Individuals have an understanding of concepts such as “tall man,” “hot weather,” and “low price.” These concepts can be communicated with minimal loss of understanding between people. Computers, however, must have the descriptors “tall,” “hot,” and “low” quantified somehow. The non-fuzzy method of quantifying these descriptors would be to arbitrarily define a range of acceptable values. For example, “tall” could be defined as “height greater than six feet.” The problem with this approach is that a height of 5.9999 feet would not be classified as “tall” while a height of 6.0001 feet would. This poses no real mathematical problem; the definition is arbitrary. This description does not adequately describe the way a person would perceive height, however. Fuzzy logic provides a method to quantify “tall” without resorting to an arbitrary delineation and can be used to quantify linguistic descriptors such as “tall,” “hot,” and “low.” In this example, fuzzy logic would allow for the height of 5.9999 feet to be “tall” to some degree and “not tall” to some degree while the height of 6.0001 feet could be “tall” to a greater degree and “not tall” to a lesser degree.

2.3.1 Basic Fuzzy Set Theory

Traditional set theory is based on the Aristotelian premise that the intersection of the set “A” and its complement, “not A” is the empty set. Otherwise stated, an element in the universe containing the sets “A” and “not A” can belong to either “A” or “not A”

(Figure 2.5). The element is contained entirely within "A" or "not A." Fuzzy set theory introduces the concept of degree of set membership. In a fuzzy universe containing the complementary sets "A" and "not A," an element can belong to both sets to some degree with the interesting consequence that the intersection of "A" and "not A" is not necessarily the empty set.

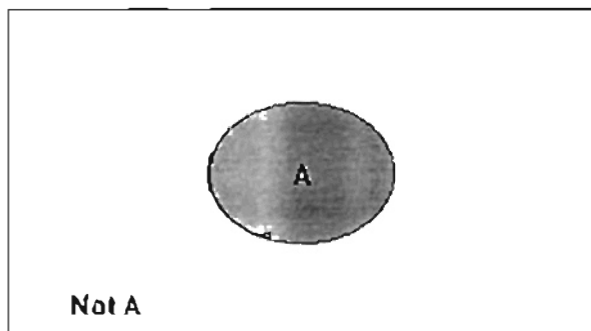


Figure 2.5: Venn diagram illustrating the set "A" and its complement, "Not A."

Another example of a fuzzy set would be the set of "hot" temperatures. The degree of membership of this set as a function of temperature is known as a membership function (Figure 2.6). Other sets could be added, such as "cold," "cool," "warm," and "hot," so that an entire temperature range is defined linguistically (Figure 2.7).

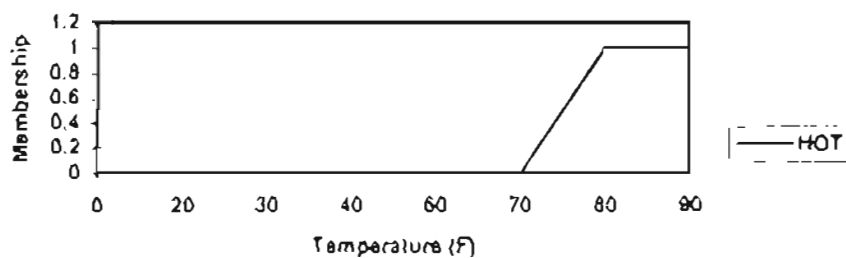


Figure 2.6: Hot temperature membership function

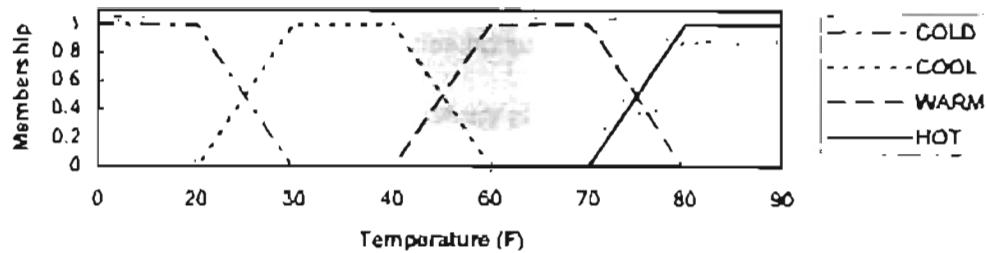


Figure 2.7: Fuzzy temperature spectrum

Fuzzy set theory is useful because it can provide an interface between human linguistic and mechanical, quantitative perceptions of the universe. With fuzzy information processing, machines can be programmed to make decisions within an environment containing vagueness, much as people do. An example of fuzzy inferencing and defuzzification is provided in Appendix A.

2.3.2 History of Fuzzy Logic

Fuzzy set theory was proposed in 1964 by Lotfi Zadeh (1965). It has since evolved from an academic novelty largely ignored by the scientific community to a versatile tool for solving engineering problems. Other philosopher-mathematicians, such as Max Black and Jan Lukasiewicz, have suggested other types of multi-valued logic or vagueness theory earlier (Black 1937; Lukasiewicz 1970), but Dr. Zadeh's fuzzy set theory is what is used today in many applications. Fuzzy logic was well received in the Orient and in Europe, but was slow to gain acceptance in the United States. American scientists and mathematicians were reluctant to accept a paradigm that suggested that scientific and engineering problems could be addressed using approximate reasoning. Japanese scientists and engineers

exploited this technology and provided Japanese consumers with fuzzy dishwashers, fuzzy camcorders, and fuzzy automatic transmissions. One of the successes of fuzzy logic control is the train in Sendai, Japan, that operates with the fuzzy predictive control system presented by Seiji Yasunobu (1985). Many of the consumer products once only available to Japanese consumers are now available to American consumers, although these products are often marketed not as “fuzzy” but as “intelligent.”

2.3.3 Fuzzy Logic Applied to Anesthesia Monitoring

Fuzzy logic has been applied to anesthesia monitoring and control with modest success. Fuzzy logic feedback control of blood pressure has been accomplished by several groups of researchers (Meier 1992; Ying 1992; Tsutsui 1994; Zbinden 1995). Some have suggested that the use of fuzzy logic to control blood pressure is probably unnecessary, but that fuzzy logic may be useful for controlling more ambiguous process variables or as a “supervising” entity in a multivariable control system (Martin 1994). Another fuzzy feedback control strategy has been to control inspired oxygen and inhalant anesthesia concentration (Curatolo 1996). More sophisticated adaptive fuzzy logic control has been applied to muscle relaxant delivery (Linkens 1991; Linkens 1992; Mason 1994). Fuzzy logic has also been used in an intelligent alarm system for cardioanesthetic monitoring (Rau 1995). None of these applications provide the assessment capabilities we are striving to achieve.

2.4 SIGNIFICANCE OF CURRENT WORK

This project is unique in that it proposes a numerical index of anesthetic depth that incorporates both time domain and frequency domain processed EEG variables related

linguistically with a fuzzy rulebase. Other efforts to create a univariate quantitative measure of anesthetic depth have included bispectral analysis (Ning 1990; Sebel 1995) of Fourier-decomposed EEG waveforms. While bispectral indices may be useful indicators of anesthetic depth, the index proposed in this work synthesizes more diverse information in a more intuitive manner resulting in a machine-generated assessment of anesthetic depth comparable to that rendered by an anesthesiologist. A similar qualitative approach has been proposed by Gurman (1994). He has generated a matrix of crisp rules relating spectral edge frequency and blood pressure to adequacy of anesthesia. Our approach is different in that our rulebase is fuzzy and we use other variables as inputs to our system.

2.4.1 Description

This system described in this thesis monitors changes in power distribution within the EEG spectrum as well as EEG burst suppression and mean arterial pressure. A matrix of fuzzy logic rules (fuzzy rulebase) was generated that relate mean arterial pressure, burst suppression ratio, processed EEG power spectrum variables, and their time rates of change over multiple time intervals to an index of adequacy of anesthesia. Input data is converted to the anesthetic depth index with the fuzzy rulebase via fuzzy logic algorithms. The resulting index correlates with the assessment of anesthetic depth provided by an anesthesiologist.

2.4.2 Application

A monitoring system such as this one could be used in an intensive care environment and during long surgical procedures to assist the attending anesthesiologist, especially if this monitoring approach proved applicable to combinations of anesthetic

agents. As discussed previously, common practice in modern surgical anesthesia is to use a combination of anesthetic agents such as neuromuscular blockers, beta blockers, and analgesics. The employment of these multiple agents may tend to mask traditional clinical observables. A system similar to the one proposed could provide insight into the patient's level of consciousness not available using traditional means of assessing anesthetic depth.

The use of a single index for a gauge of anesthetic depth could also be useful for feedback control. Rather than attempting to control multiple variables in the control system, this approach combines the multiple variables into one "set-point" variable, therefore making possible control schemes much less complex.

3.0

METHOD

The development of our fuzzy anesthesia monitoring model proceeded in three phases. The data collection phase consisted of experimentation and acquisition of data. Comparison between acquired data and clinical assessment of anesthetic depth occurred in the data analysis phase. The assembly of the model using the commercial fuzzy logic software shell constituted the model development phase.

3.1 DATA COLLECTION

The experiments performed were designed to be of sufficient duration to ensure that pharmacokinetic phenomena could be observed. These pharmacokinetic phenomena could be investigated more efficiently at multiple infusion rates. Due to the high cost of propofol, limited availability of subject animals, and our desire to keep the experimental protocol simple, each experiment was conducted using only two infusion rates administered for one hour each. To minimize complexity, no surgical procedure was associated with the regular data collection experimental protocol. In the absence of incision or other painful surgical stimuli, the anesthesiologist applied a hemostat (clamp) to the base of the tail of the subject dog to evaluate patient awareness of noxious stimuli.

Six mixed-breed dogs were used to acquire initial data for model development. Each dog was administered a 10 mg/kg bolus infusion dose of propofol, intubated, then connected to a Harvard Apparatus Model 2400 syringe infusion pump from which propofol was initially administered at the rate of 0.1 ml/kg/min for one hour. At the beginning of the second hour, the infusion rate was changed to 0.05 ml/kg/min. Infusion

was continued for one additional hour. The respiration of the dog was controlled using a ventilator for the duration of the experiment. Blood pressure was monitored invasively using a pressure transducer in a catheter inserted into an artery in a hind leg and either a Datascope model 2000 or a Datascope Passport EL electrocardiogram (ECG) monitor. ECG data acquisition commenced immediately following catheterization. The dog was also connected to an Aspect A-1000 EEG monitor using a four-channel referential electrode montage (Figure 3.1) and needle electrodes. The electrodes were inserted immediately following induction and intubation and both EEG and ECG data were acquired continuously until the dog would raise its head at the conclusion of the experiment. This protocol was also used to collect data from six purpose-bred beagle dogs for model verification. The beagle data were not used for model development. Information regarding experiment date, dog weight, identification number, and breed is provided in Appendix B.

During each experiment, the attending anesthesiologist would assess depth of anesthesia in the subject by monitoring jaw tone, and palpebral and corneal reflexes at five-minute intervals. The assessment for each of these observables was rated on a five-point scale where a score of “1” indicates “sufficiently anesthetized” and “5” indicates “awake.” An example clinical assessment worksheet is provided in Appendix C. The response of the dog to the 10 second application of a hemostat to the base of its tail (tail clamp) was monitored every 15 minutes during the infusion period.

Blood samples were taken from the subject every 15 minutes during the two-hour infusion period. After termination of infusion, samples were collected every 2 minutes until extubation. Samples were also collected every 30 minutes for two hours following extubation. These samples were used for pharmacokinetic analysis not discussed in this thesis. A summary of blood propofol data can be found in Appendix D.

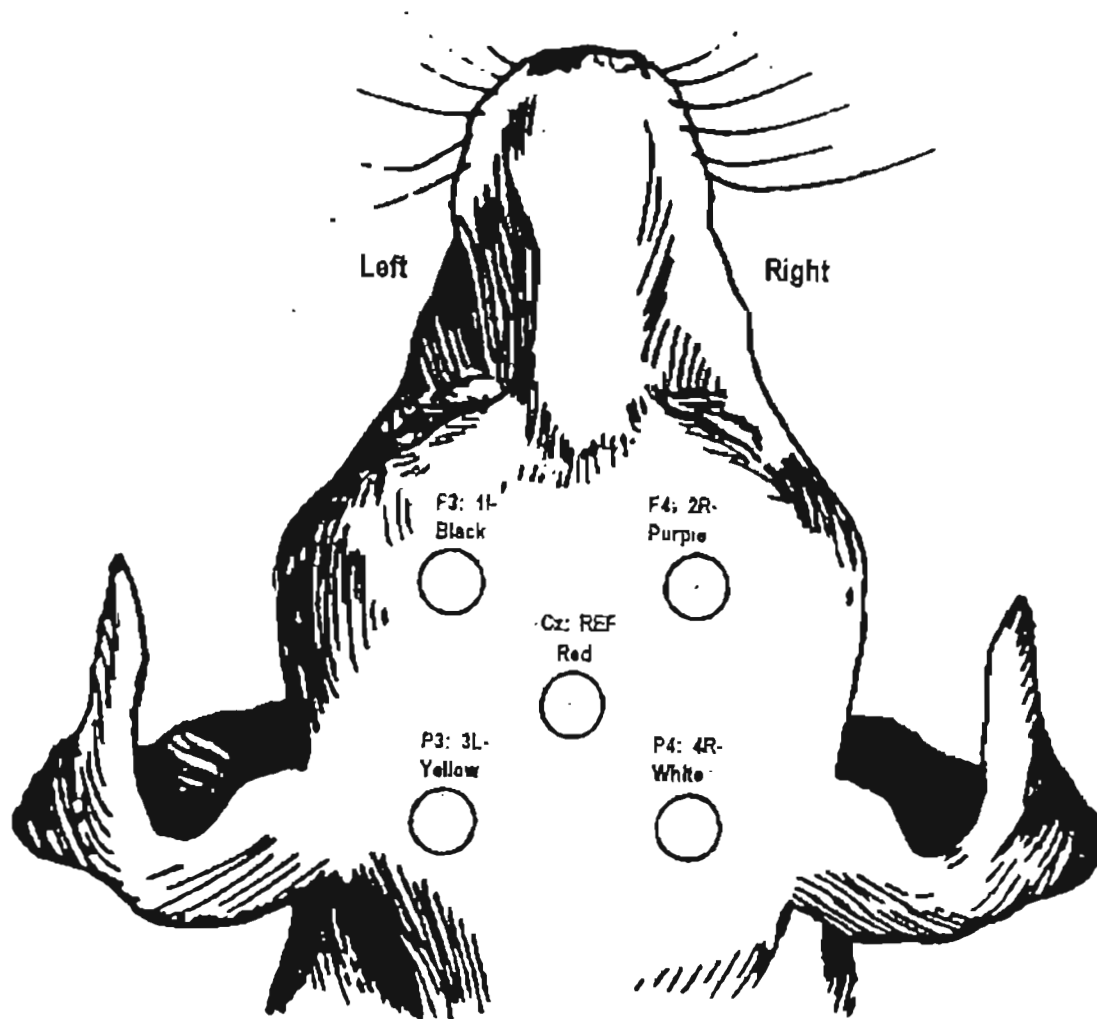


Figure 3.1: EEG electrode montage

Data from the infusion pump and EEG were acquired using software running on a Pentium-90 personal computer. The data acquisition software was written specifically for this purpose. Calculations internal to the EEG monitor were determined using a 0.5125 second epoch duration. Data from the EEG were acquired every 5 seconds and data from the pump were acquired every 30 seconds. The ECG monitor was videotaped using a tripod-mounted Sony 8 mm video camera. Data from the videotaped ECG monitor were transcribed manually from playback of the videotape. ECG data were transcribed at 30 second intervals. ECG data during tail clamp episodes were transcribed at 2 second intervals. The configuration of experimental apparatus is illustrated in Figure 3.2. Listings of the variables acquired from the EEG, ECG, and pump are presented in Tables 3.1, 3.2, and 3.3, respectively.

An additional experiment was performed using another mongrel dog and a modified version of the experimental protocol previously described. This experiment used only one infusion rate of 0.05 ml/kg for the two-hour duration of infusion. A 10 mg/kg bolus injection of propofol was administered after one hour. The purpose of this experiment was to verify assumptions regarding effect of propofol infusion rate on various EEG variables.

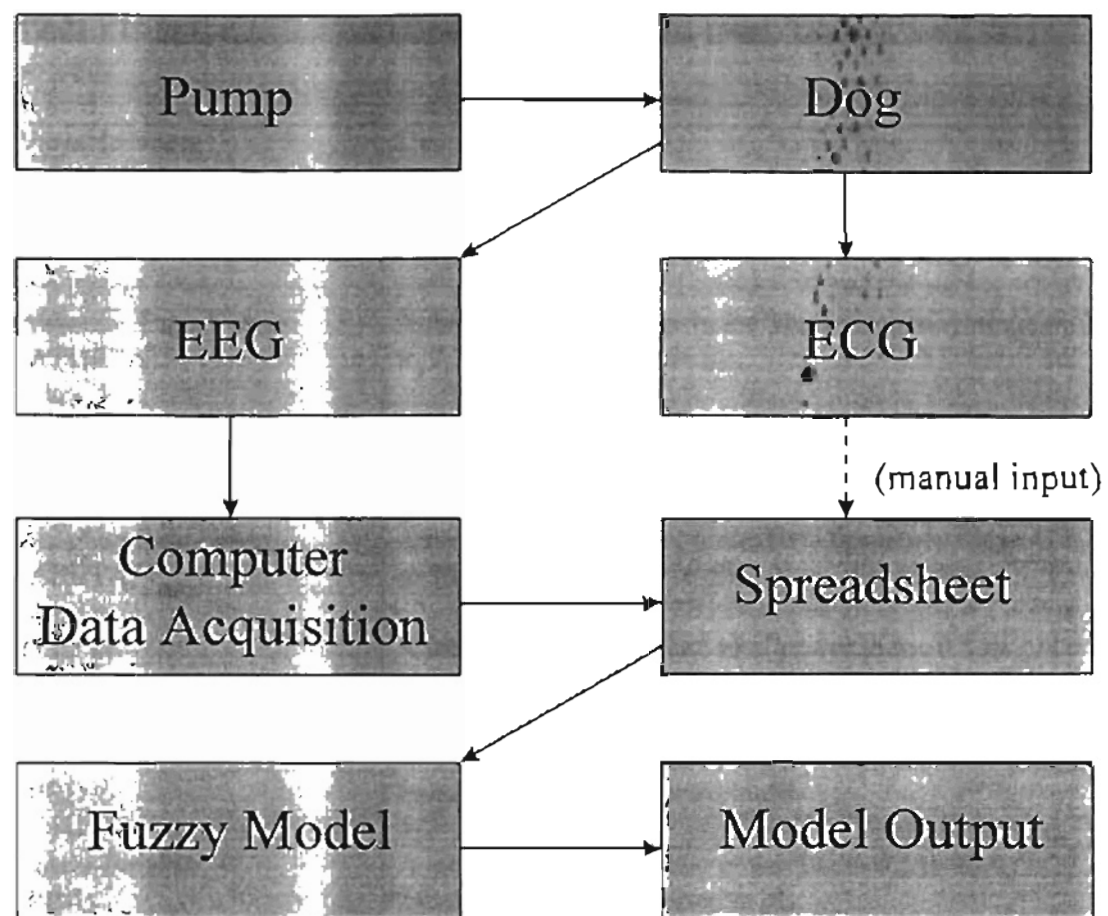


Figure 3.2: Experimental schematic diagram

Table 3.1. EEG data acquired (Aspect Medical Systems 1996). One epoch = 0.5125 seconds.

Variable Name	Description
Absolute Delta Power (ADELTA)	A measure of the power in the Delta frequency range (0.5 to 3.75 Hz). Reported in dB.
Absolute Theta Power (ATHETA)	A measure of the power in the Theta frequency range (4.0 to 7.75 Hz). Reported in dB.
Absolute Alpha Power (AALPHA)	A measure of the power in the Alpha frequency range (8.0 to 13.5 Hz). Reported in dB.
Absolute Beta Power (ABETA)	A measure of the power in the Beta frequency range (13.75 to 30.0 Hz). Reported in dB.
Total Power (TOTPOW)	A measure of the absolute total power in the 0.5 to 30 Hz frequency range. Reported in dB.
Power Band I (PBI)	A measure of the absolute power in the 30.0 to 40.0 Hz frequency range. Reported in dB.
Power Band II (PBII)	A measure of the absolute power in the 0.5 to 40.0 Hz frequency range. Reported in dB.
Relative Delta Power (RDELTA)	Percentage of Total Power expressed in the Delta frequency range.
Relative Theta Power (RTHETA)	Percentage of Total Power expressed in the Theta frequency range.
Relative Alpha Power (RALPHA)	Percentage of Total Power expressed in the Alpha frequency range.
Relative Beta Power (RBETA)	Percentage of Total Power expressed in the Beta frequency range.
Power Band Ratio (PBRAT)	The ratio of Power Band I power to Power Band II power expressed as a percentage.
Spectral Edge Frequency (SEF)	The frequency at which 95% of Total Power is expressed at lower frequencies.

Table 3.1. EEG data acquired. (Cont'd)

Variable Name	Description
Median Frequency (MEDFRQ)	The frequency at which 50% of Total Power is expressed at lower frequencies.
Asymmetry Value (ASYM)	Ratio of Channel 1 (or Channel 3) Total Power to sum of Total Powers of Channels 1&2 (or Channels 3&4)
Bispectral Index (BIS)	Bispectral index calculated via proprietary Aspect Medical Systems algorithm.
Alternate index (BISALT)	Alternative bispectral index calculated via proprietary Aspect Medical Systems algorithm.
Suppression Ratio (SR)	The percentage of epochs in the last 63 seconds in which the EEG signal is considered suppressed.
EMG Band 1 (EMGLO)	The absolute power in the 70-110 Hz frequency range. Reported in dB.
EMG Band 2 (EMGHI)	The absolute power in the 70-300 Hz frequency range. Reported in dB.
Bispectral Signal Quality (SQI)	The percentage of good epochs and suppressed epochs in the last 61.5 seconds that can be used in the Bispectral Index calculation.
Power Spectrum Signal Quality (PSQI)	The percentage of good epochs in the last spectral smoothing period.
Asymmetry Signal Quality (ASYSQI)	The percentage of good epochs in the last spectral smoothing period. Represents lowest of the Power Spectrum Signal Qualities for the hemispheric channel pairs.
Suppression Ratio Signal Quality (BSRSQI)	Percentage of good epochs in the last 63 seconds that can be used for calculation of Suppression Ratio.
Artifacts (ARTF)	Hexadecimal code for signal anomalies recognized by Aspect proprietary Artifact Detection Algorithm.

Table 3.2. ECG data acquired.

Variable	Description
Systolic Arterial Pressure (SAP)	Blood pressure during systolic phase of heartbeat. Expressed in mmHg.
Diastolic Arterial Pressure (DAP)	Blood pressure during diastolic phase of heartbeat. Expressed in mmHg.
Mean Arterial Pressure (MAP)	Mean arterial blood pressure time-averaged from pressure readings acquired during a sampling interval. Expressed in mmHg.
Heart Rate	The rate at which the heart of the patient beats. Expressed in beats per minute.

Table 3.3. Infusion pump data acquired.

Variable	Description
Infusion Rate	Rate at which propofol is administered. Expressed in ml/min.
Infused Volume	Cumulative volume of propofol infused. Expressed in ml.

Data were also collected during the neutering of a male German shepherd. The anesthesia protocol during this procedure was the same as in the previous experiments except that the propofol infusion rate was changed according to clinical requirements at the discretion of the attending anesthesiologist. Blood samples were not taken during this experiment, however. The purpose of this experiment was to evaluate both the model and equipment configuration in a surgical environment.

As mentioned previously, data were also collected from six beagles for the purposes of model verification. The protocol for data collection remained the same as for

the six initial experiments. One potential anomaly must be noted, however. Not only were these dogs all of the same breed, but several of the dogs were of similar age, size, and markings, suggesting the possibility that these dogs were from the same litter. If this is the case, the results might be affected by the lack of genetic variability in the sample being studied.

A summary of information regarding the individual dogs used as experimental subjects is provided in Appendix D.

3.2 DATA ANALYSIS

The ECG, EEG, pump, and clinical assessment data for each experiment were written into a Microsoft Excel spreadsheet. The acquired data and the clinical assessments were plotted as a function of time. For ECG data, heart rate was plotted individually and systolic, mean, and diastolic blood pressure were plotted together. The EEG data collected represented 25 variables for four EEG channels and two channel pairs (Channels 1 & 2 and Channels 3 & 4). Therefore data representing a total of 150 EEG variables were collected at five-second intervals for approximately 2.5 hours, or nominally 270,000 data points for each experiment from the EEG alone. For each EEG variable, the four channels of data were plotted together on the same plot. Data from the channel pairs were omitted on this series of plots. Pump data (infusion rate and infused volume) were plotted individually. Clinical assessments (jaw tone, corneal reflex, palpebral reflex, and overall clinical assessment) were plotted individually as well. One entire set of plots for one experiment are presented in Appendix E.

Plots of EEG and ECG data as functions of time were visually compared to plots of the clinical assessments as functions of time to determine which variables correlated

significantly. Particular emphasis was placed on analysis of variables traditionally used in assessment of anesthetic depth, such as spectral edge frequency, median frequency, bispectral index, and power in the delta (0-4 Hz), theta (4-8 Hz), alpha (8-13 Hz), and beta (13-30) power bands. The high-frequency electromyographic (EMG) bands were selected for further analysis as well. These EEG data were rescaled linearly without regard to units so that the final values were roughly on a scale of 1 to 5. This rescaling was executed for the purpose of facilitating direct comparison of the EEG variables to the 1 to 5 scale of the clinical assessments. The scaling equations and parameters are presented in Table 3.4. The scaling parameters were determined from values of ABETA, EMGLO, and TOTPOW observed during the high-infusion rate period of each experiment. These variables tended to approach a steady-state value within the first hour of each experiment. This baseline value of each variable was determined by visualization and used as the lower scaling parameter for each experiment. The upper scaling parameter represents an average maximum value of each variable for all experiments as determined by visualization.

3.2.1 EEG Input

The plots of the rescaled data provided insight into which EEG variables would be suitable for inclusion in our fuzzy model. Comparisons were made visually rather than through use of statistical correlation analysis. Given the relatively small sample size in our experiments, the subjective nature of the clinical assessments, and our proposed method of model development, the statistical correlation study would not be justified. The variables chosen for inclusion into the model are listed in Table 3.5. Note that not all of the variables traditionally monitored for assessing anesthetic depth are included in the set of variables. In general, the power distribution variables, and suppression ratio were

Table 3.4. Scaling Methodology for ABETA, TOTPOW, and EMGLO.

Transformation equation: $\theta' = 4 \cdot \frac{\theta - p}{q - p} + 1$

where:

θ = Original value (ABETA, TOTPOW, or EMGLO).

θ' = Transformed (rescaled) variable value.

p = Lower scaling parameter (dB)

q = Upper scaling parameter (dB)

Experiment	ABETA		EMGLO		TOTPOW	
	p	q	p	q	p	q
1 (0502)	38	65	30	64.3	46	65
2 (0608)	44	65	21	64.3	53	65
3 (0615A)	52	65	40	64.3	62	65
4 (0615P)	44	65	32	64.3	57	65
5 (0616)	47	65	31	64.3	56	65
6 (0811)	40	65	30	64.3	48	65
7 (0107A)	45	65	32	64.3	52	65
8 (0107P)	46	65	32	64.3	55	65
9 (0108A)	45	65	30	64.3	54	65
10 (0108P)	45	65	30	64.3	56	65
11 (0109A)	45	65	31	64.3	56	65
12 (0109P)	47	65	31	64.3	57	65
Pulse Experiment (0911)	44	65	32	64.3	54	65
Surgical Experiment (1213)	45	65	28	64.3	55	65

TABLE 3.5. Model Input Variables.

Variable	Definition	Physiological Significance
Absolute Beta Power (ABETA)	A measure of the power in the Beta frequency band. (13.75-30.0 Hz)	As propofol anesthesia deepens, Beta activity decreases.
Absolute Beta Power Rate (ABETArate)	Rate of change of Absolute Beta Power over five minute period.	Provides quantification of Absolute Beta Power trends.
Total Power (TOTPOW)	A measure of the absolute total power in the Delta, Theta, Alpha, and Beta frequency bands. (0.5 to 30 Hz)	As anesthesia deepens, total power decreases.
Relative Beta Power (RBETA)	The fraction of total power that is due to Beta activity.	As anesthesia deepens, power in the Beta frequency band decreases, but relative power in other frequency bands increases. Provides indication of power distribution within 0.5 - 30 Hz frequency band.
EMG Low Band Power (EMGLO)	The absolute power in the low EMG band. (70-110 Hz)	EMG power is a measure of muscle activity. As anesthesia deepens, EMG activity decreases.
EMG Low Band Power Rate (EMGrate)	Rate of change of EMG Low Band Power over five minute period.	Provides quantification of EMG Low Band Power trends.
Suppression Ratio (SR)	The percentage of epochs within a sampling window that are considered "suppressed." (i.e., generating a potential of less than $\pm 5\mu\text{V}$ for greater than 240 ms)	Provides an indication of periods of relative brain inactivity. Usually indicative of deep anesthesia.

chosen. The power distribution variables were selected to provide a gauge of power distribution throughout the 0-30 Hz spectrum. Suppression ratio was included because it provides a reliable indicator of when the brain is electrically “quiet.” For ease of analysis, data from only one channel, Channel 2, were considered.

3.2.2 Mean Arterial Pressure

With most anesthetic agents, hypotension (low blood pressure) is a key concern. Typically, blood pressure decreases with increasing depth of anesthesia. With propofol, however, we have observed no meaningful correlation between depth of anesthesia and blood pressure at surgically adequate infusion rates. Therefore blood pressure was not included in the set of input variables for fuzzy model development. Any application of this modeling methodology to drugs other than propofol should not initially exclude blood pressure as an input, however.

During the experiments, the anesthesiologist would typically be concerned if the mean arterial pressure would drop below 65 mmHg: the minimum pressure required to keep tissues adequately perfused (Robertson 1992). Early attempts at model development included mean arterial pressure as an input, with the 65 mmHg pressure as a “tripwire.” The final form of the model as it will be discussed here does not include mean arterial pressure or any other cardiovascular input. If the mean arterial pressure were to be included in a monitoring system to serve as a control variable used to activate a “tripwire,” it can be included independently of the fuzzy system.

3.3 MODEL DEVELOPMENT

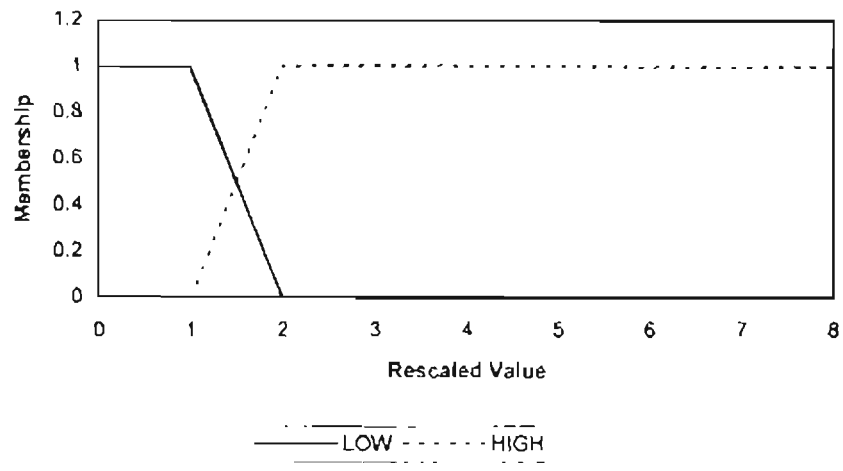
A model was developed using the set of input variables listed in Table 3.3. The model was constructed using the commercially available fuzzy logic programming shell, TILShell version 3.0, from Togai Infralogic, Inc., Irvine, CA. (now incorporated into Ortech Engineering, Houston, TX). The output of the model is the variable AWARE, which is an index of anesthetic depth. The goal of this model is to approximate the clinical determination of anesthetic depth as determined by an anesthesiologist.

Once the variables for fuzzy system input were selected, membership functions were defined for all input variables and for the output variable (Figure 3.3). Note that the membership functions for Absolute Beta Power (ABETA), Total Power (TOTPOW), and power in the low EMG band (EMGLO) are scaled using the scaling methodology previously discussed. These input variables are scaled using patient-specific parameters. This allows for ease of model development and implementation. The use of scaled input provides for more efficient use of programming resources. Two other input variables used in the model are the rate of change of absolute beta power (ABETArate) and the rate of change of power in the EMG low frequency band (EMGrate). These rates of change are not instantaneous, but determined over a time interval of five minutes. The method of calculating ABETArate and EMGrate is illustrated in Table 3.6.

Table 3.6: Calculation of ABETArate and EMGrate.

Variable	Formula ($\Delta t = 5$ minutes)
ABETArate	$ABETArate(t) = \frac{ABETA(t) - ABETA(t - \Delta t)}{\Delta t}$
EMGrate	$EMGrate(t) = \frac{EMGLO(t) - EMGLO(t - \Delta t)}{\Delta t}$

Membership functions for ABETA, EMGLO, and TOTPOW (dimensionless)



Membership functions for ABETArate and EMGrate (dB/s)

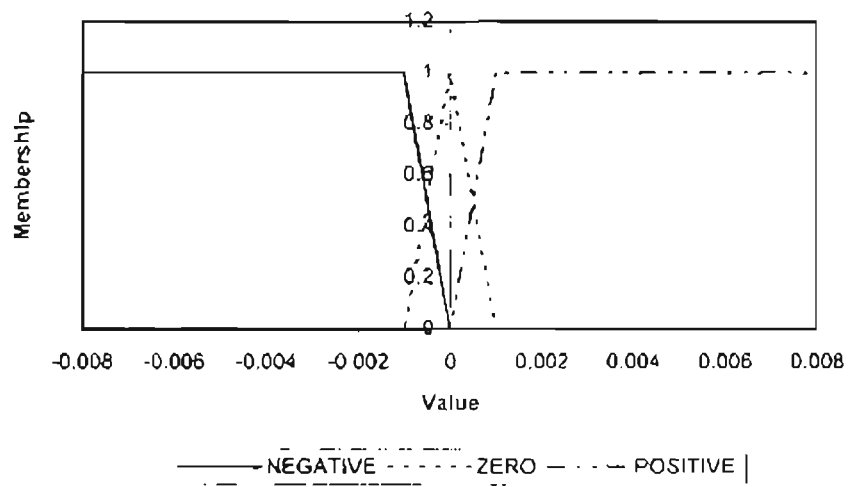
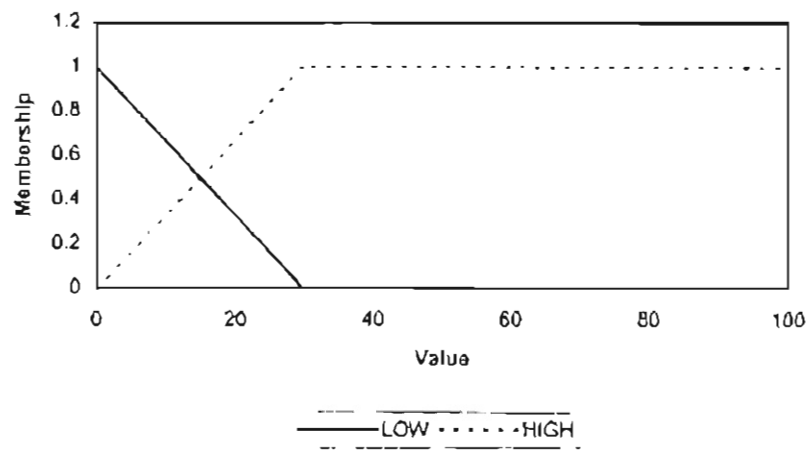
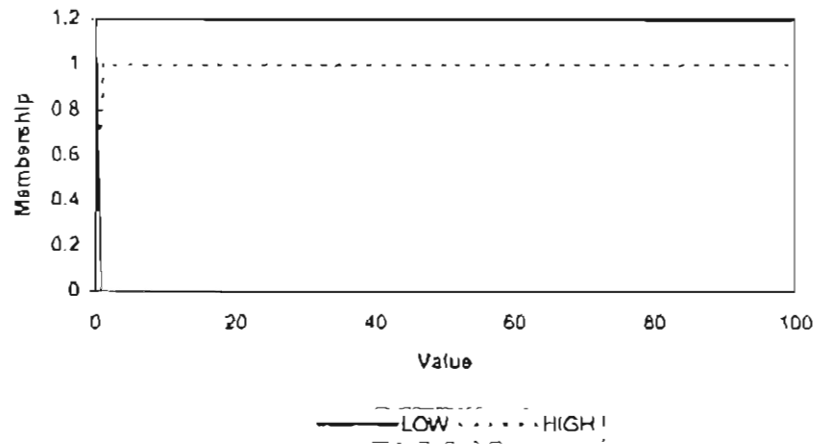


Figure 3.3: Input and output variable membership functions.

Membership functions for RBETA (percentage)



Membership functions for Suppression Ratio (percentage)



Membership functions for model output

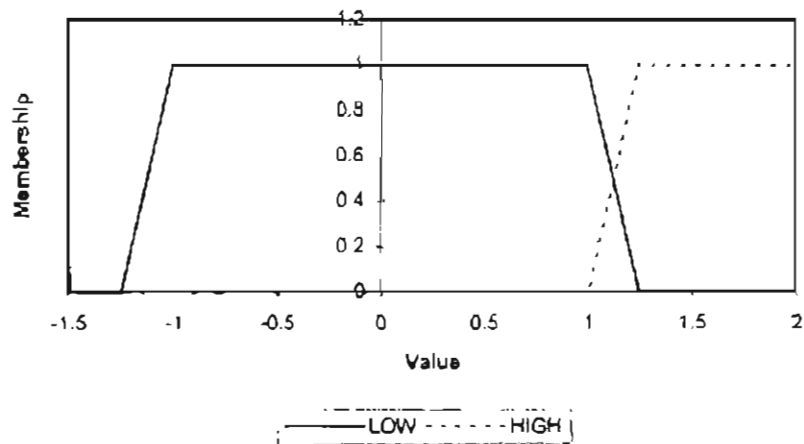


Figure 3.3 (Cont'd): Input and output variable membership functions.

A matrix of 38 rules relating the membership functions of the input variables was generated based on physiological heuristics. An example of a typical rule would be, "If ABETA is low and if ABETArate is negative, then AWARE is low." Each rule is physiologically based and enumerated in Appendix F.

Slight electrode movement, patient movement, or non-continuous electromagnetic interference would occasionally generate spurious data. These spurious data would be the source of "noise." Rather than incorporate physically meaningless data in to the model, some data were smoothed using a MATLAB program that uses wavelet smoothing (Ganti, 1996) to remove "noise" from the original signal. An example comparison of raw and smoothed data is provided in Figure 3.4. The data sets selected for wavelet smoothing were Absolute Beta Power (ABETA), Relative Beta Power (RBETA), Total Power (TOTPOW), and power in the low EMG band (EMGLO). Each of these data sets for each experiment were smoothed using the default smoothing level available with the program used. The resulting sets of smoothed data were concatenated and assembled into data files for each experiment using Microsoft Excel Version 7.0.

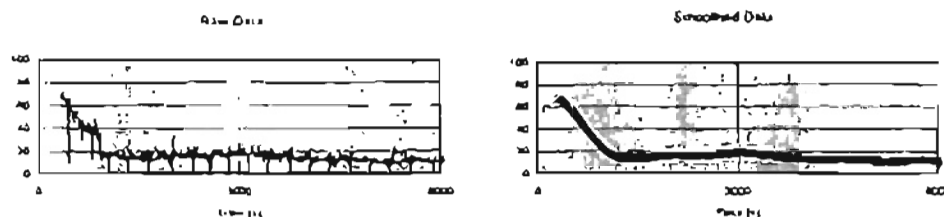


Figure 3.4: Comparison of raw and smoothed values of relative beta power (experiment 1).

The simulations using the model were executed within TILShell. A block of code was written in a TILShell simulation module which designated the data file to be read, the

scaling parameters to be used, and performed the scaling calculations. The resulting output was written to another data file for each simulation. Details regarding the generation and execution of TILShell simulations are provided in Appendix G.

RESULTS

The output resulting from the fuzzy model was analyzed in two ways. The trends evident in the model output were compared with those that would be expected based on physiological principles alone. Also, the output from the model was compared against the overall clinical assessment determined by the anesthesiologist.

4.1 ANALYSIS FROM PHYSIOLOGICAL PRINCIPLES ALONE

The first iteration of data analysis was to determine if the EEG input and model output were physiologically consistent. What is meant by physiological consistency is that none of the inputs and outputs contradict one another based on current understanding of EEG principles. As anesthesia deepens, a patient would be expected to exhibit less high frequency EEG activity. Consequently, physiological consistency would require that the variables used in this model, ABETA, EMG, and TOTPOW, would decrease as anesthesia deepens. The expectations for RBETA are unclear because it is the quotient of ABETA and TOTPOW. Rates of change of RBETA are therefore related to the comparative rates of change of ABETA and TOTPOW.

Consider the example of a patient subject to a “lightening” of anesthesia. One would expect that as anesthesia lightens, both ABETA and TOTPOW would increase. If one considers also the rule of thumb that a lighter plane of anesthesia generally implies more high frequency (BETA) activity than low frequency activity, one might conclude that RBETA would also increase. This is not the case, however, when TOTPOW increases faster than ABETA. In this case, RBETA should decrease: a somewhat counterintuitive

result. For the purposes of this analysis, however, the rate of ABETA increase is assumed to be generally faster than the rate of TOTPOW increase. The expected trend would therefore be an increase in RBETA as anesthetic depth lightens.

The data from experiment 1 provide an excellent example of what is meant by physiological consistency. Note the trends in ABETA (Figure 4.1). Immediately following induction, ABETA decreases to a relatively constant level for the first hour, then increases slightly following the infusion rate change at the beginning of the second hour, then increases rapidly to a high level following termination of infusion. The dip in the ABETA level at $t = 7200s$ corresponds to a data smoothing artifact. The input variables EMG and TOTPOW also show the trends that would be expected (Figures 4.2 and 4.3). The model output also corresponds to what would be intuitively expected (Figure 4.4). Note that the values for model output appear to be two parallel lines after $t = 3600s$. Although the plot may appear to be line plot, it is actually a scatter plot with many data points close together. Consequently, very rapid changes in model output appear to form parallel lines and are not immediately obvious as rapid discontinuities.

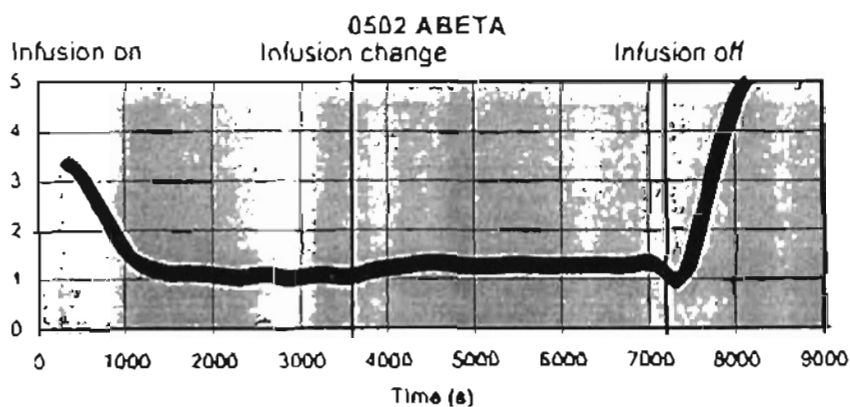


Figure 4.1: Dimensionless absolute power in Beta frequency band (Experiment 1).

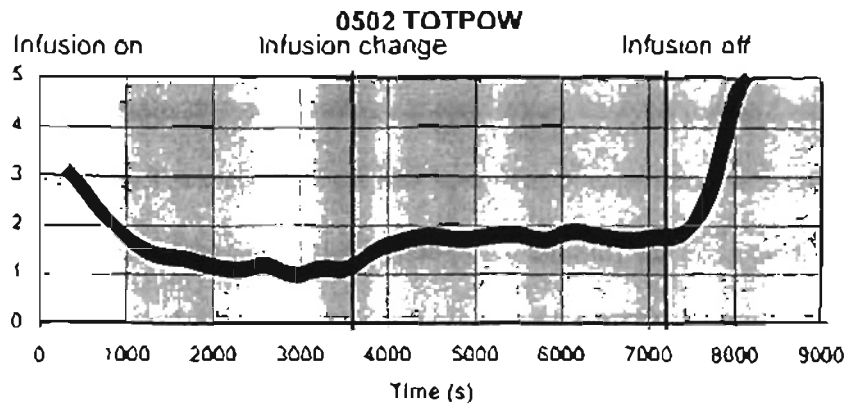


Figure 4.2: Dimensionless total absolute power in 0-30Hz frequency band (Experiment 1).

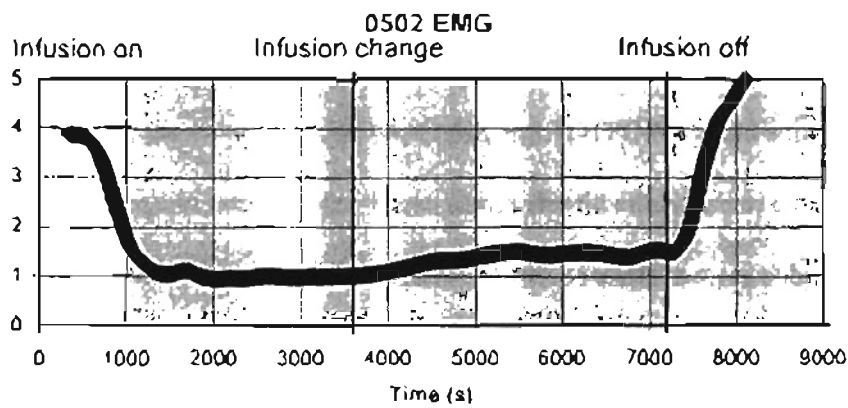


Figure 4.3: Dimensionless absolute power in EMG low frequency band (Experiment 1).

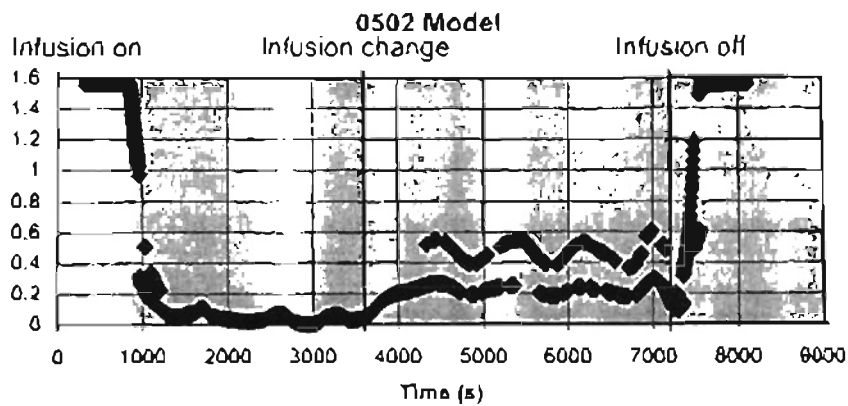


Figure 4.4: Model output (Experiment 1).

4.1.1 Initial Six Experiments

Results of the physiological consistency analysis for the first six experiments are presented in Table 4.1. For the first hour of each experiment when propofol was administered at the high infusion rate (1 ml/kg/min), the expected trend would be either a low level or a decrease to a low level in each of ABETA, EMG, TOTPOW, and RBETA measurements. As a reflection of its input, the model output should also show either a low level or a decrease to a low level during the first hour. All six experiments yielded this trend as expected.

For the second hour of each experiment at half the original infusion rate (0.5 ml/kg/min), the values of ABETA, EMG, and TOTPOW should show an increase shortly after the infusion rate change. These values should either rise to a plateau or increase as the experiment proceeds. Interpretation of these results is more subjective, however. While subject to the lower infusion rate, the patients are more likely to show responses to external stimuli such as the application of tail clamps. The consequence is that a clean, monotonic trend in one of the input variables or the model output is not likely to be evident. Local minima, maxima, and other oscillatory behavior with periodicity corresponding to tail clamp application was evident. Nonetheless, consistency was observed.

Trends in ABETA were consistent for 3 of the 6 experiments, trends in EMG were consistent for 6 of the 6 experiments, and trends in TOTPOW were consistent for 5 of the 6 experiments. The model yielded consistent trends for 4 of the 6 experiments. What intuitively appears to be contrary behavior of RBETA is not (Figure 4.5). What has been observed with RBETA is a slight decrease or maintenance of a relatively constant level during the second hour of the experiment. Therefore either TOTPOW increases slightly

TABLE 4.1 Physiological consistency of model input and output variables for initial experiments.

	High Infusion Rate $0 < t < 1$ hr	Low Infusion Rate $1 \text{ hr} < t < 2$ hr	Infusion Pump Off $2 \text{ hr} < t$
Expected Trends ABETA, EMG, TOTPOW, MODEL	Low level or decrease to constant low level	Increase shortly after 2 hr mark to higher level, or continuous increase to 2 hr mark.	Increase to constant high level
Consistency with expected trends			
	High Infusion Rate $0 < t < 1$ hr	Low Infusion Rate $1 \text{ hr} < t < 2$ hr	Infusion Pump Off $2 \text{ hr} < t$
Experiment 1			
ABETA	Yes	Yes	Yes
EMG	Yes	Yes	Yes
TOTPOW	Yes	Yes	Yes
MODEL	Yes	Yes	Yes
Experiment 2			
ABETA	Yes	Yes	No
EMG	Yes	Yes	No
TOTPOW	Yes	Yes	No
MODEL	Yes	Yes	Yes
Experiment 3			
ABETA	Yes	No	No
EMG	Yes	Yes	No
TOTPOW	Yes	Yes	No
MODEL	Yes	Yes	Yes
Experiment 4			
ABETA	Yes	No	Yes
EMG	Yes	Yes (to $t = 1.9$ hr)	Inconclusive
TOTPOW	Yes	Yes (Oscillatory)	Yes
MODEL	Yes	No	Yes
Experiment 5			
ABETA	Yes	No	Inconclusive
EMG	Yes	Yes	Yes
TOTPOW	Yes	No	Inconclusive
MODEL	Yes	No	Yes
Experiment 6			
ABETA	Yes	Yes	Yes
EMG	Yes	Yes	Yes
TOTPOW	Yes	Yes	Yes
MODEL	Yes	Yes	Yes

faster than ABETA or ABETA and TOTPOW increase at the same rate. This is not in opposition to what would be expected physiologically.

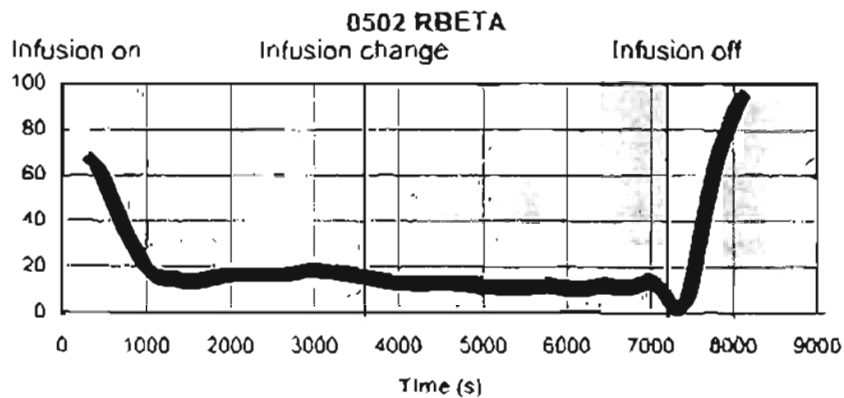


Figure 4.5 Relative power in Beta frequency band (Experiment 1).

When the infusion pump is turned off, the input variables and the model output should increase to a relatively high level, perhaps to the highest levels observed. The relatively short duration of this period makes trend analysis somewhat speculative, however. For experiments 2 and 3 (Figures 4.6 - 4.8, 4.10 - 4.11) during this non-infusion period after $t = 7200$ s. most of the input variables are physiologically inconsistent, but consistent model output values are obtained for the duration of this period (Figures 4.9 and 4.12). This phenomenon is possibly attributable to the inclusion of rules in the rulebase which address rates of change of EMG and ABETA. A more likely explanation is that the magnitudes of ABETA and RBETA were sufficiently great to counteract the decrease.

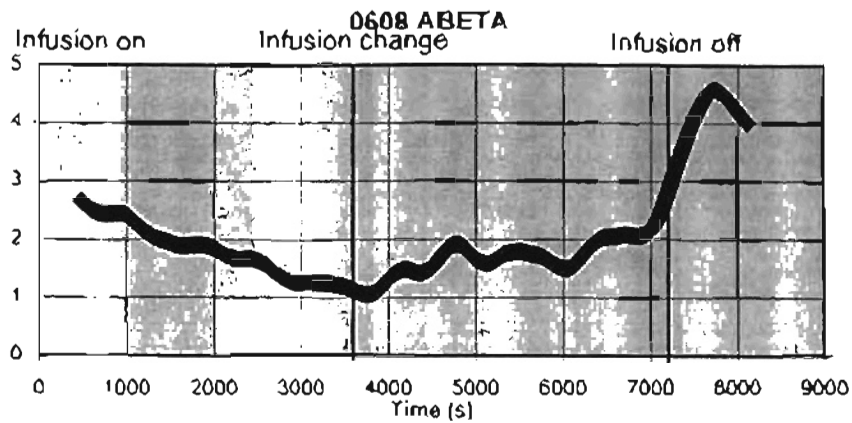


Figure 4.6 Dimensionless absolute power in Beta frequency band (Experiment 2).

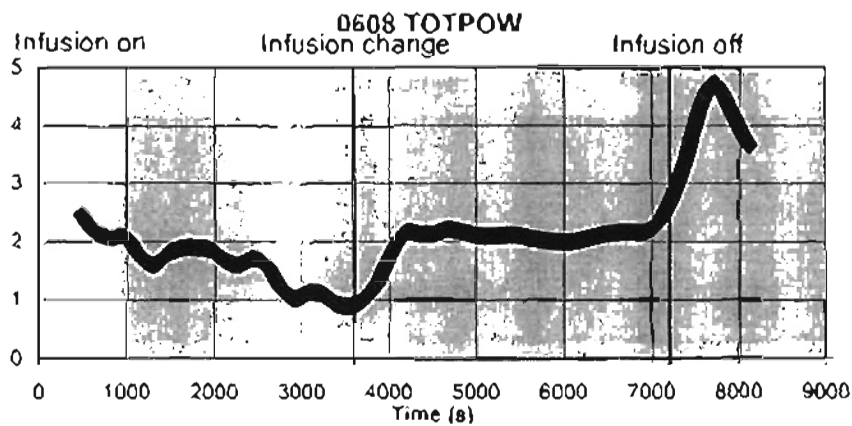


Figure 4.7 Dimensionless total absolute power in 0-30Hz frequency band (Experiment 2).

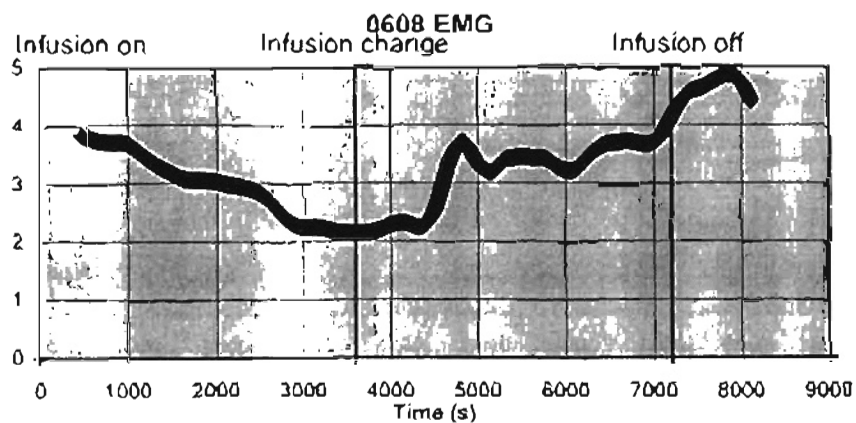


Figure 4.8 Dimensionless absolute power in EMG low frequency band (Experiment 2).

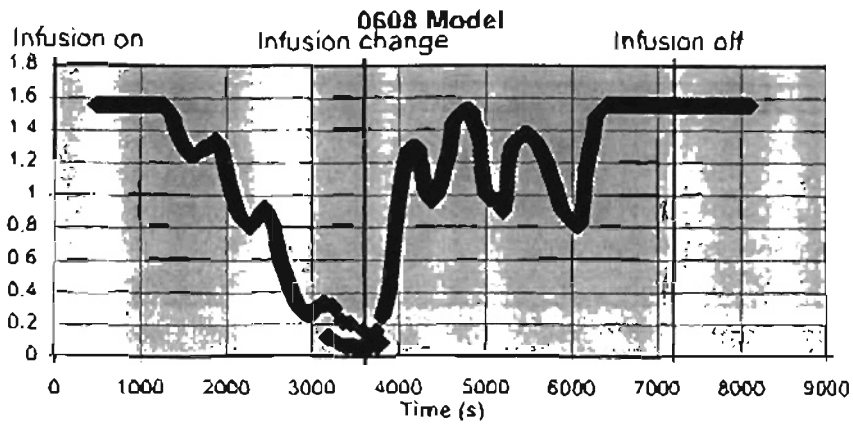


Figure 4.9 Model output (Experiment 2)

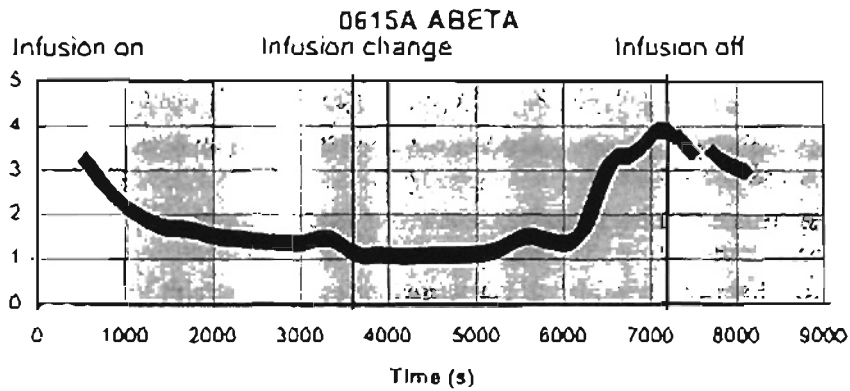


Figure 4.10 Dimensionless absolute power in Beta frequency band (Experiment 3).

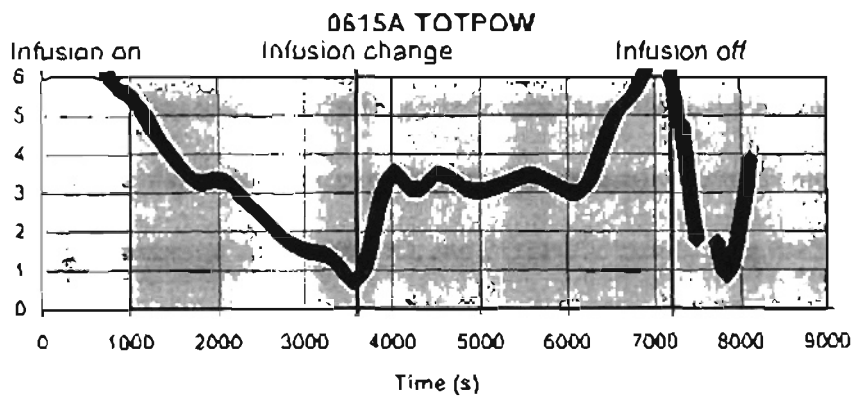


Figure 4.11 Dimensionless total absolute power in 0-30Hz frequency band (Experiment 3).

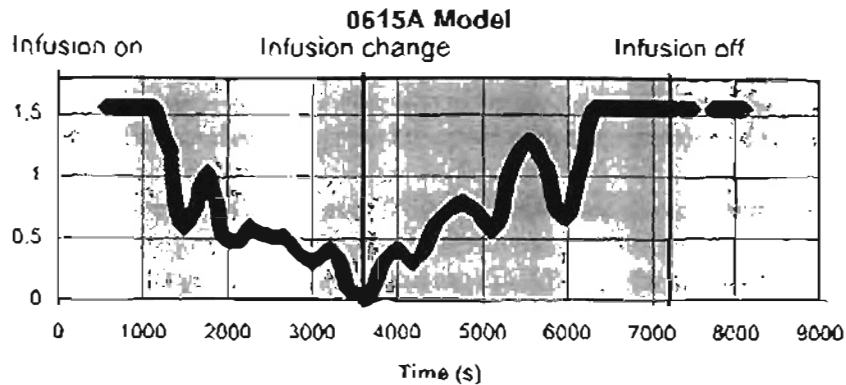


Figure 4.12 Model output (Experiment 3)

4.1.2 Verification Experiments

To validate the model constructed using the data collected during the first six experiments, six more experiments were conducted using the same experimental protocol. The results of this series of experiments did not show the same degree of physiological consistency. A summary of these results is presented in Table 4.2. In general, the input variables were consistent for the first hour of each experiment, but model output values oscillated for the first 40 minutes of each experiment, providing no proof of agreement with expected trends.

For the second hour during administration of the lower infusion rate, the input variables for the verification experiments were generally contradictory. Experiment 7 yielded increases of ABETA, EMG, and TOTPOW shortly after the 3600 s mark as expected, but all three variables dropped off after the 6000 s mark contrary to expectation. Experiment 8 showed physiologically consistent EMG trends, but also showed a decrease in ABETA after 3600s and a decrease in TOTPOW after 6000 s. Values of ABETA and

TOTPOW for experiment 9 showed no obvious consistent trend between 3600 s and 7200s. The EMG values might be considered to follow the expected trend, but the magnitude of the post-infusion-change increase coupled with the existence of two relative maxima within the interval between 3600s and 7200s makes the assessment of consistency speculative. Experiment 10 yields a general decrease in ABETA for the interval between 3600s and 7200s and TOTPOW decreases in the interval from 5400s to 7200s; both results are thoroughly inconsistent with the expected result. For experiment 11, ABETA essentially hovers around a constant value as do ABETA and EMG for experiment 12. The model output for verification experiments 1, 2, and 5 do seem to be physiologically consistent, however.

Results for the infusion-off period ($t > 7200s$) for each verification experiment showed that, in general, if the inputs were inconsistent, the outputs were inconsistent. Verification experiments 1, 4, and 6 were inconsistent in all input and output variables while the remaining experiments were generally consistent.

TABLE 4.2 Physiological consistency of model input and output variables for verification experiments.

	High Infusion Rate $0 < t < 1$ hr	Low Infusion Rate $1 \text{ hr} < t < 2$ hr	Infusion Pump Off $2 \text{ hr} < t$
Expected Trends ABETA, EMG, TOTPOW, MODEL	Low level or decrease to constant low level	Increase shortly after 2 hr mark to higher level, or continuous increase to 2 hr mark.	Increase to constant high level
Consistency with expected trends			
	High Infusion Rate $0 < t < 1$ hr	Low Infusion Rate $1 \text{ hr} < t < 2$ hr	Infusion Pump Off $2 \text{ hr} < t$
Experiment 7			
ABETA	Yes	No	No
EMG	Yes	No	No
TOTPOW	Yes	No	No
MODEL	No	Yes	No
Experiment 8			
ABETA	Yes (after 0.25 hr)	No	Yes
EMG	Yes	Yes	Yes
TOTPOW	Yes (after 0.25 hr)	No	Inconclusive
MODEL	No	Yes	Yes
Experiment 9			
ABETA	Yes (after 0.25 hr)	No	Yes
EMG	Yes (after 0.25 hr)	No	Yes
TOTPOW	No	No	Yes
MODEL	No	No	Yes
Experiment 10			
ABETA	Yes	No	No
EMG	Yes	Yes	No
TOTPOW	No	No	No
RBETA	Yes	No	No
MODEL	No	No	No
Experiment 11			
ABETA	Yes (after 0.4 hr)	No	Yes
EMG	Yes	Yes	Yes
TOTPOW	Yes (after 0.4 hr)	Yes	No
MODEL	No	Yes	Yes
Experiment 12			
ABETA	Yes (after 0.4 hr)	No	No
EMG	Yes	No	No
TOTPOW	Yes (after 0.4 hr)	Yes	No
MODEL	No	No	No

4.2 ANALYSIS FROM CLINICAL ASSESSMENT

The limitation of the preceding method of analysis is that it is based on physiological principles alone. Comparisons of the model with the assessments rendered by our anesthesiologist provide a more detailed and meaningful method of analysis by noting subtle patient-specific and experiment-specific responses to anesthesia. In this light, the model can be viewed as a sort of non-linear function approximator with the anesthesiologist assessment of anesthetic depth as the function being approximated. The clinical assessments were originally scaled between “1” (indicating deep anesthesia) and “5” (indicating awake). These values were rescaled linearly to correspond to maximum and minimum values that would result from the model. The span of model output ranges from 0 to 1.56. The rescaling methodology used transformed an assessment of “1” to 0 and an assessment of “4” to 1.56 (the assignment of an assessment of “5” was rare). After the transformation, the model output can be compared directly to the anesthesiologist-determined clinical assessment.

The vectors of model output values and clinical assessments were of different dimensions. To make direct comparisons, the number of model output values was reduced to the number of clinical assessments by parametrically matching clinical assessment values with model output values obtained at the same time or as close to the same time as possible. The model output values were determined for a time interval of 5 seconds and the clinical assessments were determined every 5 minutes. The uncertainty introduced by comparing a clinical assessment with a model output value not exactly concurrent would therefore be negligible, especially considering that each clinical assessment would take at least 15 to 30 seconds to determine. Each experiment was analyzed by time interval according to infusion pump rate. The number and percentage of model output values

within three possible clinical assessment uncertainties were determined and are presented in Tables 4.13 through 4.16.

The input variables and model output for each of the experiments will be analyzed experiment by experiment in the sections that follow. Observations regarding both adherence to physiological consistency and correspondence to the veterinarian clinical assessment will be discussed.

4.2.1 Initial Six Experiments

The six experiments which are described in the following sections were the experiments used for model development. These experiments used mixed-breed dogs as subjects.

4.2.1.1 Experiment 1

The deviations between the clinical assessment and the model are generally small for experiment 1 (Table 4.3). In Table 4.3 and subsequent similar tables, the spread of data is presented as the number and percentage of data points from the infusion period designated in the leftmost column within the specified rescaled clinical assessment uncertainty in the top row. The column headed by “n” represents the total number of data points from the specified infusion period. For example, the values in the “Low Infusion Rate” row of Table 4.3 should be read as follows: 8 of 11 data points are within ± 0.26 clinical assessment units of the actual clinical assessment, 11 of 12 data points are within ± 0.52 clinical assessment units, and 12 of 12 are within ± 0.78 clinical assessment units.

Two deviations of significant magnitude occur at the beginning of the experiment until $t = 1000s$ and shortly after the cessation of infusion at $t = 7200s$ (Figures 4.13, 4.15). At the beginning of the experiment, the veterinarian immediately assessed the subject as

being deeply anesthetized while the model suggested light anesthesia for the first 15 minutes followed by a five-minute decrease to a level indicative of deep anesthesia (Figure 4.14). The second significant deviation occurring between $t = 7200s$ (termination of infusion) and $t = 8100s$ is the result of the model determining a rate of anesthetic lightening greater than that determined by the anesthesiologist. The greater rate indicated by the model is likely due to the increased rates of change of ABETA and EMG during this interval (Figures 4.16, 4.17).

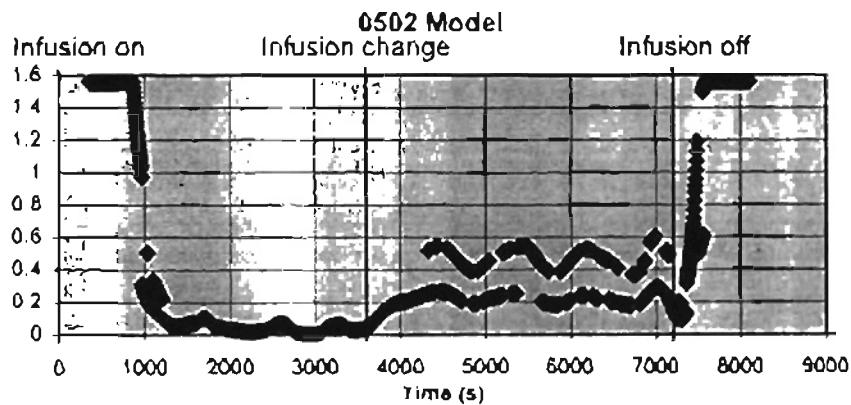


Figure 4.13 Model output (Experiment 1).

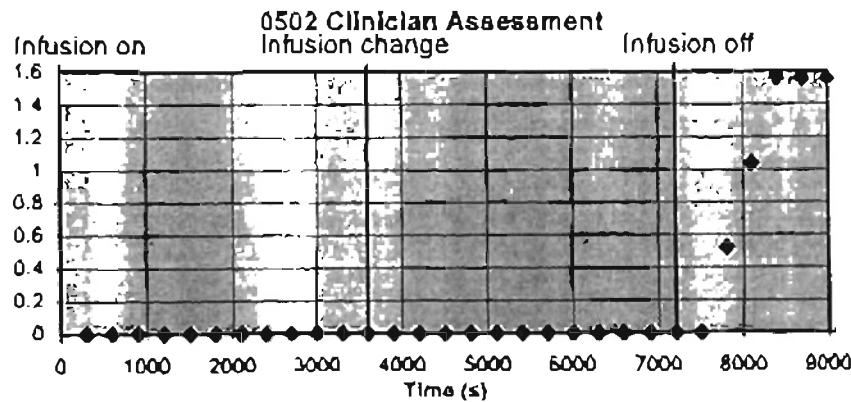


Figure 4.14 Rescaled clinical assessment (Experiment 1).

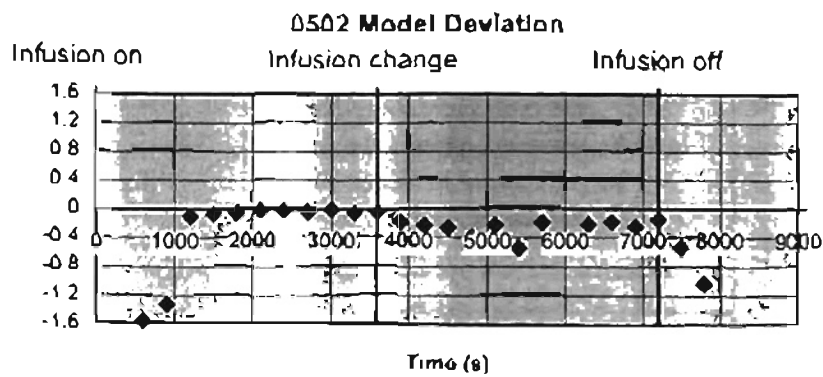


Figure 4.15 Model deviation from clinical assessment (Experiment 1).
Deviation = clinical assessment - model

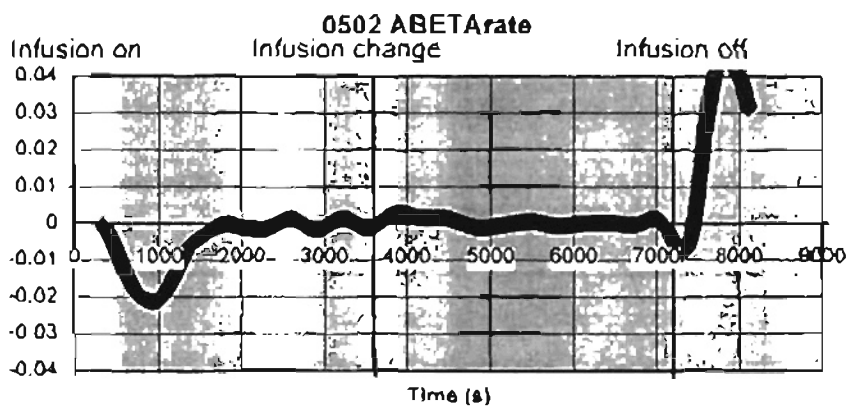


Figure 4.16 Rate of change in absolute beta power over five minutes: Experiment 1 (dB/s)

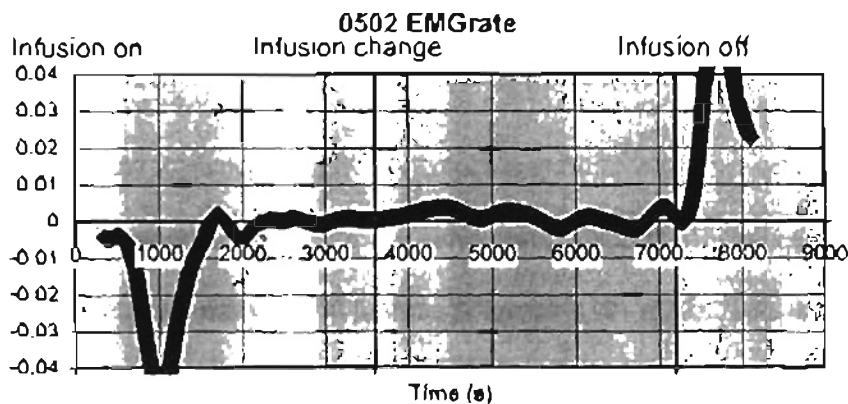


Figure 4.17 Rate of change in absolute EMG power over five minutes: Experiment 1 (dB/s)

TABLE 4.3 Comparison of model with overall clinical assessment for experiment 1. Uncertainty expressed in rescaled clinical assessment units.

	Trend agreement (Yes / No) and number and percentage of data within specified uncertainty of rescaled clinical assessment					Description of deviations
	Trend	Uncertainty				
		\pm 0.26	\pm 0.52	\pm 0.78	n	
Experiment 1						
High Infusion Rate 0 < t < 1 hr	Yes	9 82%	9 82%	9 82%	11	Model values greater for first 0.25 hr.
Low Infusion Rate 1 hr < t < 2 hr	Yes	8 67%	11 92%	12 100%	12	Oscillations may correspond to tail-clamp events.
Infusion Pump Off 2 hr < t	Yes	0 0%	0 0%	1 33%	3	Rate of increase to maximum value greater for model

In Figure 4.4, experiment 1 model output, the model shifts back and forth rapidly between two levels during the low infusion rate hour, resulting in what appears to be two parallel levels. This phenomenon is actually due to discontinuities caused by rapid rule-shifting within the fuzzy rulebase.

4.2.1.2 Experiment 2

The model showed a much slower rate of anesthetic deepening than the clinical assessment for the first 45-50 minutes (Figures 4.18 - 4.20). This is attributable to a relatively slow rate of decrease in ABETA, EMG, and TOTPOW (Figures 4.21-4.23). The second hour at the lower infusion rate shows some oscillation in the model, but this is likely due to tail clamping episodes. The model deviates from the clinical assessment 45 minutes into the second hour, increasing to its highest levels before cessation of infusion

and 15 minutes prior to the clinical assessment at the higher levels (rescaled clinical assessment values greater than or equal to 1.6). This phenomenon is attributable to the rate of increase in EMG and ABETA (Figures 4.24 and 4.25).

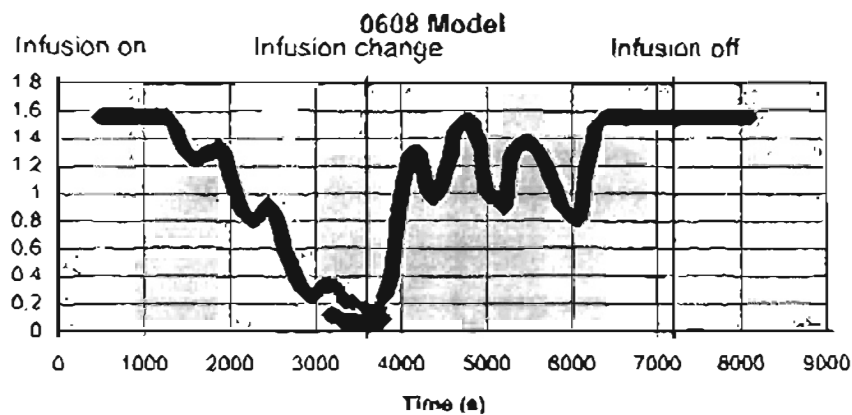


Figure 4.18: Model output (Experiment 2).

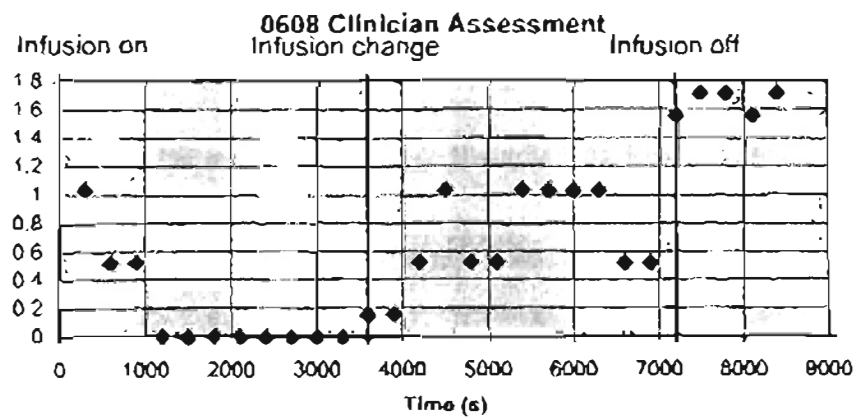


Figure 4.19: Rescaled clinical assessment (Experiment 2).

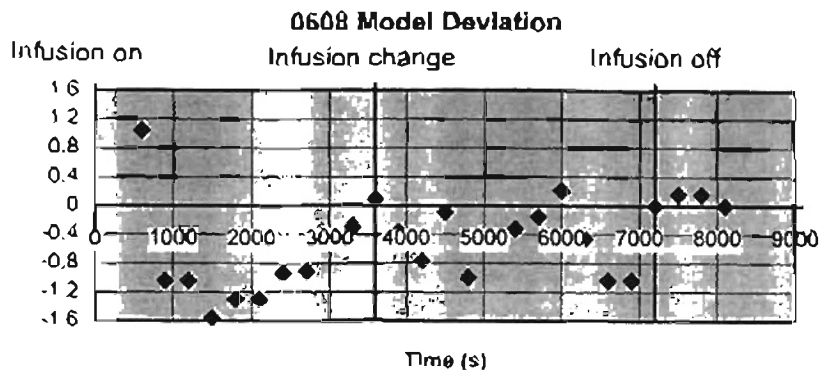


Figure 4.20: Model deviation from clinical assessment (Experiment 2).
Deviation = clinical assessment - model

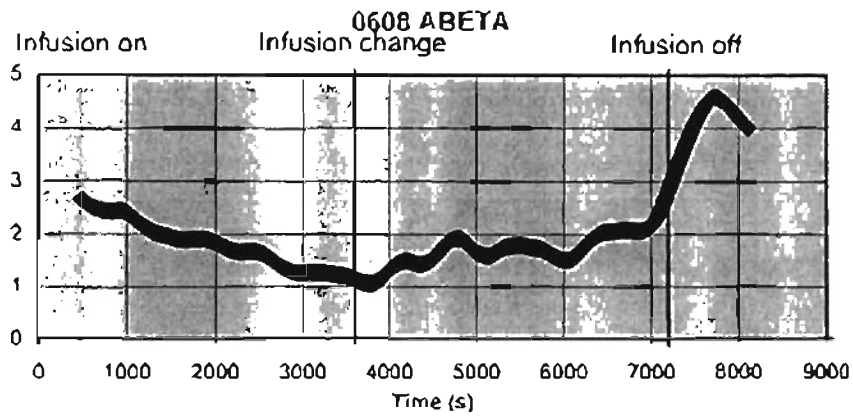


Figure 4.21: Dimensionless absolute power in Beta frequency band (Experiment 2).

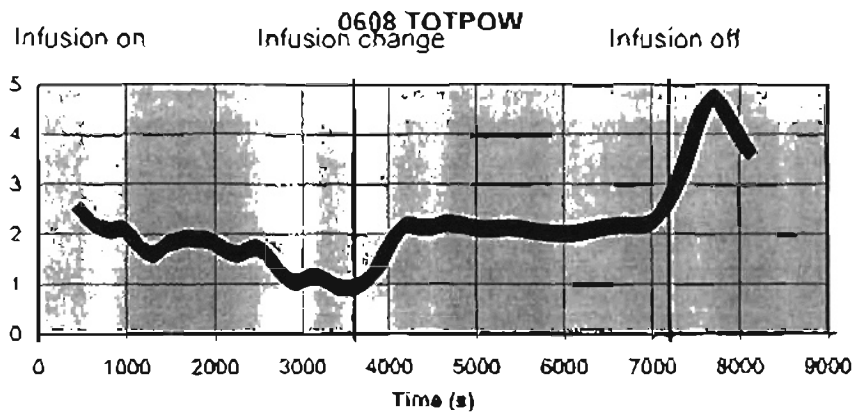


Figure 4.22: Dimensionless total absolute power in 0-30Hz frequency band (Experiment 2).

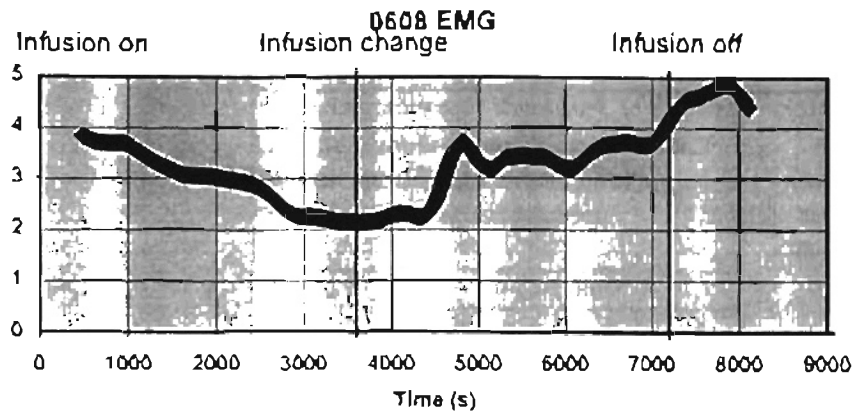


Figure 4.23: Dimensionless absolute power in EMG low frequency band (Experiment 2).

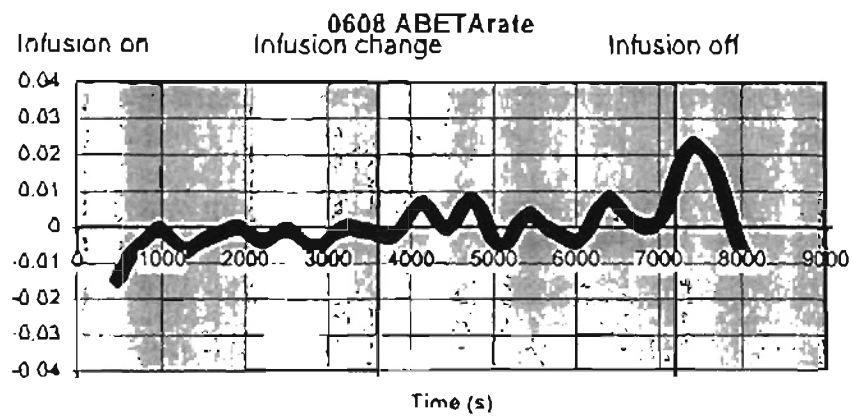


Figure 4.24: Rate of change in absolute beta power over five minutes: Experiment 2. (dB/s)

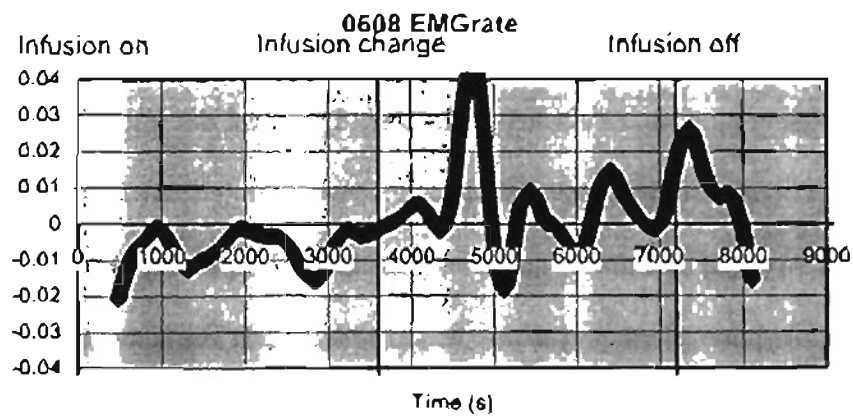


Figure 4.25: Rate of change in absolute EMG power over five minutes: Experiment 2. (dB/s)

TABLE 4.4 Comparison of model with overall clinical assessment for experiment 2. Uncertainty expressed in rescaled clinical assessment units.

	Trend agreement (Yes / No) and number and percentage of data within specified uncertainty of rescaled clinical assessment					Description of deviations
	Trend	Uncertainty				
		\pm 0.26	\pm 0.52	\pm 0.78	n	
Experiment 2						
High Infusion Rate $0 < t < 1$ hr	Yes	1 9%	3 27%	3 27%	11	Model values greater for first 0.8 hr. Model requires 0.5 hr longer to record lowest levels
Low Infusion Rate $1 \text{ hr} < t < 2$ hr	Yes	4 33%	8 67%	9 75%	12	Oscillations may correspond to tail-clamp events.
Infusion Pump Off $2 \text{ hr} < t$	Yes	4 100%	4 100%	4 100%	4	

4.2.1.3 Experiment 3

Deviation is significant for the first 20 minutes of experiment 3 (Figures 4.26 - 4.28). The rate of anesthetic deepening suggested by the model is slower than that observed by the anesthesiologist. This is attributable to a slow rate of decrease in TOTPOW for this interval (Figure 4.29). For the second hour at the lower infusion rate the model and the clinical assessment compare favorably (Table 4.5). Although data are incomplete for the period following cessation of infusion, figures 4.26 and 4.27 suggest that the model and clinical assessment would compare favorably for this interval as well.

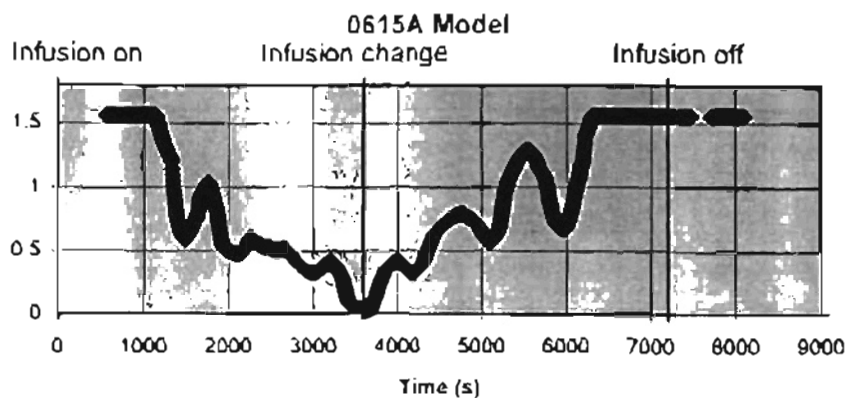


Figure 4.26: Model output (Experiment 3).

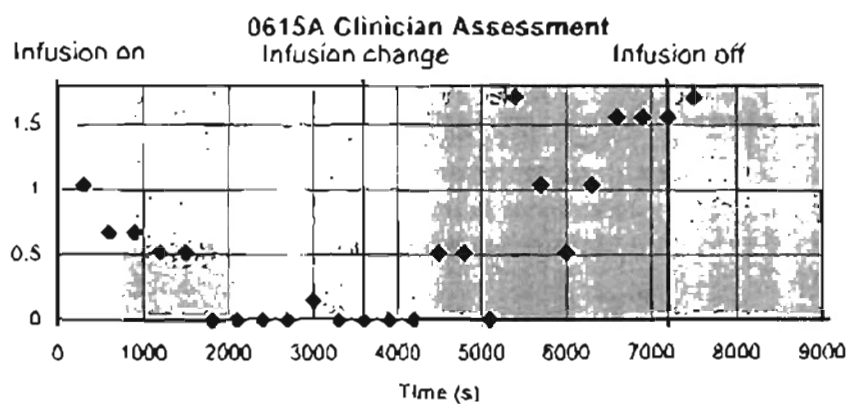


Figure 4.27: Rescaled clinical assessment (Experiment 3).

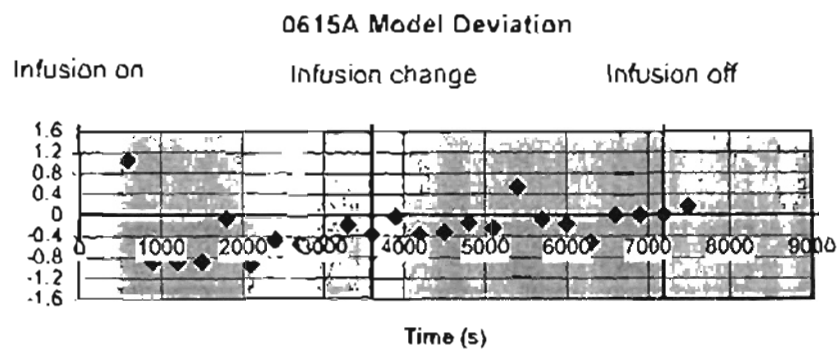


Figure 4.28: Model deviation from clinical assessment (Experiment 3).
Deviation = clinical assessment - model

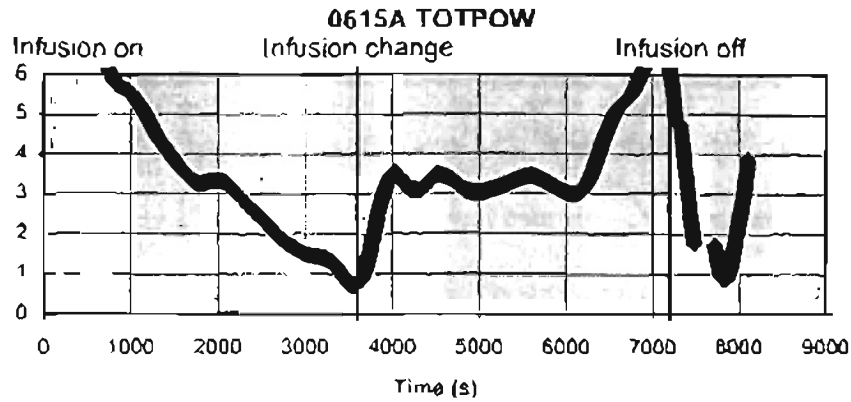


Figure 4.29: Dimensionless total absolute power in 0-30Hz frequency band (Experiment 3).

TABLE 4.5 Comparison of model with overall clinical assessment for experiment 3.
Uncertainty expressed in rescaled clinical assessment units.

	Trend agreement (Yes / No) and number and percentage of data within specified uncertainty of rescaled clinical assessment					Description of deviations
	Trend	Uncertainty				
		\pm 0.26	\pm 0.52	\pm 0.78	n	
Experiment 3						
High Infusion Rate $0 < t < 1$ hr	Yes	2 18%	5 45%	6 55%	11	Model values greater for first 0.3 hr. Model requires 0.5 hr longer to record lowest levels
Low Infusion Rate $1 \text{ hr} < t < 2$ hr	Yes	8 67%	10 83%	12 100%	12	Oscillations may correspond to tail-clamp events.
Infusion Pump Off $2 \text{ hr} < t$	N/A	1 100%	1 100%	1 100%	1	

4.2.1.4 Experiment 4

The model and clinical assessment compare favorably for most of the data from experiment 4 (Figures 4.30-4.32, Table 4.6). A significant deviation occurs at approximately 20 minutes into the second hour (low infusion rate). This deviation is due to a corresponding decrease in TOTPOW (Figure 4.33), causing a dip in the model output suggesting an overprediction of anesthetic depth. The experiment was terminated shortly after infusion was stopped.

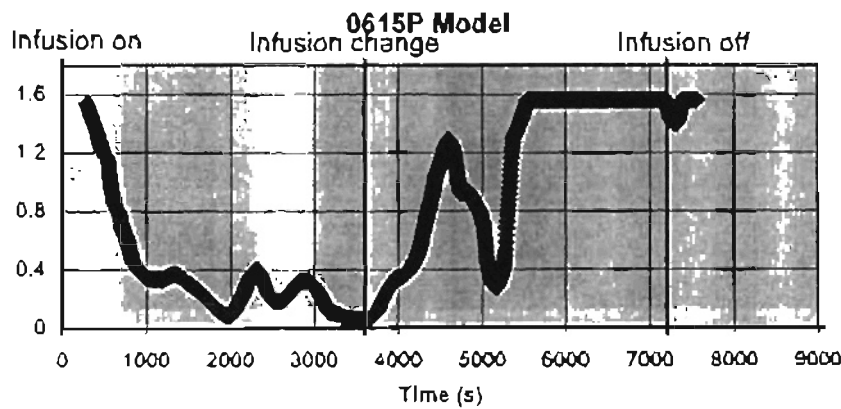


Figure 4.30: Model output (Experiment 4).

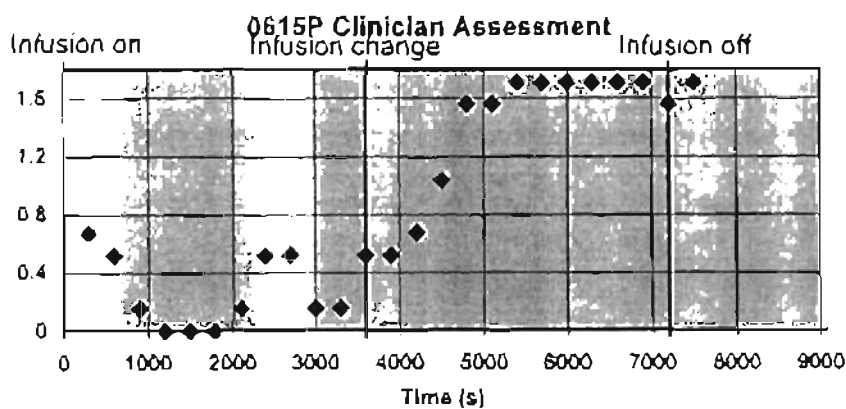


Figure 4.31: Rescaled clinical assessment (Experiment 4).

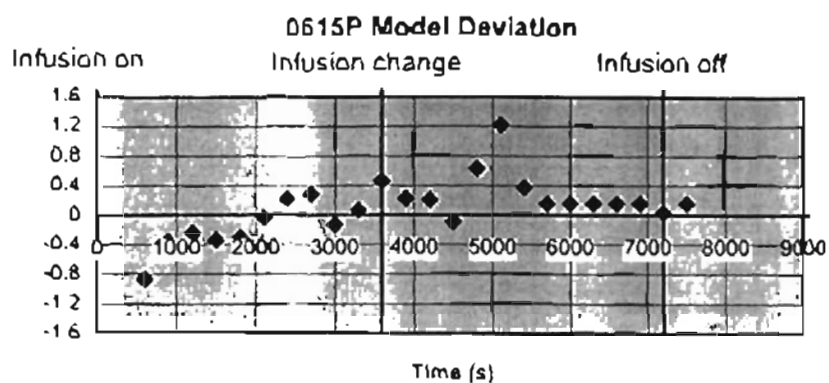


Figure 4.32: Model deviation from clinical assessment (Experiment 4).

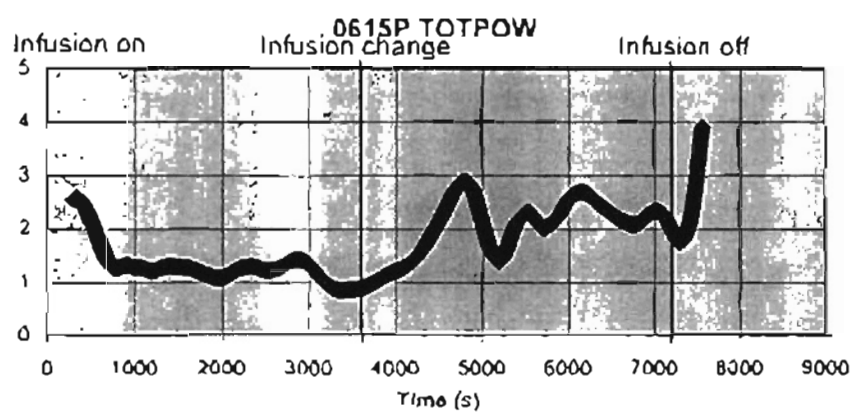


Figure 4.33: Dimensionless total absolute power in 0-30Hz frequency band (Experiment 4)

TABLE 4.6 Comparison of model with overall clinical assessment for experiment 4. Uncertainty expressed in rescaled clinical assessment units.

	Trend agreement (Yes / No) and number and percentage of data within specified uncertainty of rescaled clinical assessment					Description of deviations
	Trend	Uncertainty				
		\pm 0.26	\pm 0.52	\pm 0.78	n	
Experiment 4						
High Infusion Rate 0 < t < 1 hr	Yes	5 45%	10 91%	10 91%	11	
Low Infusion Rate 1 hr < t < 2 hr	Yes	9 75%	10 83%	11 92%	12	
Infusion Pump Off 2 hr < t	N/A	1 100%	1 100%	1 100%	1	

4.2.1.5 Experiment 5

The clinical assessment and model output for experiment 5 do not compare quite as favorably as for some of the other experiments (Figures 4.34-4.36, Table 4.7). This experiment is unique among the first six experiments in that the anesthesiologist did not span the clinical assessment range of “1” to “4” (0 to 1.6 rescaled), but instead only spanned “1” to “3”. (0 to 1.07 rescaled). The patient was obviously not as responsive to stimuli. This was reflected in the EEG input as well, however. The inputs, ABETA and EMG did not show much variation as a function of time (Figures 4.37 and 4.38). Also, ABETA and TOTPOW appeared to be inconsistent 40 minutes after the infusion rate change (Figures 4.37 and 4.39).

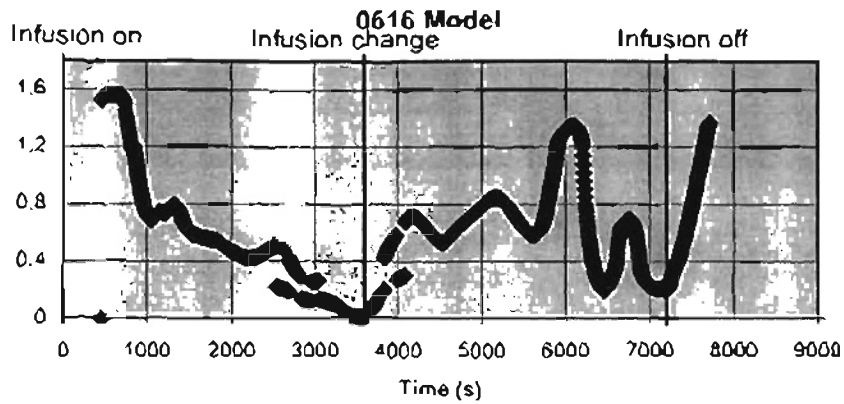


Figure 4.34: Model output (Experiment 5)

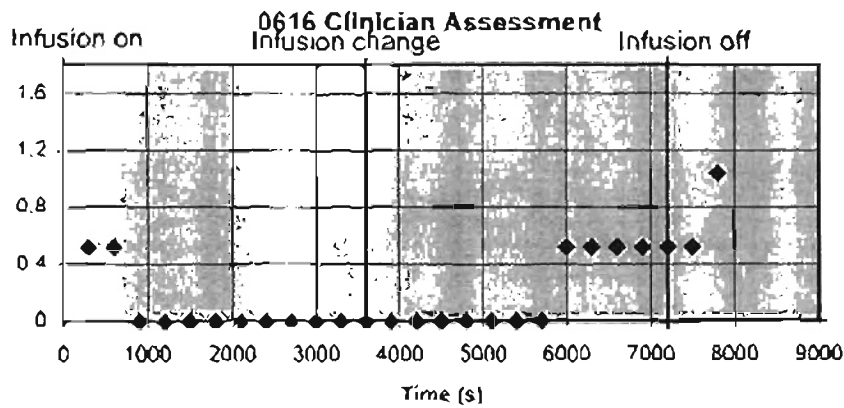


Figure 4.35: Rescaled clinical assessment (Experiment 5).

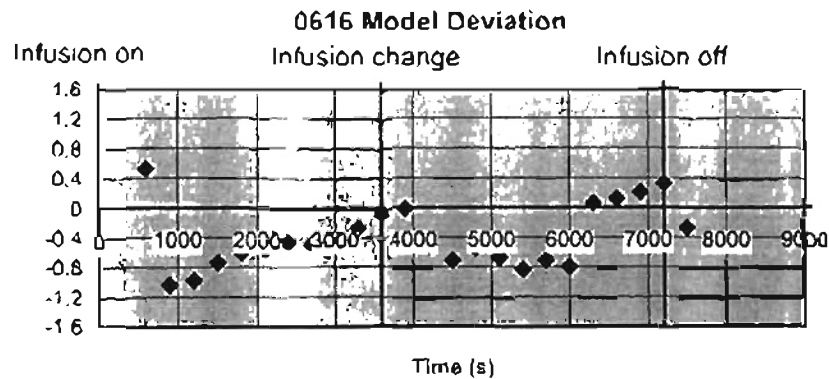


Figure 4.36: Model deviation from clinical assessment (Experiment 5).

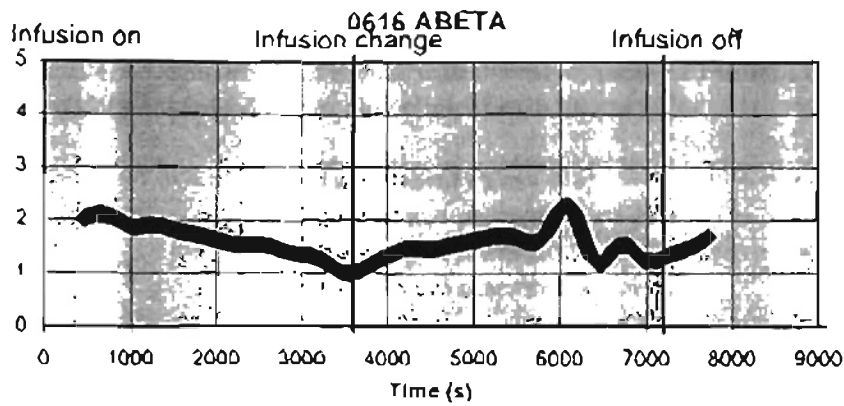


Figure 4.37: Dimensionless absolute power in Beta frequency band (Experiment 5).

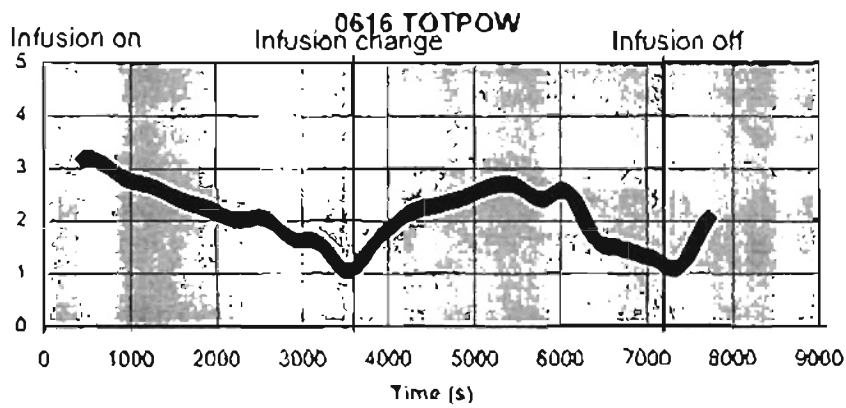


Figure 4.38: Dimensionless total absolute power in 0-30Hz frequency band (Experiment 5).

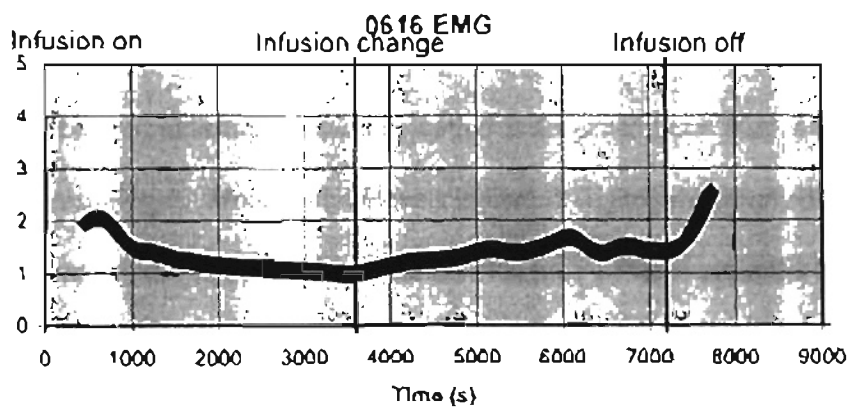


Figure 4.39: Dimensionless absolute power in EMG low frequency band (Experiment 5).

TABLE 4.7 Comparison of model with overall clinical assessment for experiment 5. Uncertainty expressed in rescaled clinical assessment units.

	Trend agreement (Yes / No) and number and percentage of data within specified uncertainty of rescaled clinical assessment					Description of deviations
	Trend	Uncertainty				
		\pm 0.26	\pm 0.52	\pm 0.78	n	
Experiment 5						
High Infusion Rate 0 < t < 1 hr	Yes	2 18%	6 55%	9 82%	11	Model values greater for first 0.3 hr. Model requires 0.5 hr longer than clinician to record lowest levels
Low Infusion Rate 1 hr < t < 2 hr	Yes	4 33%	6 50%	10 83%	12	Oscillations may correspond to tail-clamp events.
Infusion Pump Off 2 hr < t	N/A	0 0%	1 100%	1 100%	1	

4.2.1.6 Experiment 6

For the first hour of experiment 6 during administration at the high infusion rate, model output indicated anesthetic depth that deepened faster than that observed by the anesthesiologist. Model output levels indicated slightly deeper anesthesia than that observed by the anesthesiologist for the first hour of the experiment (Figures 4.40 - 4.42, Table 4.8). The depth of anesthesia inferred by the model output is kept low by the substantial burst suppression in the first hour (Figure 4.43). The end of this period of burst suppression is the likely source for the five-minute period of rapid rule shifting beginning at $t = 4000$ s (Figure 4.43). The rate of anesthetic lightening during the period of low

infusion in the second hour was slower for the model than that observed by the anesthesiologist after $t = 5100$ s. The relatively slow rate of lightening is attributable to the corresponding trends evident in the inputs ABETA, TOTPOW, and EMG (Figures 4.44 - 4.46).

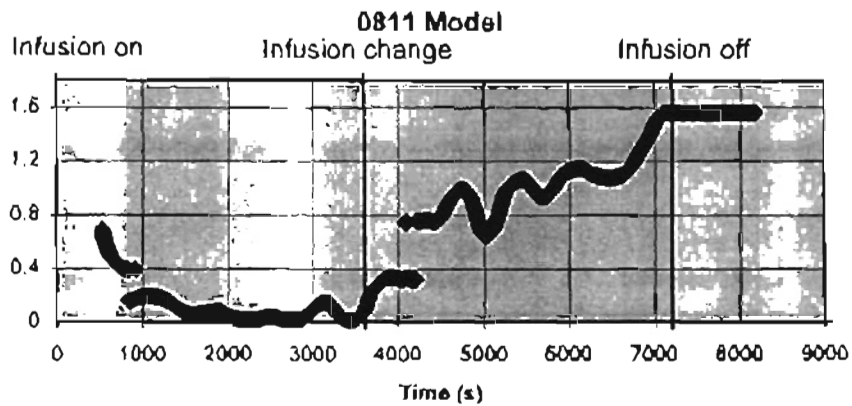


Figure 4.40: Model output (Experiment 6).

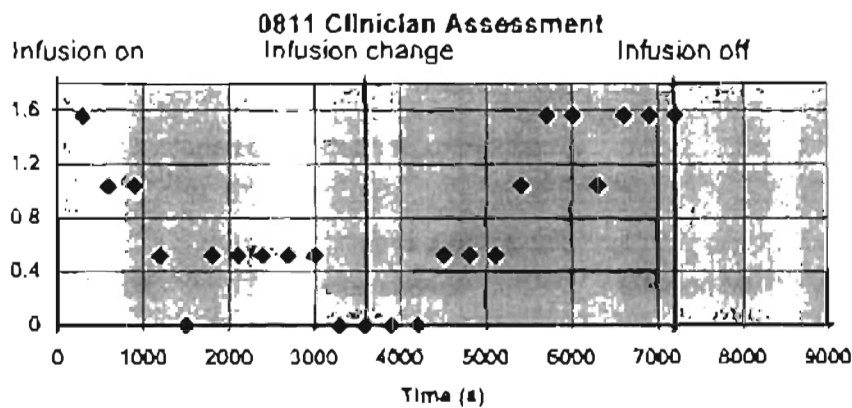


Figure 4.41: Rescaled clinical assessment (Experiment 6).

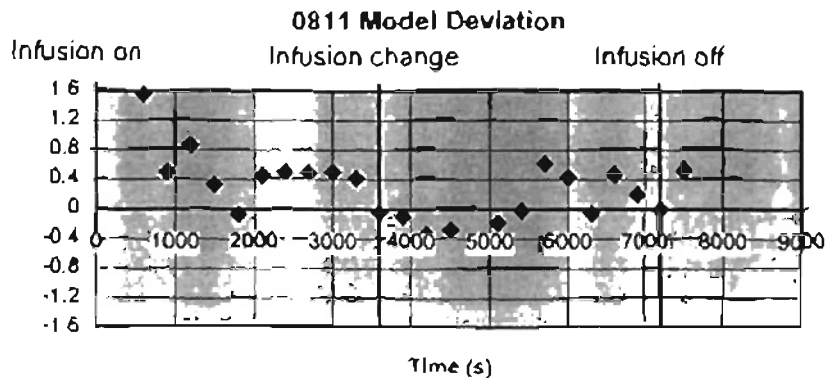


Figure 4.42: Model deviation from clinical assessment (Experiment 6).

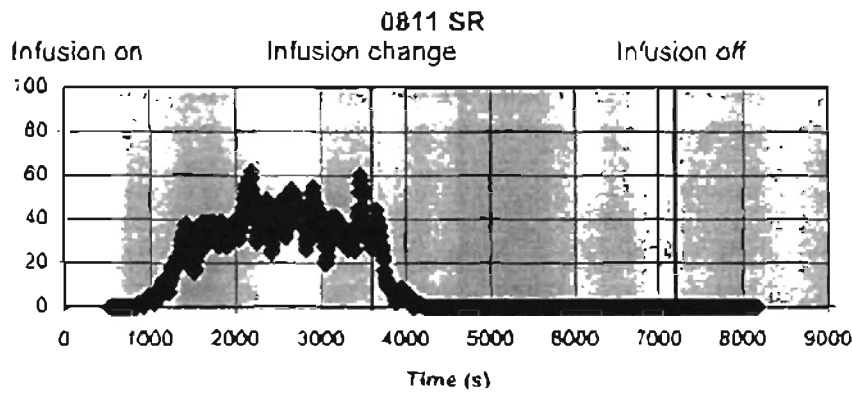


Figure 4.43: Suppression Ratio (Experiment 6).

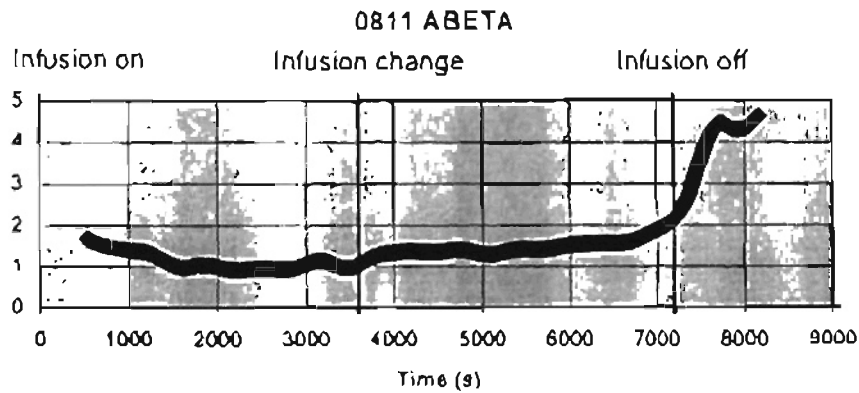


Figure 4.44: Dimensionless absolute power in Beta frequency band (Experiment 6).

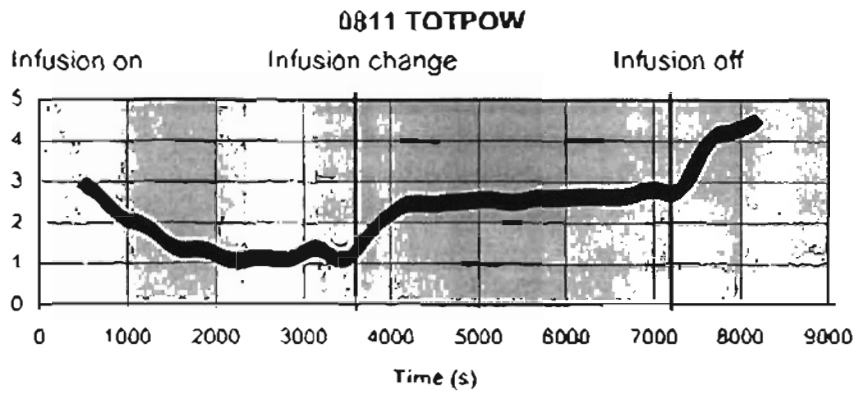


Figure 4.45: Dimensionless total absolute power in 0-30Hz frequency band (Experiment 6).

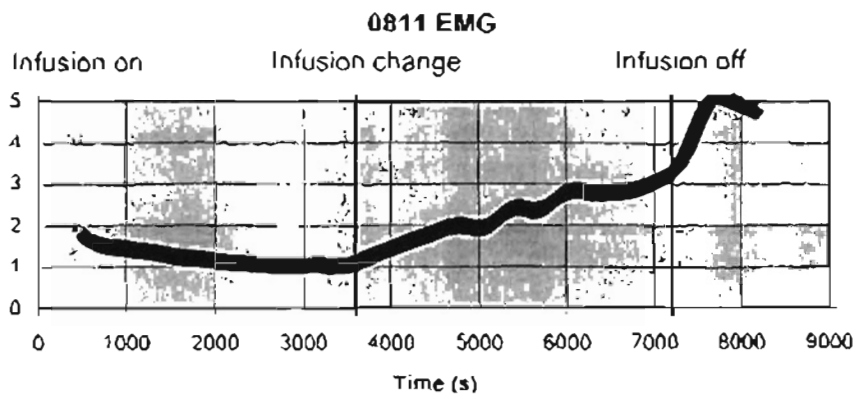


Figure 4.46: Dimensionless absolute power in EMG low frequency band (Experiment 6).

TABLE 4.8 Comparison of model with overall clinical assessment for experiment 6. Uncertainty expressed in rescaled clinical assessment units.

	Trend agreement (Yes / No) and number and percentage of data within specified uncertainty of rescaled clinical assessment					Description of deviations
	Trend	Uncertainty				
		\pm 0.26	\pm 0.52	\pm 0.78	n	
Experiment 6						
High Infusion Rate 0 < t < 1 hr	Yes	2 18%	9 82%	9 82%	11	Oscillations may correspond to tail-clamp events.
Low Infusion Rate 1 hr < t < 2 hr	Yes	6 50%	11 92%	12 100%	12	
Infusion Pump Off 2 hr < t	N/A	0 0%	2 100%	2 100%	2	

4.2.1.7 Summary of results of first six experiments

The agreement between the model and the data from the first six experiments is quite good. Although good agreement should be expected between the model and the data used to develop it, the high quality of the agreement for all six experiments was a surprise.

4.2.1 Six validation experiments

The six experiments which are described in the following sections were the experiments used for model verification. These experiments used beagles bred for laboratory use as subjects.

4.2.2.1 Experiment 7

In general, for this experiment there appears to be little correspondence between the model and the clinical assessment (Figures 4.47-4.49, Table 4.9). The model output makes some sense intuitively in that deep anesthesia is suggested for the first hour during the period of high infusion. Compared to the clinical assessment, however, correlation seems coincidental and rare. The clinical assessment is initially very deep, whereas the model is not. The times during which the deepest levels of anesthesia are observed by the anesthesiologist do not correspond to the times during which the model suggests deep anesthesia. The model suggests light anesthesia at the beginning of the experiment and deep levels 40 minutes into the hour of high infusion. After the infusion rate change, depth of anesthesia rapidly lightens according to the model. The clinical assessment is not in agreement, however. The deviation at the beginning of the experiment and shortly after the infusion rate change can be traced to the inputs ABETA, TOTPOW, and EMG (Figures 4.50-4.52). Burst suppression was evident toward the end of the first hour which accounts for the model output indicating deep anesthesia at this time (Figure 4.53). These input values show trends corresponding to similar trends in the model output. Some of these trends seem physiologically inconsistent. After infusion is ceased, ABETA, TOTPOW, and EMG decrease: contrary to what is expected. This physiological inconsistency is the likely explanation for the significant deviation between $t = 8400$ s and $t = 9000$ s.

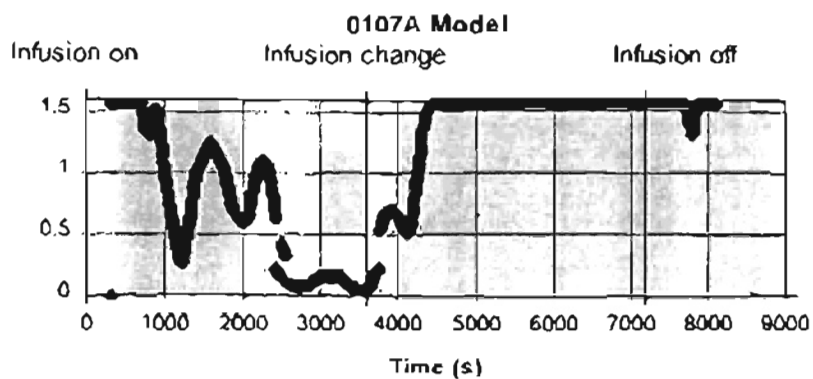


Figure 4.47: Model output (Experiment 7).

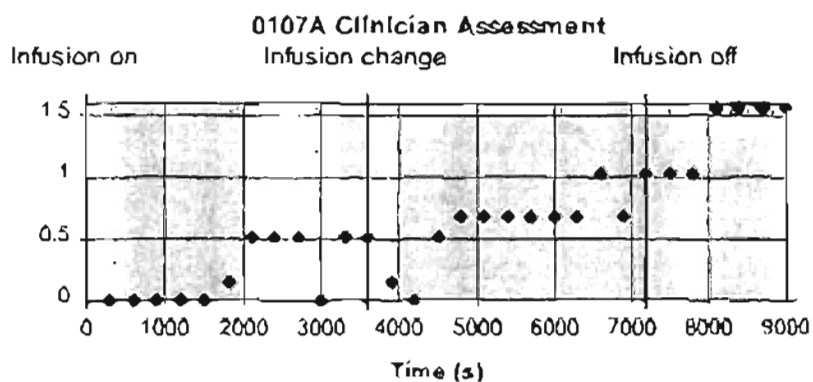


Figure 4.48: Rescaled clinical assessment (Experiment 7).

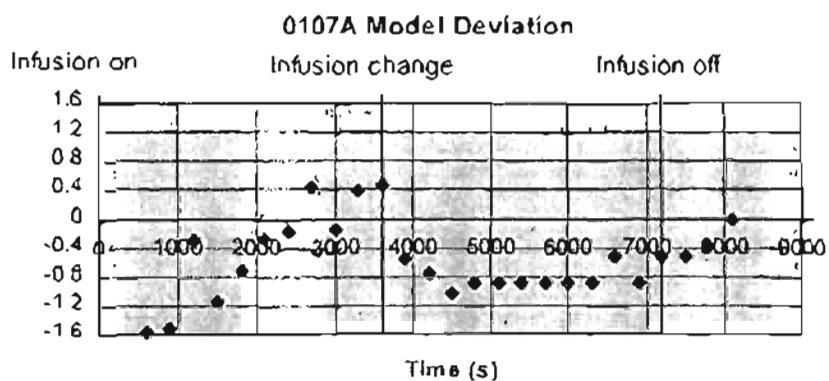


Figure 4.49: Model deviation from clinical assessment (Experiment 7).

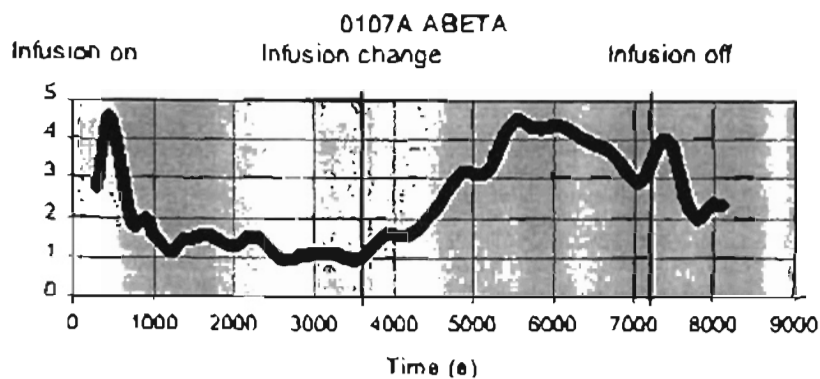


Figure 4.50: Dimensionless absolute power in Beta frequency band (Experiment 7).

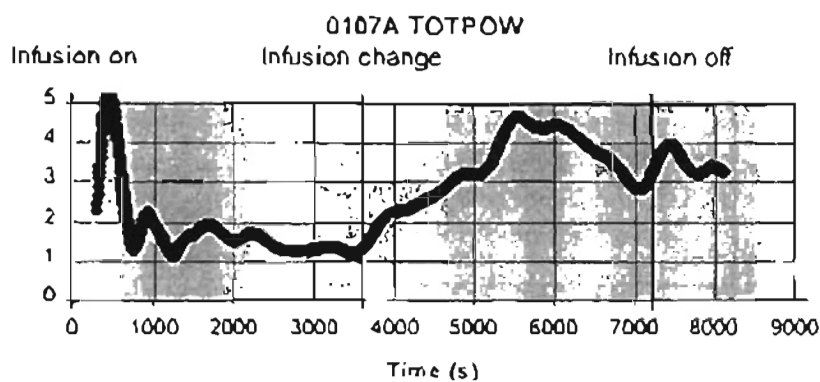


Figure 4.51: Dimensionless total absolute power in 0-30Hz frequency band (Experiment 7).

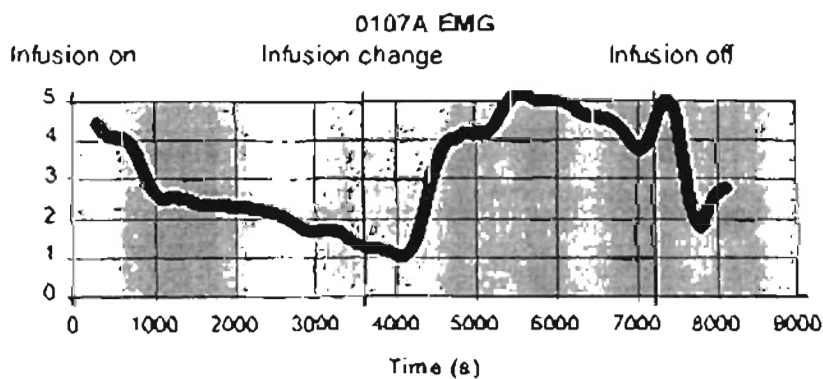


Figure 4.52: Dimensionless absolute power in EMG low frequency band (Experiment 7).

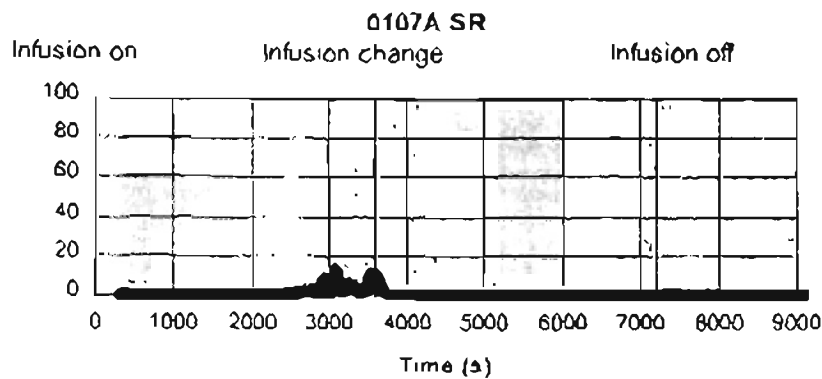


Figure 4.53: Suppression Ratio (Experiment 7).

TABLE 4.9 Comparison of model with overall clinical assessment for experiment 7.
Uncertainty expressed in rescaled clinical assessment units.

	Trend agreement (Yes / No) and number and percentage of data within specified uncertainty of rescaled clinical assessment					Description of deviations
	Trend	Uncertainty				
		\pm 0.26	\pm 0.52	\pm 0.78	n	
Experiment 7						
High Infusion Rate $0 < t < 1$ hr	No	2 18%	7 64%	8 73%	11	Model values greater for first 0.5 hr.
Low Infusion Rate $1 \text{ hr} < t < 2$ hr	Yes	0 0%	0 0%	4 33%	12	Model values significantly greater.
Infusion Pump Off $2 \text{ hr} < t$	Yes	3 100%	3 100%	3 100%	3	

4.2.2.2 Experiment 8

For experiment 8, the initial clinical assessments indicated deep anesthesia. The model output, however, did not indicate deep anesthesia for the first 40 minutes at the high

infusion rate (Figures 4.54-4.56, Table 4.10). After the infusion rate change, a slight increase in the mean level of model output is observed, but the rate of increase is not as rapid as that observed by the anesthesiologist. The input variables ABETA, TOTPOW, and EMG are peculiar in that they show little variation between the hour of high infusion and the hour of low infusion (Figures 4.57-4.59). The levels of ABETA and EMG increase immediately once infusion is terminated at $t = 7200$ s, however.

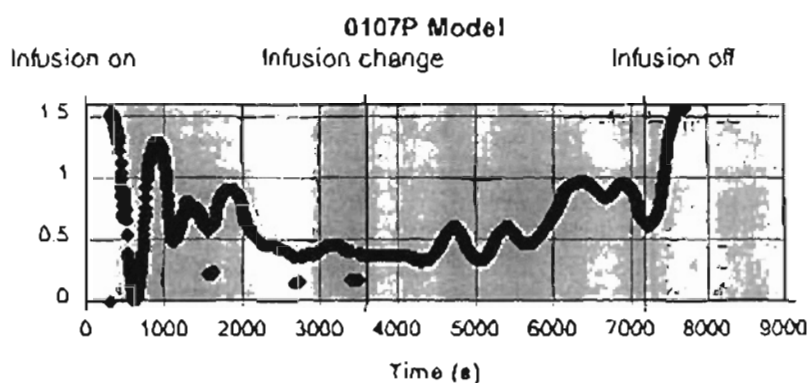


Figure 4.54: Model output (Experiment 8).

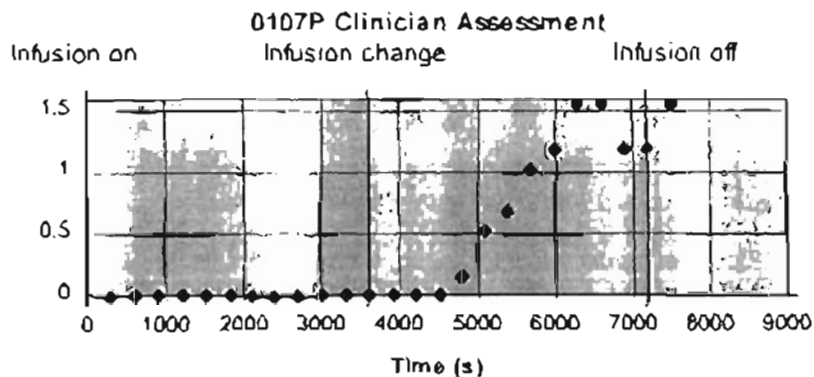


Figure 4.55: Rescaled clinical assessment (Experiment 8).

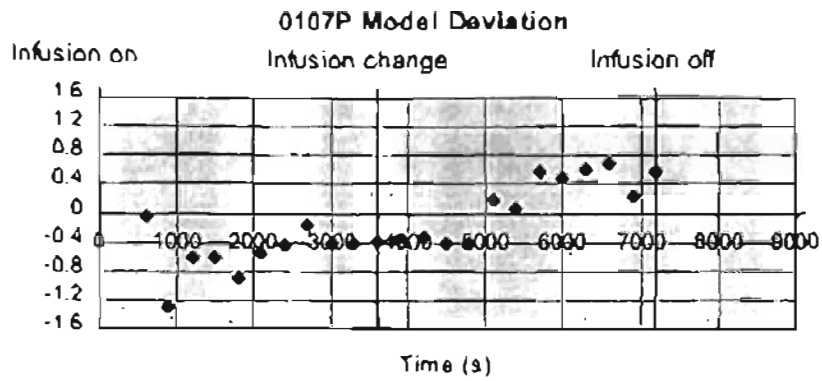


Figure 4.56: Model deviation from clinical assessment (Experiment 8).

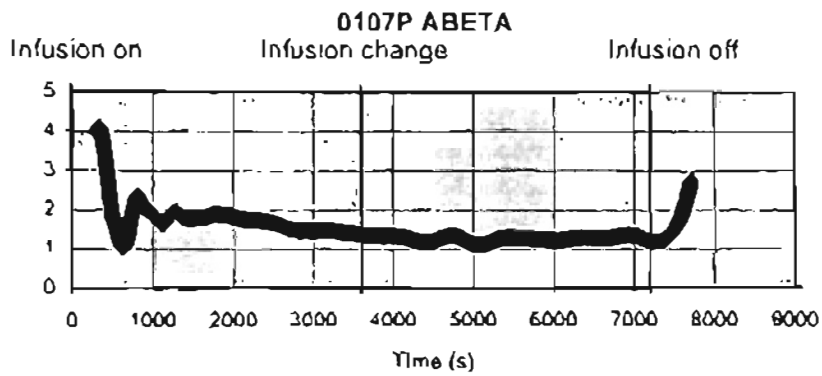


Figure 4.57: Dimensionless absolute power in Beta frequency band (Experiment 8).

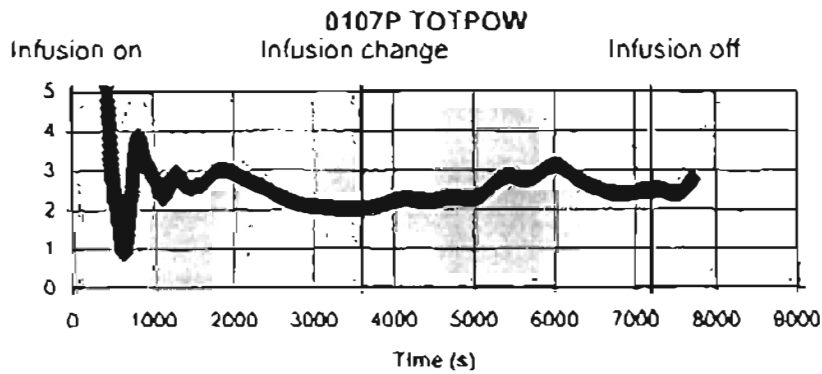


Figure 4.58: Dimensionless total absolute power in 0-30Hz frequency band (Experiment 8).

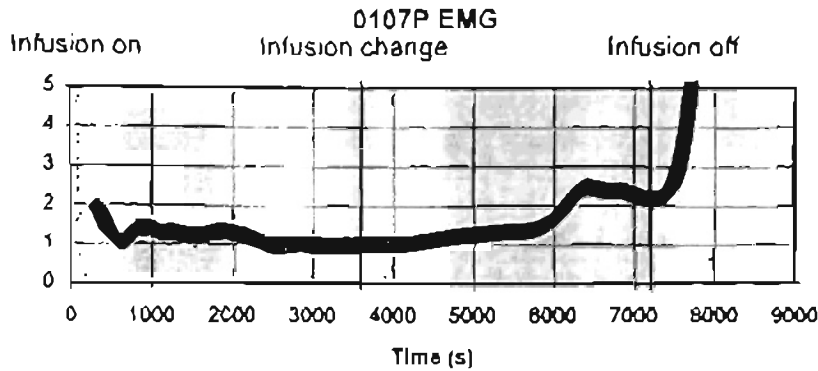


Figure 4.59: Dimensionless absolute power in EMG low frequency band (Experiment 8)

TABLE 4.10 Comparison of model with overall clinical assessment for experiment 8. Uncertainty expressed in rescaled clinical assessment units.

	Trend agreement (Yes / No) and number and percentage of data within specified uncertainty of rescaled clinical assessment					Description of deviations
	Trend	Uncertainty				
		\pm 0.26	\pm 0.52	\pm 0.78	n	
Experiment 8						
High Infusion Rate $0 < t < 1$ hr	No	2 18%	6 55%	9 82%	11	Model oscillates for first 0.6 hr around mean level greater than clinical assessment.
Low Infusion Rate $1 \text{ hr} < t < 2$ hr	Yes	3 25%	8 67%	12 100%	12	Rate of model increase slower.
Infusion Pump Off $2 \text{ hr} < t$	N/A	1 100%	1 100%	1 100%	1	

4.2.2.3 Experiment 9

There is significant deviation during both the high and low infusion rate intervals (Figures 4.60-4.62, Table 4.11). The input variables appear to be featureless (Figures 4.63-4.65) resulting in similarly featureless model output.

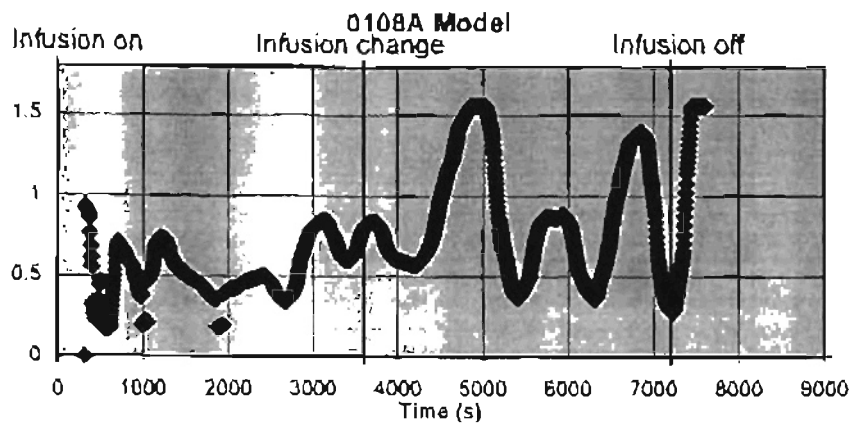


Figure 4.60: Model output (Experiment 9).

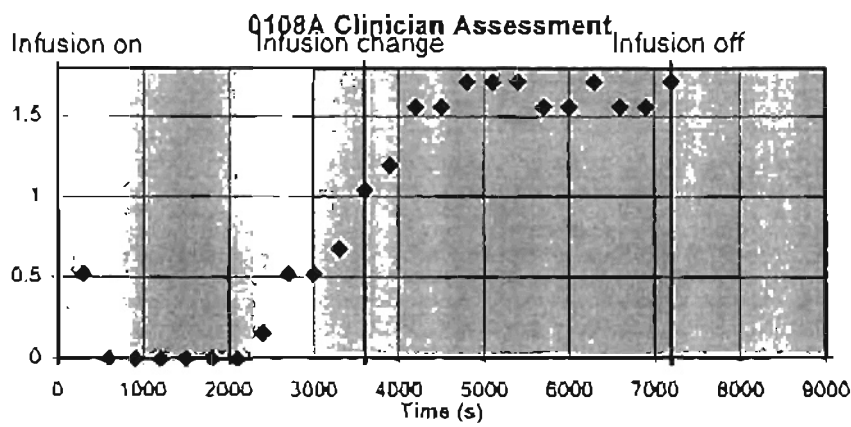


Figure 4.61: Rescaled clinical assessment (Experiment 9).

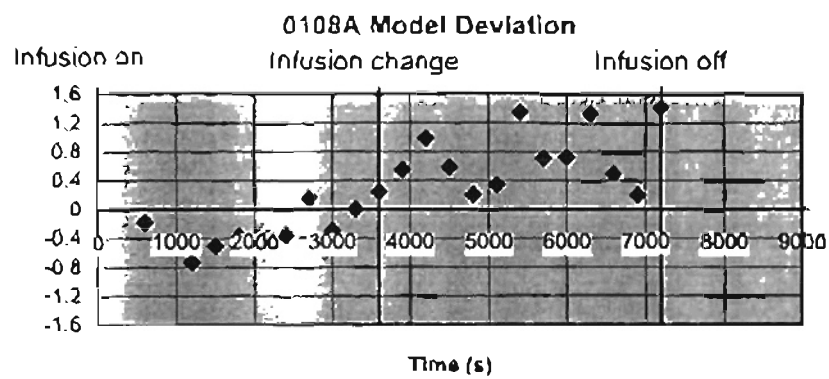


Figure 4.62: Model deviation from clinical assessment (Experiment 9).

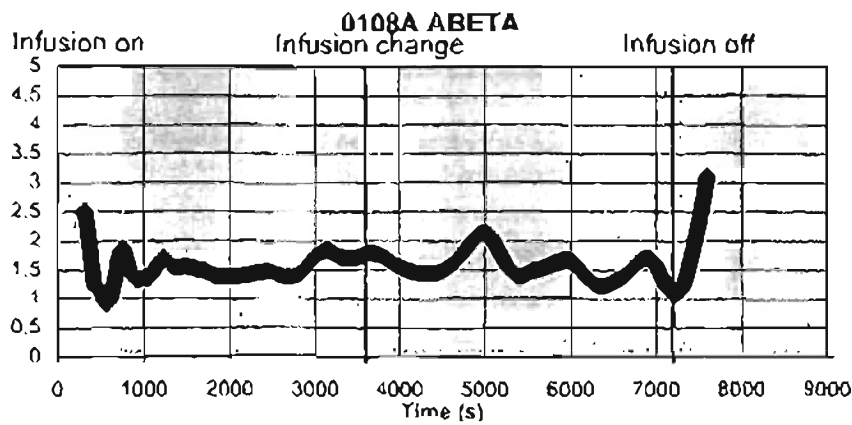


Figure 4.63: Dimensionless absolute power in Beta frequency band (Experiment 9).

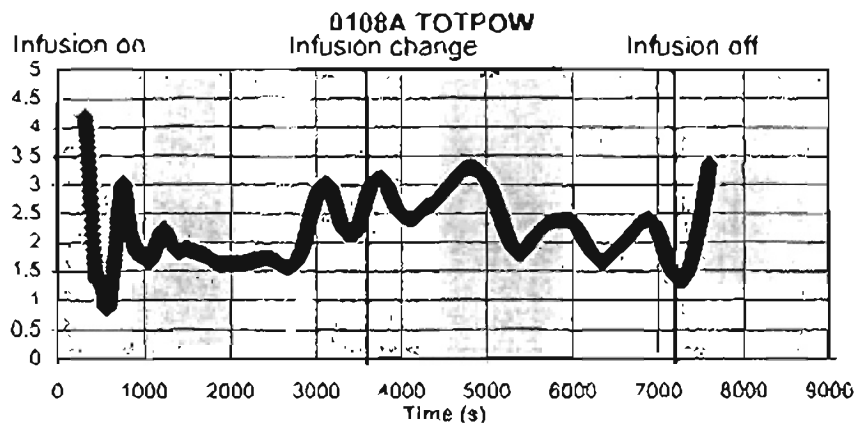


Figure 4.64: Dimensionless total absolute power in 0-30 Hz frequency band (Experiment 9).

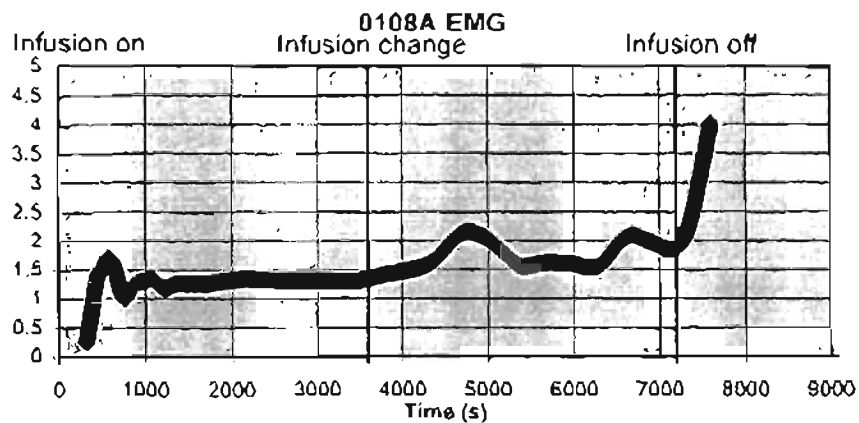


Figure 4.65: Dimensionless absolute power in EMG low frequency band (Experiment 9).

TABLE 4.11 Comparison of model with overall clinical assessment for experiment 9.
Uncertainty expressed in rescaled clinical assessment units.

	Trend agreement (Yes / No) and number and percentage of data within specified uncertainty of rescaled clinical assessment					Description of deviations
	Trend	Uncertainty				
		\pm 0.26	\pm 0.52	\pm 0.78	n	
Experiment 9						
High Infusion Rate $0 < t < 1$ hr	No	4 36%	10 91%	11 100%	11	Model values greater than clinician values for first 0.3 hr. Model requires 0.5 hr longer to record lowest levels
Low Infusion Rate $1 \text{ hr} < t < 2$ hr	No	2 67%	4 33%	8 67%	12	Increase in clinical assessment obvious but no obvious trend in model observed.
Infusion Pump Off $2 \text{ hr} < t$	N/A	0 0%	1 100%	1 100%	1	

4.2.2.4 Experiment 10

Like experiment 9, this experiment shows significant deviation between the clinical assessment and the model (Table 4.12). After 30 minutes at the high infusion rate, the model and clinical assessment diverge (Figures 4.66 - 4.68). Again, this puzzling lack of obvious trends in the output are due to relatively featureless (Figures 4.69 and 4.71) or physiologically inconsistent input (Figure 4.70).

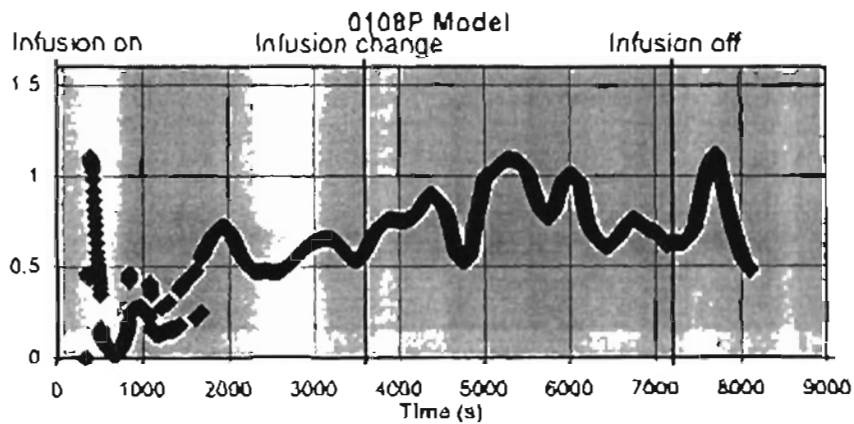


Figure 4.66: Model output (Experiment 10).

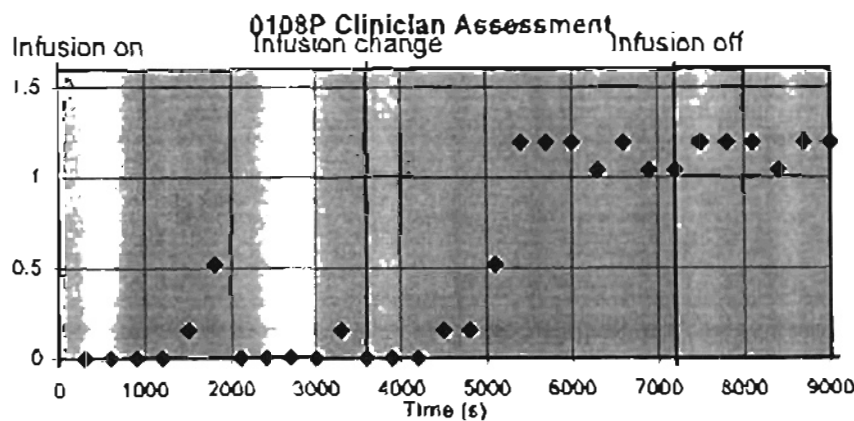


Figure 4.67: Rescaled clinical assessment (Experiment 10).

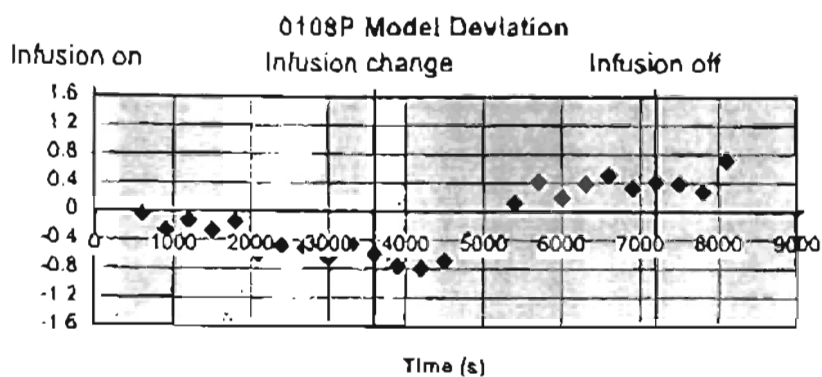


Figure 4.68: Model deviation from clinical assessment (Experiment 10).

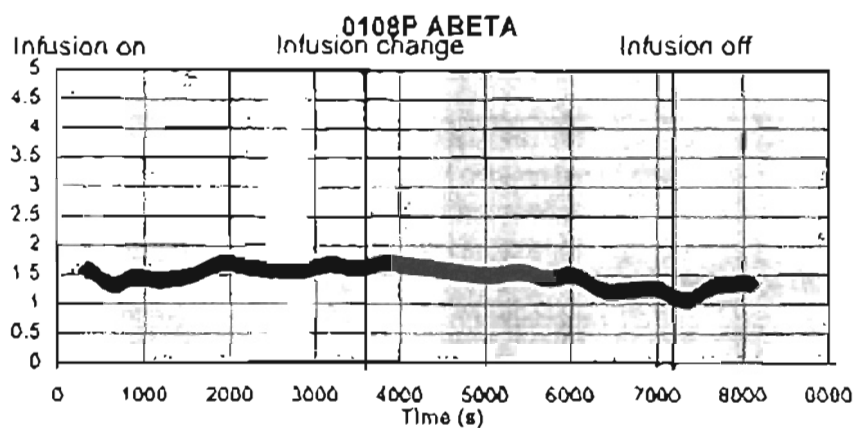


Figure 4.69: Dimensionless absolute power in Beta frequency band (Experiment 10).

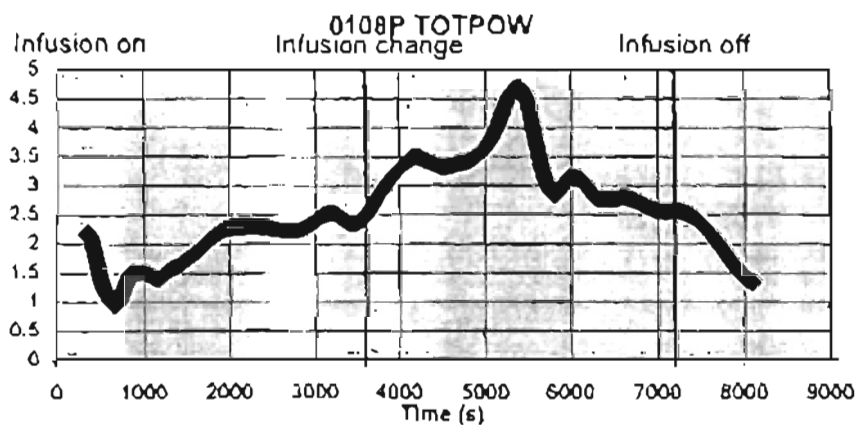


Figure 4.70: Dimensionless total absolute power in 0-30Hz frequency band (Experiment 10).

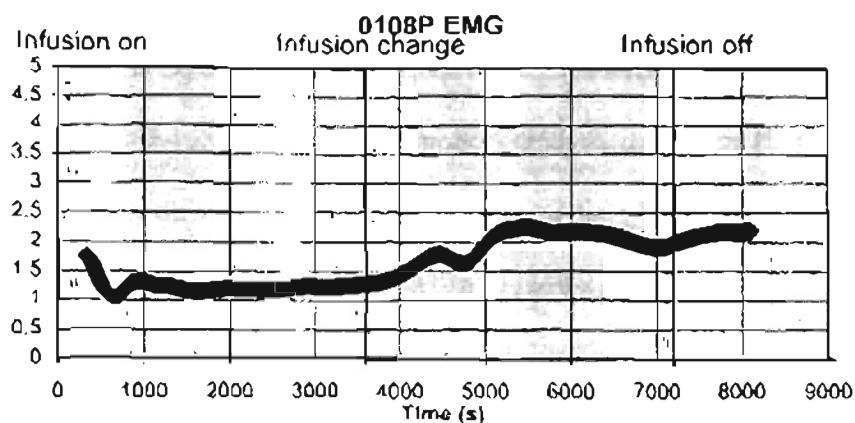


Figure 4.71: Dimensionless absolute power in EMG low frequency band (Experiment 10)

TABLE 4.12 Comparison of model with overall clinical assessment for experiment 10. Uncertainty expressed in rescaled clinical assessment units.

		Trend agreement (Yes / No) and number and percentage of data within specified uncertainty of rescaled clinical assessment				Description of deviations	
		Trend	Uncertainty				
			\pm 0.26	\pm 0.52	\pm 0.78		n
Experiment 10							
High Infusion Rate $0 < t < 1$ hr	Yes	3 27%	8 73%	11 100%	11	Model output yields maximum at $t = 1.5$ hr Clinical assessment relatively constant. Model has maximum at $t = 2.2$ hr.	
Low Infusion Rate $1 \text{ hr} < t < 2$ hr	No	2 17%	9 75%	11 92%	12		
Infusion Pump Off $2 \text{ hr} < t$	No	0 0%	2 67%	3 100%	3		

4.2.2.5 Experiment 11

This experiment showed some correlation between the clinical assessment and the model (Table 4.13). Although the model output values for the first hour at the high infusion rate do not show anesthesia as deep as that observed by the anesthesiologist, they appear to be hovering around a baseline suggesting deep anesthesia (Figures 4.72 - 4.74). The deviations for the first 20 minutes of the experiment are attributable to TOTPOW (Figure 4.76). Although ABETA appears to be relatively featureless for the first two hours of the experiment (Figure 4.75), TOTPOW registers a significant change corresponding to the change in infusion rate. A similar but more subtle change in EMG occurs as well (Figure 4.77). These changes observable in the input variables manifest themselves in the model output. From the infusion rate change to the 90 minute mark, the clinical assessment was much deeper than the assessment suggested by the model. For the next 30 minutes there was little deviation.

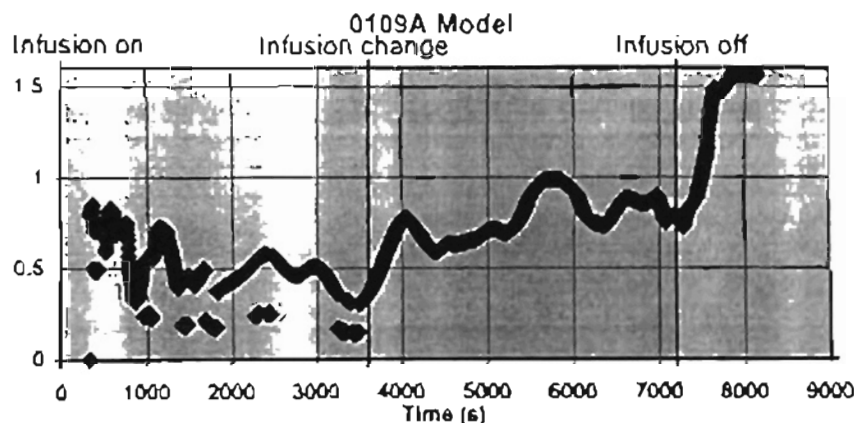


Figure 4.72: Model output (Experiment 11).

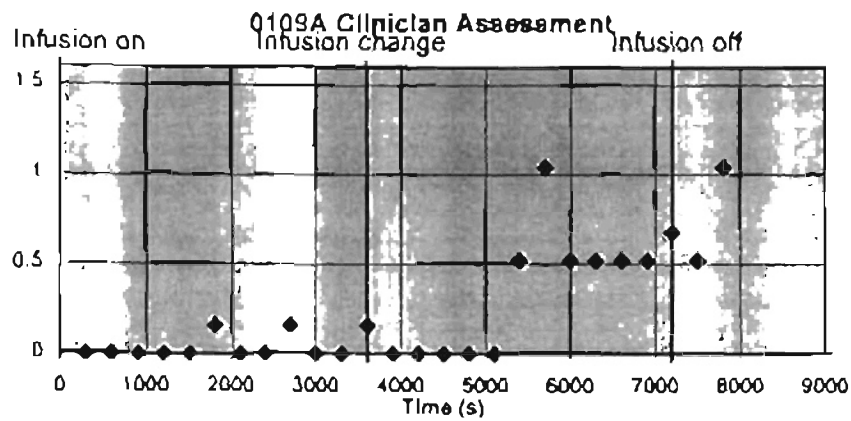


Figure 4.73: Rescaled clinical assessment (Experiment 11).

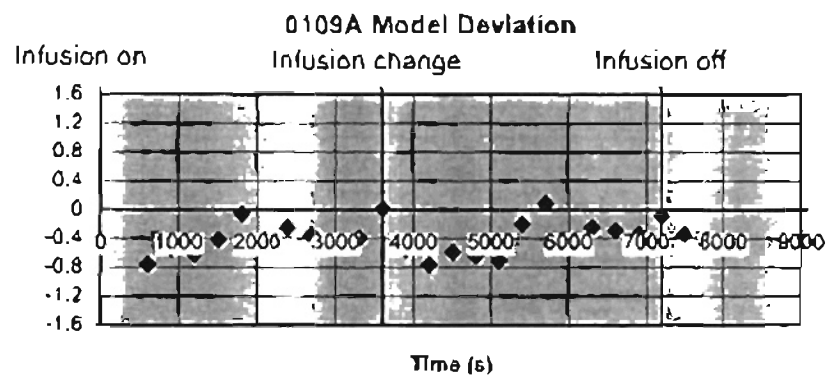


Figure 4.74: Model deviation from clinical assessment (Experiment 11).

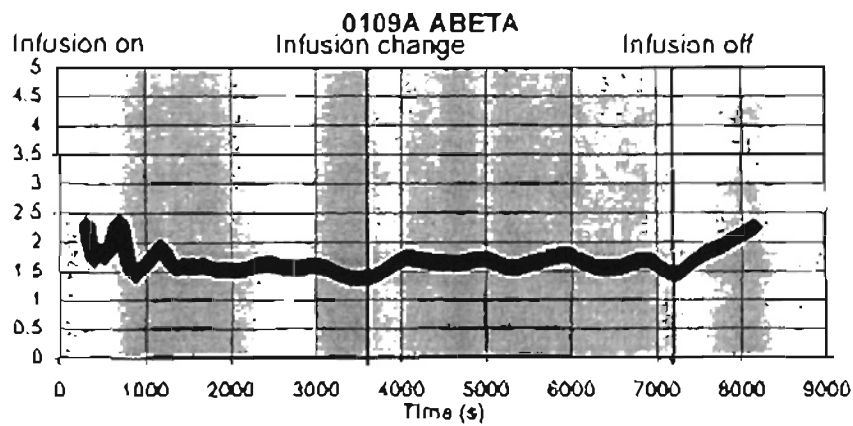


Figure 4.75: Dimensionless absolute power in Beta frequency band (Experiment 11).

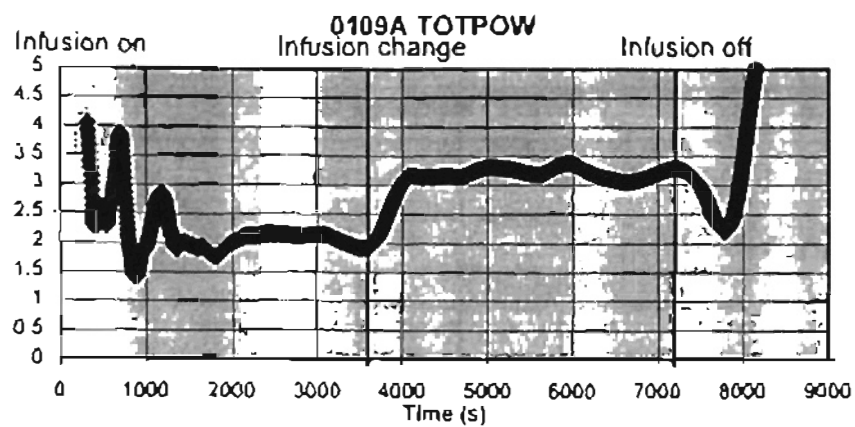


Figure 4.76: Dimensionless total absolute power in 0-30Hz frequency band (Experiment 11).

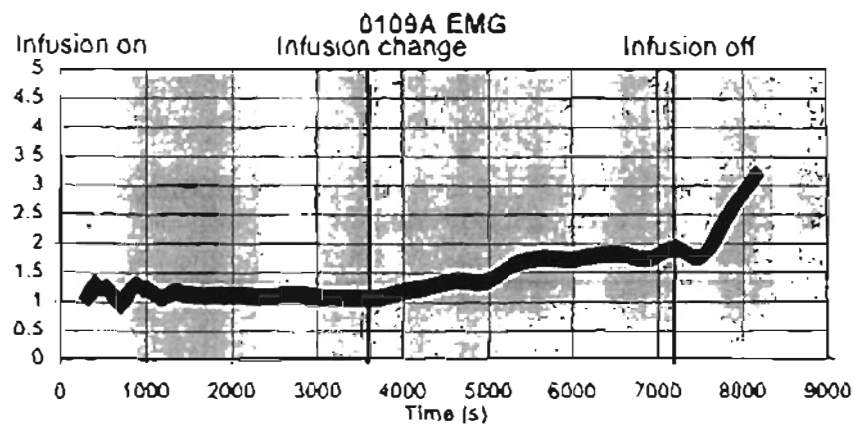


Figure 4.77: Dimensionless absolute power in EMG low frequency band (Experiment 11).

TABLE 4.13 Comparison of model with overall clinical assessment for experiment 11. Uncertainty expressed in rescaled clinical assessment units.

	Trend agreement (Yes / No) and number and percentage of data within specified uncertainty of rescaled clinical assessment					Description of deviations
	Trend	Uncertainty				
		\pm 0.26	\pm 0.52	\pm 0.78	n	
Experiment 11						
High Infusion Rate $0 < t < 1$ hr	Yes	3 27%	8 73%	11 100%	11	Rate of model increase slower beginning at infusion rate change. Clinical assessment increase begins 0.4 hr later.
Low Infusion Rate $1 \text{ hr} < t < 2$ hr	Yes	4 33%	7 58%	12 100%	12	
Infusion Pump Off $2 \text{ hr} < t$	Yes	0 0%	3 100%	3 100%	3	

4.2.2.6 Experiment 12

This experiment is another example of an experiment in which the anesthesiologist did not apply a broad span of assessments for the duration of the experiment. The first 40 minutes of the experiment provided examples of significant deviation between model and clinical assessment due to oscillatory behavior in ABETA and TOTPOW and a relatively slow decrease in EMG (Figures 4.78 - 4.83). Levels of ABETA and EMG remained relatively constant from the 40 minute mark during the high infusion period to the termination of infusion. No significant change was observed as a result of the change to the low infusion rate at the end of the first hour. There was a slight change at the infusion rate change in TOTPOW, however. During the second hour at the low infusion rate, model

output values oscillated and hovered around a mean level slightly higher than the lowest level attained during the first hour. At the termination of infusion, there were significant changes in ABETA, TOTPOW, and EMG followed by a peculiar decrease approximately 12 minutes later.

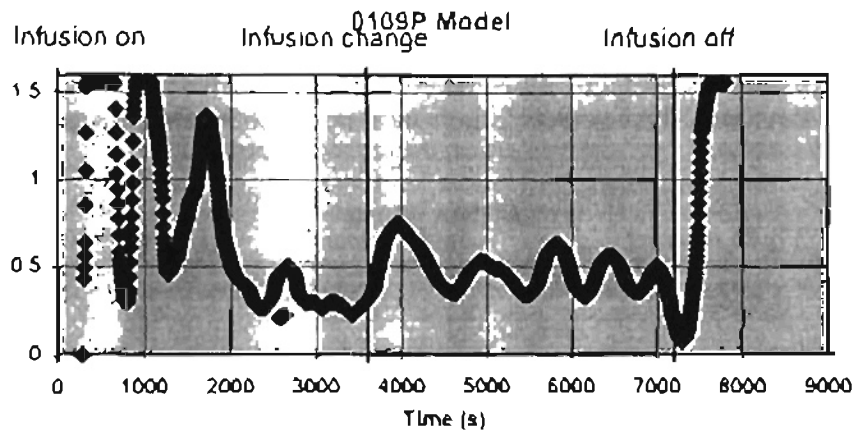


Figure 4.78: Model output (Experiment 12).

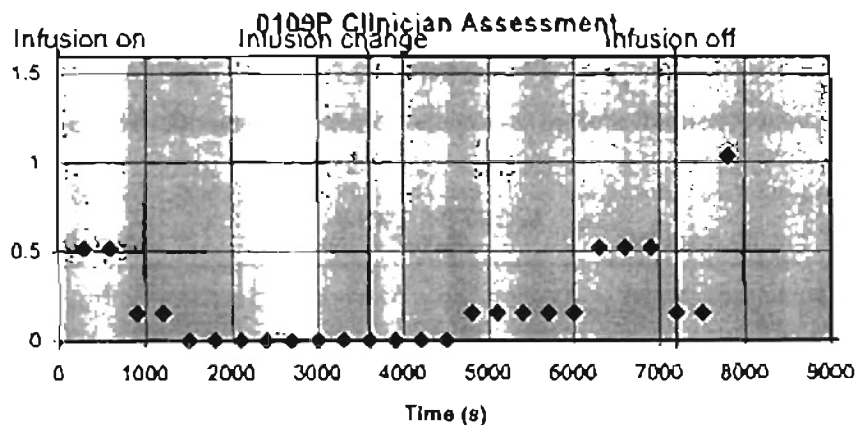


Figure 4.79: Rescaled clinical assessment (Experiment 12).

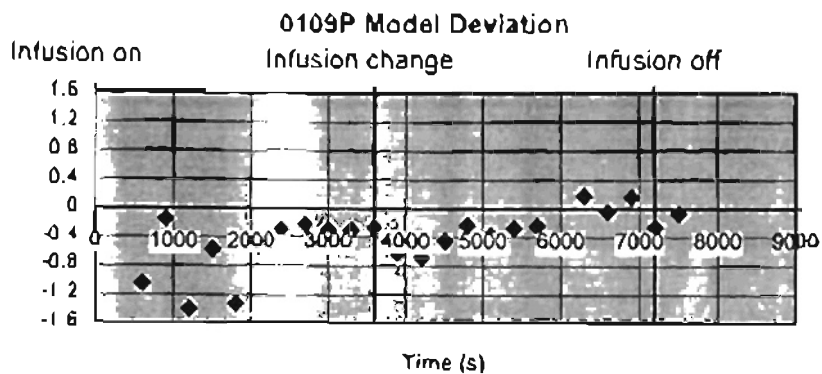


Figure 4.80: Model deviation from clinical assessment (Experiment 12).

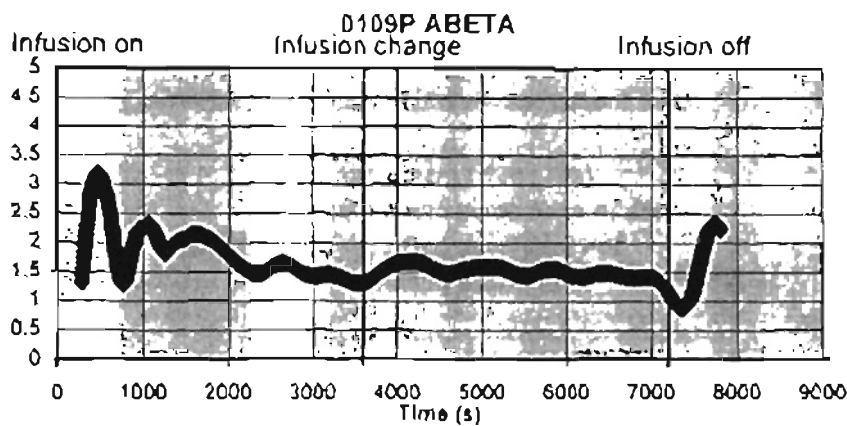


Figure 4.81: Dimensionless absolute power in Beta frequency band (Experiment 12).

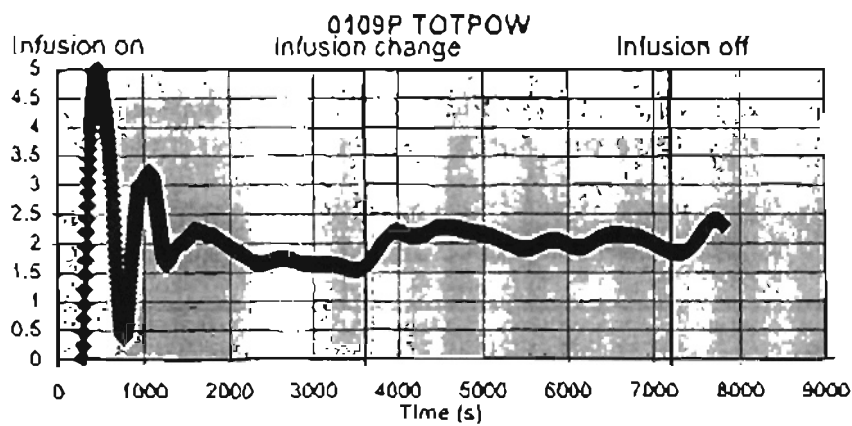


Figure 4.82: Dimensionless total absolute power in 0-30Hz frequency band (Experiment 12).

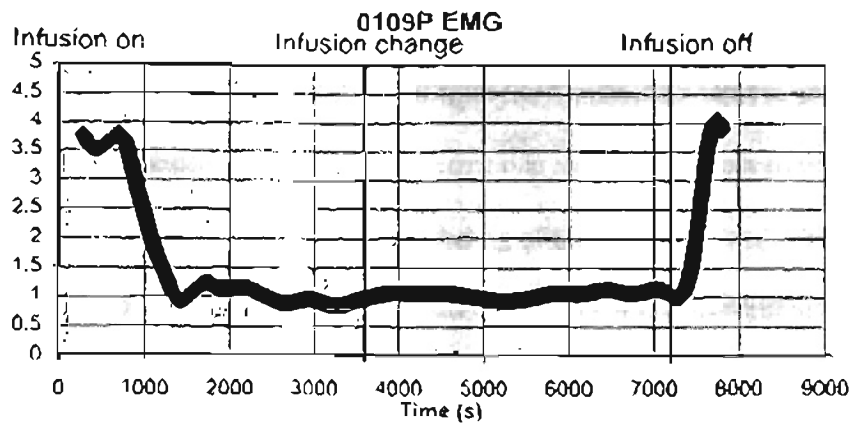


Figure 4.83: Dimensionless absolute power in EMG low frequency band (Experiment 12).

TABLE 4.14 Comparison of model with overall clinical assessment for experiment 12. Uncertainty expressed in rescaled clinical assessment units.

		Trend agreement (Yes / No) and number and percentage of data within specified uncertainty of rescaled clinical assessment				Description of deviations	
		Trend	Uncertainty				
			\pm 0.26	\pm 0.52	\pm 0.78		n
Experiment 12							
High Infusion Rate $0 < t < 1$ hr	Yes	3 27%	6 55%	8 73%	11	Oscillatory model decrease slower for first 0.6 hr.	
Low Infusion Rate $1 \text{ hr} < t < 2$ hr	Yes	5 42%	10 83%	12 100%	12		
Infusion Pump Off $2 \text{ hr} < t$	N/A	1 100%	1 100%	1 100%	1		

4.2.3 Comparison of initial experiments with verification experiments.

In general, the model output from the verification experiments did not agree with the clinical assessment to the same extent that the model output from the initial six experiments agreed with the corresponding clinical assessment (Tables 4.15 and 4.16). This is certainly not surprising considering that the initial experiments were used to develop the model. Also, laboratory beagles were used for the verification experiments whereas mixed breed dogs were used for the model development experiments. The verification experiments demonstrated slightly greater agreement with clinical assessment during the high infusion rate regime than the initial experiments. The initial experiments were closer to the clinical assessments during the low infusion rate, however. Existence and quality of data for the post-infusion period limits the validity of any analysis or comparison of data for this interval.

TABLE 4.15. Comparison of Model with Overall Clinical Assessment for Initial Experiments. (Experiments 1 - 6)

	Trend agreement (Yes / No) and number and percentage of data within specified uncertainty of rescaled clinical assessment					Description of deviations
	Trend	Uncertainty				
		± 0.26	± 0.52	± 0.78	n	
TOTALS						
High Infusion Rate 0 < t < 1 hr	6 Yes	21 32%	42 64%	46 70%	66	
Low Infusion Rate 1 hr < t < 2 hr	6 Yes	39 54%	56 78%	66 92%	72	
Infusion Pump Off 2 hr < t	2 Yes 4 N/A	6 50%	9 75%	10 83%	12	
GRAND TOTALS		66 44%	107 71%	122 81%	150	

TABLE 4.16. Comparison of Model with Overall Clinical Assessment for Verification Experiments. (Experiments 7 - 12)

	Trend agreement (Yes / No) and number and percentage of data within specified uncertainty					Description of deviations
	Trend	Uncertainty				
		\pm 0.26	\pm 0.52	\pm 0.78	n	
TOTALS						
High Infusion Rate 0 < t < 1 hr	3 Yes 3 No	17 26%	45 68%	58 88%	66	
Low Infusion Rate 1 hr < t < 2 hr	4 Yes 2 No	16 22%	38 53%	58 81%	72	
Infusion Pump Off 2 hr < t	2 Yes 1 No 3 N/A	5 42%	11 92%	12 100%	12	
GRAND TOTALS						
		38 25%	94 63%	128 85%	150	

4.3 PULSE EXPERIMENT

The purpose of this experiment was to determine the response of EEG variables to changes in infusion rate. This was accomplished by inducing anesthesia in a mixed-breed dog using the same protocol as used in the other experiments, but rather than immediately infusing the subject with 0.1 ml/kg of propofol, the lower infusion rate of 0.05 ml/kg was used. This infusion rate was maintained for one hour to obtain a nominally "steady state" anesthetic depth, then a 10 mg/kg bolus dose of propofol was administered and EEG data were collected for one more hour. The infusion was maintained during the second hour at the 0.05 ml/kg infusion rate.

The expectations for this experiment were that ABETA, TOTPOW, and EMGLO would decrease immediately following the bolus injection and then increase as the propofol was cleared. Modest burst suppression was expected immediately following the bolus injection as well. The expectation for the model was that it should indicate light anesthesia for the first hour with a relatively short period of deeper anesthesia immediately following administration of the bolus, then progressive lightening of the anesthesia as the experiment continued. The results are shown in Figures 4.84 - 4.90.

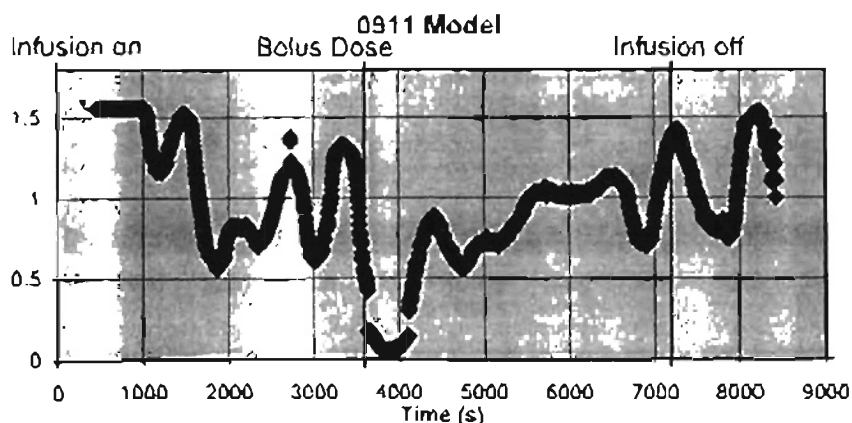


Figure 4.84: Model output (Pulse experiment).

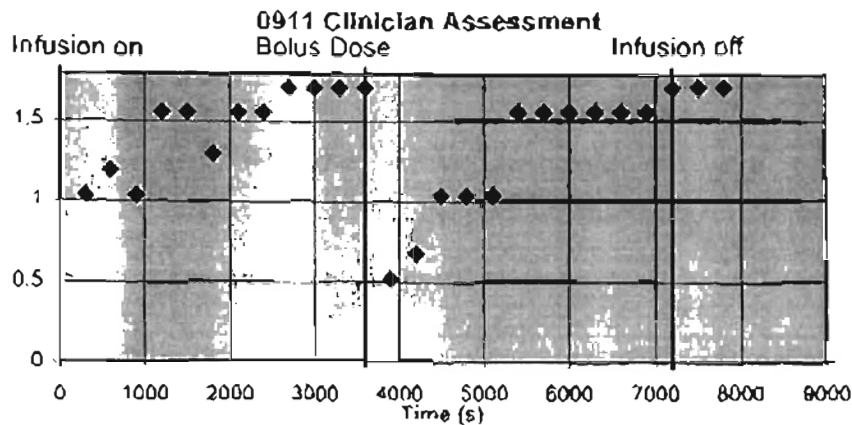


Figure 4.85: Rescaled clinical assessment (Pulse experiment).

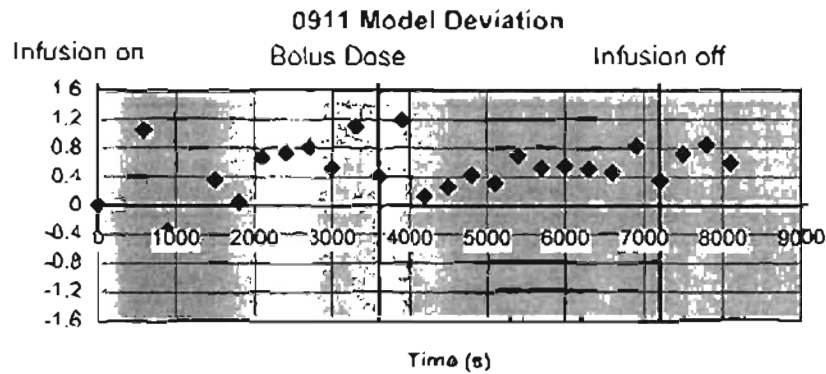


Figure 4.86: Model deviation from clinical assessment (Pulse experiment).

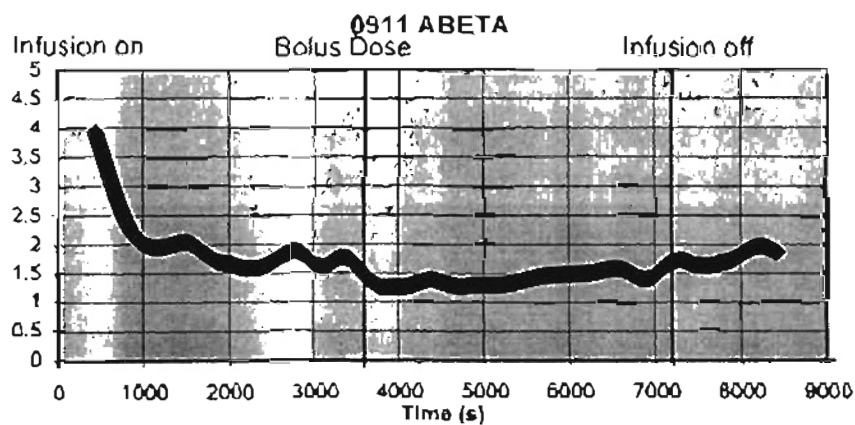


Figure 4.87: Dimensionless absolute power in Beta frequency band (Pulse experiment).

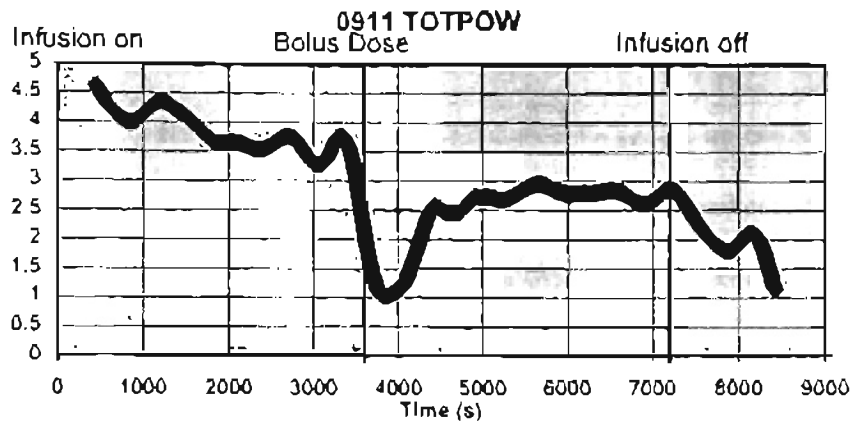


Figure 4.88: Dimensionless total absolute power in 0-30Hz frequency band (Pulse experiment).

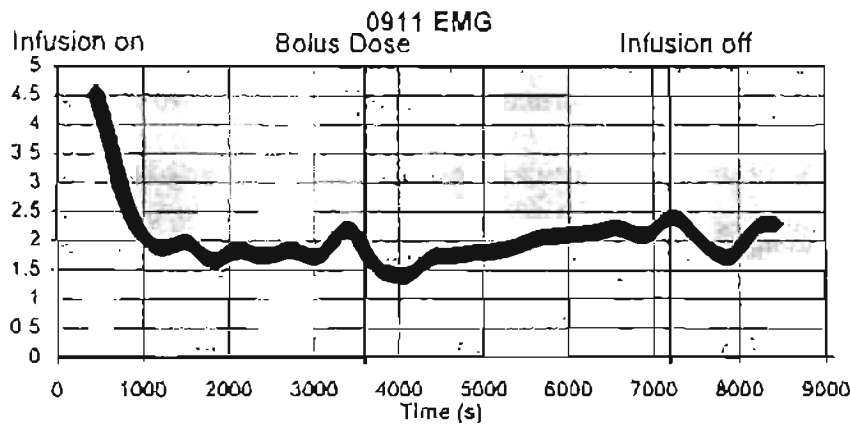


Figure 4.89: Dimensionless absolute power in EMG low frequency band (Pulse experiment).

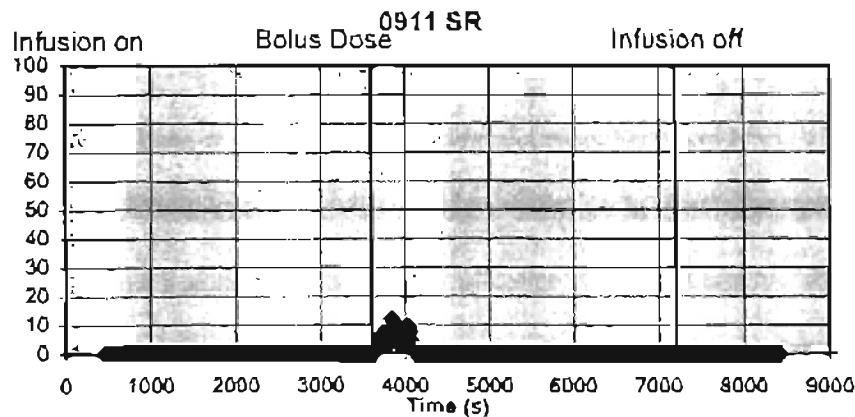


Figure 4.90: Suppression Ratio (Pulse experiment).

As expected, ABETA, EMGLO, and TOTPOW all attain their minimum values immediately after the bolus injection. Suppression occurs immediately after the bolus injection as well. Both the model and clinical assessment indicate the deepest anesthetic plane immediately after the bolus injection. Model trends generally agree with clinical assessment trends, particularly at and immediately following the bolus injection.

4.4 SURGICAL EXPERIMENT

This experiment was intended to fulfill three purposes. First, it provided another set of data for fine tuning and further development of the fuzzy model. Second, it provided assurance to the anesthesiologist that the infusion rates used in the other experiments were adequate and consistent with those used in a surgical scenario. Third, it provided an opportunity to test the compatibility of surgery with data acquisition.

4.4.1 Data Analysis

Induction dosage and initial infusion rates were set as they were in the previous experiments at 10 mg /kg and 0.1 ml/kg/min, respectively. The infusion rate was changed afterward at the discretion of the anesthesiologist. An event list for the experiment is provided in Table 4.17. Due to the nature of this experiment, expected trends were difficult to predict. Plots of selected input and model output are provided in Figures 4.91 - 4.97. Trends in ABETA seem only slight, but low values in EMGLO and TOTPOW correspond with instances of suppression. The application of the monopolar cautery at $t = 1138$ s caused a EEG data acquisition interruption of approximately 4 minutes. The values obtained in this window are therefore specious. Low values in the model output

correspond with instances of burst suppression, during the beginning of the experiment at the high infusion rate and at the end of the experiment immediately following the administration of the second bolus propofol dose.

Table 4.17. Event list for surgical experiment: neutering of 6 month old male German Shepherd.

Elapsed Time		Event
s	hh:mm:ss	
0	0:00:00	Infusion pump on (3.0 ml/min)
1146	0:19:06	Incision
1138	0:18:58	Use of monopolar cautery (EEG signals interrupted)
1225	0:20:25	Infusion decrease to 2.0 ml/min
1697	0:28:17	Cutting of scrotal ligament
1746	0:29:06	Clamps applied
1857	0:30:57	Infusion increase to 2.5 ml/min
2087	0:34:47	Clamps applied
2342	0:39:02	Reduce infusion to 2.0 ml/min
2667	0:44:27	Bolus propofol injection (same as induction dose)
3260	0:54:20	Application of Bipolar Cautery
3297	0:54:57	Application of Bipolar Cautery

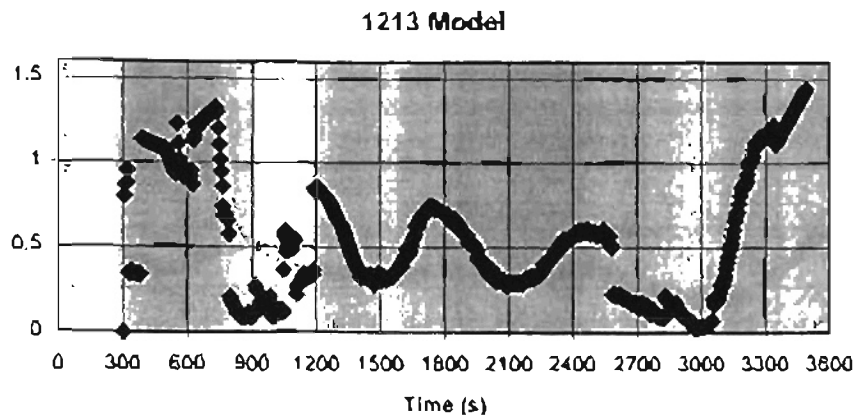


Figure 4.91: Model output (Surgical experiment).

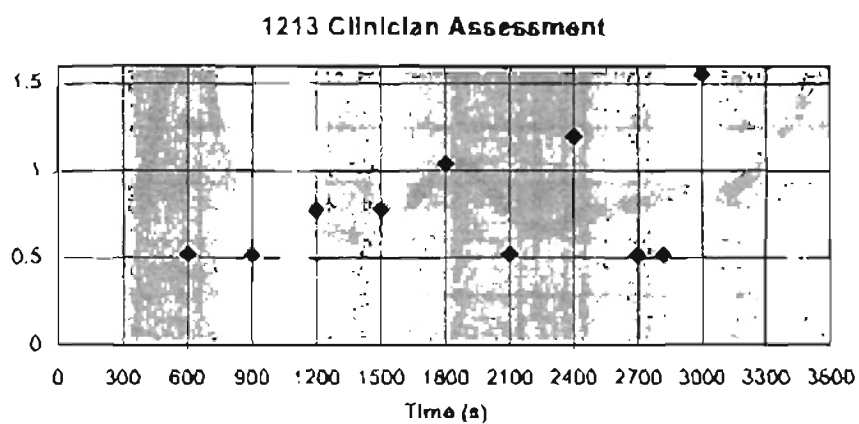


Figure 4.92: Rescaled clinical assessment (Surgical experiment).

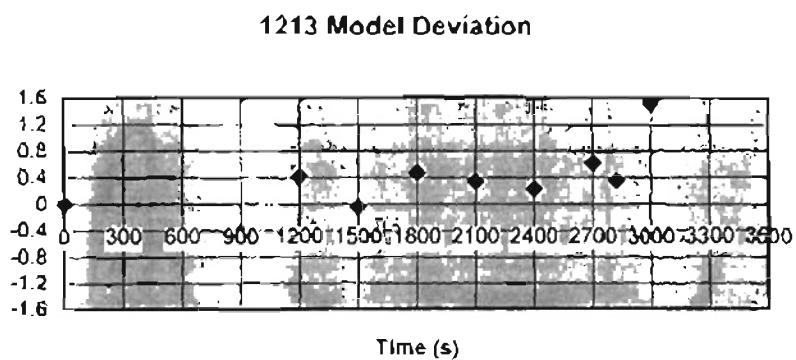


Figure 4.93: Model deviation from clinical assessment (Surgical experiment).

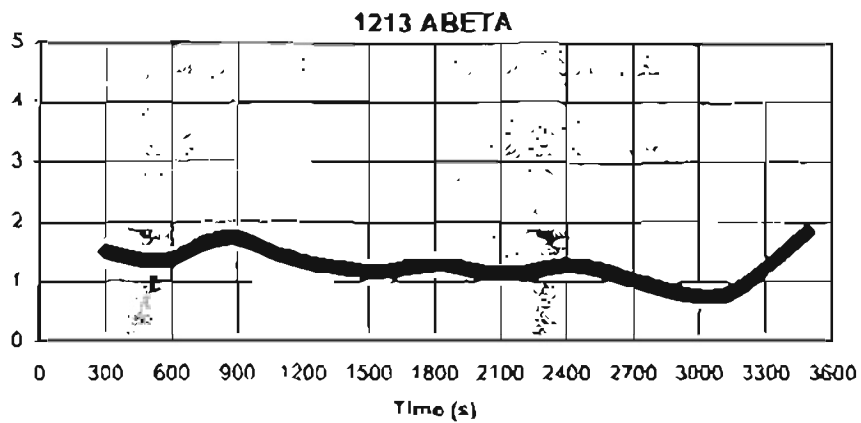


Figure 4.94: Dimensionless absolute power in Beta frequency band (Surgical experiment).

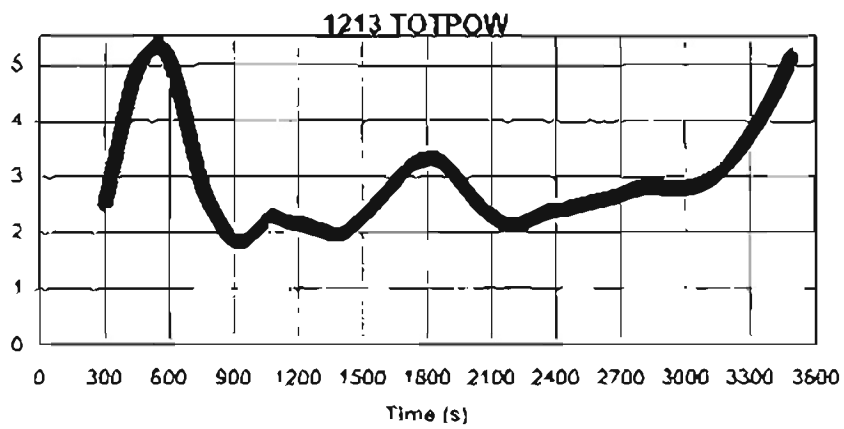


Figure 4.95: Dimensionless total absolute power in 0-30Hz frequency band (Surgical experiment).

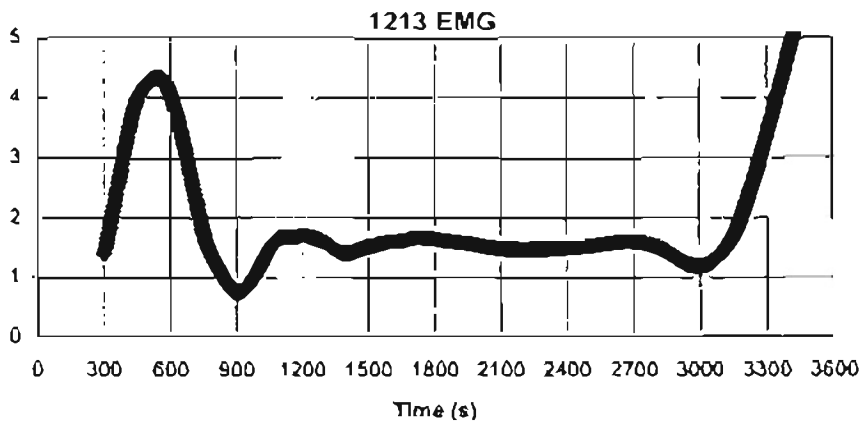


Figure 4.96: Dimensionless absolute power in EMG low frequency band (Surgical experiment).

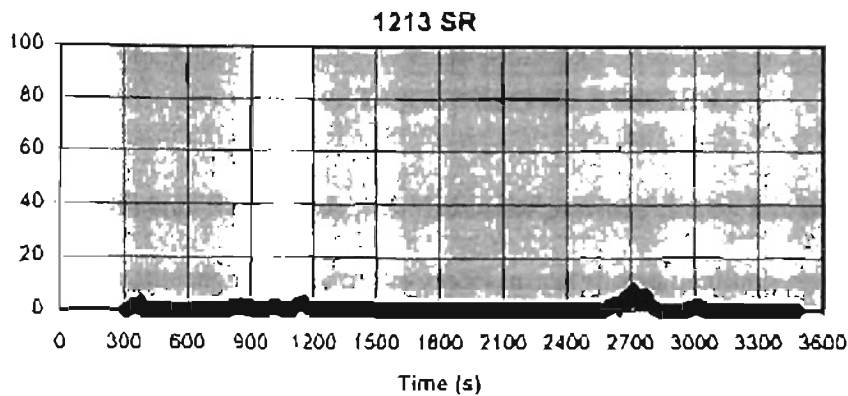


Figure 4.97: Suppression Ratio (Surgical experiment).

4.4.2 Verification of Appropriateness of Infusion Rate

The anesthesiologist was satisfied with the infusion rates used in the previous experimental protocol. The 0.1 ml/kg/min infusion rate is representative of a propofol infusion rate adequate for surgical use.

4.4.3 Surgical Application of Data Acquisition Techniques

The use of the monopolar cautery prevented four minutes of data acquisition. The bipolar cautery interrupted data acquisition for a much shorter period, but interrupted the EEG signal nonetheless. A more typical surgical environment in human medicine would have many more sources of electromagnetic fields and other sources that would likely interfere with data acquisition as it was done in this experiment. Also, moving the patient may disrupt EEG acquisition as well.

DISCUSSION OF RESULTS

Although the analysis provided in the previous chapter has been primarily quantitative, the significance of the model is best shown qualitatively. The essence of assessing anesthetic depth is qualitative; the distilled purpose of this work is to generate a computer program that can reproduce a person's opinion. Consequently, we believe statistical regression analysis or other typical quantitative techniques are less meaningful and potentially misleading as a means of assessing the quality of the proposed model.

Considering that the clinical assessment and the model require different sets of input data, a meaningful interpretation of the differences between them may be difficult to elucidate. When the clinician observes the reflexes and muscle tone of a patient, he infers depth of anesthesia. He cannot explicitly see how deep his patient is anesthetized; he can only base his opinion on the observables he can monitor. The model prediction is an assessment based on another set of observables. Again, depth of anesthesia is inferred and not measured explicitly. The physiological processes that cause subtle changes in the observables used by the clinician to assess anesthetic depth are temporally different from the processes that cause subtle changes in the observables monitored by the computer program. The philosophical question that lurks behind all of the analysis comparing these assessments is whether the anesthesiologist and the computer program are actually assessing the same thing.

Perhaps a more reasonable interpretation is that the index generated by the model is a comparable and complimentary assessment of anesthetic depth. Clearly, some of the experiments showed a distinct change in the output index corresponding to change in

infusion rate while the anesthesiologist reported no such change. In other instances, the anesthesiologist observed drastically different indicators of anesthetic depth that resulted in assessments very different from those generated by the model. At any rate, the assumption that the clinician's assessment based on one set of observables can be duplicated by a system monitoring a completely different set of observables is debatable. The two assessments are comparable, however.

Although the comparison of the clinical assessments based on physical observables and the model output based on EEG observables may not be valid as a means of quantitatively evaluating the model, this comparison has probative value for model evaluation. The validity of the comparison could be enhanced by using multiple clinicians and requiring less resolution in the continuum between light and deep anesthesia for both the clinical and model-determined assessments. Another means of qualitatively verifying the model would be to test it on-line in real time with an anesthesiologist evaluating the model-determined assessment.

5.1 EVALUATION OF MODEL

The determination of whether the proposed model accurately assesses depth of anesthesia is difficult to answer. If the question to be answered is whether the model exactly mimics the assessment of an anesthesiologist, the answer is no. But if the question is whether the model assessment identifies the same trends identified by the anesthesiologist within a comparable time, the answer would be a qualified yes. For the initial six experiments used to develop the model, the general trends observed by the anesthesiologist were reproduced by the model. Although the set of verification experiments did not yield the same degree of trend agreement, the differences and

deviations between the model and the clinical assessments are generally the result of physiologically inconsistent or contradictory input data. The quality of the model can only be as good as the quality of the model input.

The model clearly provides some indication of anesthetic depth. Developing a model that would reproduce the assessments given by the anesthesiologist exactly would be extremely difficult. In this light, the true indicators of the clinical value of the model would be its response to variations in infusion rate and whether it distinctly differentiates deep anesthesia from light anesthesia. Responses of the model to changes in infusion rate are consistent with those expected. Furthermore, model predictions corresponding to deep anesthesia are clearly distinct from those corresponding to light anesthesia.

Although the model as presented appears to have value as a means of assessing anesthetic depth, and that the relationship between model output and anesthetic depth can be described and evaluated qualitatively, what follows is a discussion of the limitations of the model regarding quantitative comparison with clinical assessment of anesthetic depth.

5.1.1 Limitations of Experimental Procedure

The experimental procedure made data analysis more difficult than necessary. The results of most of the experiments during the second hour at the low infusion rate indicate oscillatory behavior in the model output. This oscillation may be due to the application of tail clamps at 15 minute intervals. Some of the experiments show very clearly a corresponding 15 minute periodicity in these oscillations. For the kind of analysis being performed, the oscillations make the determination of conclusions difficult.

The breed and age of dog used as a subject were also not controlled. All the dogs studied were considered “young adults,” but no more specific information regarding age

was available. The six dogs used for the first experiment were medium-sized mixed breed dogs, but the six dogs used in the verification experiments were laboratory purpose-bred beagles. Differences in EEG response to anesthesia by breed have been noted (Zoran 1993). Therefore, the experimental methodology could have removed a potential bias either by examining only one breed or examining a larger, statistically significant sample of mixed breed dogs.

The subject dogs for the verification experiments appeared similar in age and appearance. The appearance was so similar that two dogs weighed approximately the same and shared similar markings, suggesting that they may have come from the same litter. If several of these dogs were related, one might expect that the results from the experiments may be subject to some bias.

5.1.2 Limitations of Model Development

Many assumptions were used to develop this model. The input variables ABETA, TOTPOW, and EMG were rescaled and made dimensionless using patient-specific parameters. The parameters used to define the input membership functions were assigned using the best judgment of the author. No major effort was extended to optimize either the scaling parameters or membership function parameters either to minimize deviation from the clinical assessment or to enhance the physiological consistency of the model. These issues are fundamental in the development of all fuzzy systems, however, and not particular to this system. These are limitations of design and can therefore be mitigated to improve the model.

The development of the fuzzy rulebase was hindered by the inability of the fuzzy logic software, TILShell, to easily accommodate complicated rules. The software was

originally designed to accelerate the design of fuzzy control systems and not for implementing fuzzy expert systems. A superior fuzzy logic software shell would allow for rules containing multiple conjunctive premises (e.g. "if A and B and C and D, then X"). The software as it exists now is only capable of using rules containing no more than two conjunctive premises conveniently (e.g. "if A and B then Y"). Certainly the logical equivalent of the multiple conjunctive argument could be determined using De Morgan's Laws and arbitrary logical intermediate variables, but this is unnecessarily complicated. The rulebase would be easier to comprehend if rules containing multiple conjunctive premises were used.

5.1.3 Limitations of Clinical Assessment

Our anesthesiologist assessed anesthetic depth using a subjective five point scale which was rescaled and compared to the model output. In practice, only values ranging from "1" to "5" were used. Examination of the experimental results indicates that these assessments appear to be consistent, but considering that they are subjective and determined by a human, some bias will exist, regardless of the training and expertise of the clinician. The endpoints of the anesthetic depth spectrum, "deep" anesthesia and "awake" are easily identifiable by objective analysis, but the continuum between these endpoints is less well defined to the clinician. It may be relatively simple to identify and assess a "1" or a "4", but less easy to assess a "2" or a "3". Consequently, a more straightforward and less subjective analysis comparing the model and the clinical assessment could have been performed with a scale requiring less differentiation among the values intervening between "deep" anesthesia and "awake".

5.1.4 Limitations of Comparison

To compare the model output and the clinical assessment, a linear relationship was assumed to exist between them so that the clinical assessment could be rescaled and compared directly with the model. The fundamental relationship between these two variables, if one exists, may not be linear, however. The direct comparisons presented in the Tables 4.3 to 4.16 are therefore somewhat speculative. What the entries in those tables represent is not necessarily the quality of the agreement between the model and the clinical assessment, but the quality of a linear correlation between the model and the clinical assessment.

5.2 IMPLEMENTATION ISSUES

The possibility of implementing this model as it currently exists is limited. The EEG is very sensitive to electromagnetic disturbances and the modern health-care milieu generates many electromagnetic disturbances. The quality of the EEG signal is often questionable even in the most optimum circumstances and the introduction of an electrocautery can rapidly destroy the ability of the monitoring system to acquire data. This is a hardware limitation and therefore restricts the quality and robustness of the monitoring system to the quality and robustness of the hardware used to implement it.

Another limiting aspect of this work is that it was done using propofol alone as an anesthetic agent. For this or a similar model to be implemented, it must be validated for the appropriate pharmaceuticals to be used. The general rules as defined in the rulebase should apply, but the patient specific parameters would likely need adjustment.

These patient-specific parameters used for scaling the input values are also a potential source of difficulty regarding model implementation. Prior to the use of this

system, these parameters must be determined. This may require calibration while the patient is anesthetized which may not be practical.

6.0

CONCLUSIONS AND RECOMMENDATIONS

The anesthesia monitoring system developed in this project provides a previously unavailable means for the quantitative assessment of anesthetic depth. Although it does not provide an assessment identical to that determined by an anesthesiologist, it provides a complimentary assessment which may on occasion provide a more sensitive determination of anesthetic depth than that provided by a clinician. This system also assesses anesthetic depth continuously. If the implementation issues are resolved, this system or a similar one may be useful in the operating rooms or critical care wards of the future.

6.1 CONCLUSIONS

Specific conclusions drawn from this work are listed below.

1. The index generated by this model reflects depth of anesthesia.
2. Agreement between model and clinical assessments very good considering that this approach to model development has not been attempted in the context of anesthesia monitoring.
3. Fuzzy logic provides a viable method of modeling complex, non-linear processes.
4. Use of fuzzy linguistic variables made model development intuitive.
5. Incorporation of EEG variables from both the time domain (Suppression Ratio) and frequency domain (power distribution) provides an extra dimension of useful clinical information to the model.
6. Experimental observations suggest that propofol anesthesia does not elicit a strong hypotensive effect at surgically adequate infusion rates, therefore supporting the

- reputation of propofol as a safe anesthetic agent. However, this model should be considered propofol-specific due to the exclusion of blood pressure as a model input.
7. The model yields good results with mixed-breed dogs, but inconsistent results with pure-bred beagles.
 8. The model could be optimized by adjusting membership functions and related scaling parameters.
 9. Use of EEG presents enormous data handling requirements.
 10. In a surgical environment, a bipolar cautery is preferred to a monopolar cautery because it causes less EEG signal disruption.

6.2 RECOMMENDATIONS

Although this model holds promise as a means of assessing anesthetic depth, certain issues must be addressed to improve the means of evaluating and implementing the model. The limitations previously discussed would need to be overcome or otherwise accounted for: particularly the items which make interpretation of the results difficult. It is very possible that both qualitative and quantitative agreement between the clinical assessment and the model are shrouded behind noisy inputs and irregular experimentation due to the variability mentioned previously. A comprehensive list of recommendations follows.

1. An alternative to evaluating the model by directly comparing it to a clinical assessment after the fact would be to evaluate it online in a clinical setting in real time. Clinical trials could be performed so that multiple anesthesiologists could gauge the adequacy of the model assessment relative to their own clinical assessment.

2. Alternative fuzzy logic software or problem-specific code may provide greater model development flexibility.
3. The automation of ECG data acquisition would make the extension of this model to other anesthetic agents considerably easier.
4. Future experiments should either use the tail clamp more infrequently or not at all. The use of the tail clamp resulted in spiking and other oscillations in the EEG signal which tended to complicate the interpretation of results.
5. The use of a larger sample of mixed breed dogs would provide a superior means of determining the existence of spurious or questionable data.
6. The assessments delivered by several veterinarians rather than one would provide a means of reducing the bias introduced by subjective assessment.
7. The model could be improved further if scaling parameters and membership functions were optimized and more complicated conjunctive rules could be used in the rulebase.
8. Optimization of the model could be made simpler with more flexible software. The generation and use of model specific code may be preferable to the use of commercial fuzzy logic software.
9. Questions regarding the robustness of the system could be resolved by multiple system trials in a surgical environment.

REFERENCES

- Arndt, V. M.; Hofmockel, R.; Benad, G. (1995). "EEG-Veränderungen unter Propofol-Alfentanil-Lachgas-Narkose." Anaesthesiologie und Reanimation 20(5): 126-133.
- Aspect Medical Systems, (1996). A-1000 EEG Monitor Serial Port Technical Specification. Natick, Massachusetts
- Black, M. (1937). "Vagueness: an exercise in logical analysis." Philosophy of Science 4: 427-455.
- Curatolo, M.; Derighetti, M.; Petersen-Felix, S.; Feigenwinter, P.; Fischer, M.; Zbinden, A. M. (1996). "Fuzzy logic control of inspired isoflurane and oxygen concentrations using minimal flow anaesthesia." British Journal of Anaesthesia 76: 245-250.
- Donegan, J. H.; Rampil, Ira J. (1990). The Electroencephalogram. Monitoring in Anesthesia and Critical Care Medicine. C. D. Blitt. New York, Churchill Livingstone: 431-459.
- Dwyer, R. C.; Rampil, Ira J.; Eger, Edmond I.; Bennet, Henry L. (1994). "The electroencephalogram does not predict depth of isoflurane anesthesia." Anesthesiology 81(2): 403-409.
- Gaitini, L.; Vaida, Sonia; Collins, Geoffrey; Somri, Mostafa (1995). "Awareness detection during Caesarian section under general anaesthesia using EEG spectrum analysis." Canadian Journal of Anaesthesia 42(5): 377-381.
- Ganti, S. S. (1996). Automated Trend Extraction of Sensor Signals for Pattern Based Data Analysis. M. S. Thesis, School of Chemical Engineering, Oklahoma State University. Stillwater, Oklahoma.
- Ghourji, A. F.; Monk, T. G.; White, P. F. (1993). "Electroencephalogram spectral edge frequency, lower esophageal contractility and autonomic responsiveness during general anesthesia." Journal of Clinical Monitoring 9: 176-185.
- Gurman, G. M. (1994). "Assessment of depth of general anesthesia: observations on processed EEG and spectral edge frequency." International Journal of Clinical Monitoring and Computing 11: 185-189.
- Kanto, J.; Gepts, E. (1989). "Pharmacokinetic implications for the clinical use of propofol." Clinical Pharmacokinetics 17(5): 308-326.

- Koch, E.; Bischoff, P.; Pichlmeier, U.; Esch, J. S. (1994). "Surgical stimulation induces changes in brain electrical activity during isoflurane/nitrous oxide anesthesia." Anesthesiology 80: 1026-1034.
- Larijani, G. E.; Gratz, Irwin; Afshar, Mary; Jacobi, Athole G. (1989). "Clinical pharmacology of propofol: an intravenous anesthetic agent." DICP, The Annals of Pharmacotherapy 23: 743-749.
- Linkens, D. A.; Hasnain, S. B. (1991). "Self-organizing fuzzy logic control and application to muscle relaxant anaesthesia." IEEE Proceedings-D 138(3): 274-284.
- Linkens, D. A.; Mahfouf, M.; Abbod, M. (1992). "Self-adaptive and self-organising control applied to nonlinear multivariable anaesthesia: a comparative model-based study." IEEE Proceedings-D 139(4): 381-394.
- Lukasiewicz, J. (1970). In Defense of Logistic. Selected Works. L. Borkowski. London, North-Holland.
- Mamdani, E. H. (1976). "Advances in linguistic synthesis of fuzzy controllers." Int. J. Man Mach. Stud. 8: 669-678.
- Martin, J. F. (1994). "Fuzzy control in anesthesia." Journal of Clinical Monitoring 10: 77-80.
- Mason, D. G.; Linkens, Derek A.; Abbod, Maysam F.; Edwards, Neil D.; Reilly, Charles S. (1994). "Automated delivery of muscle relaxants using fuzzy logic control." IEEE Engineering in Medicine and Biology 13(5): 678-686.
- Meier, R.; Nieuwland, Jacques; Zbinden, Alex. M.; Hacisalihzade, Selim. S. (1992). "Fuzzy logic control of blood pressure during anesthesia." IEEE Control Systems.
- Nayak, A.; Roy, Rob J.; Sharma, Ashutosh (1994). "Time-frequency spectral representation of the EEG as an aid in the detection of the depth of anesthesia." Annals of Biomedical Engineering 22: 501-513.
- Ning, T.; Bronzino, Joseph D. (1990). "Autoregressive and bispectral analysis techniques: EEG applications." IEEE Engineering in Medicine and Biology(3): 47-50.
- Otto, K.; Short, Charles E. (1991). "Electroencephalographic power spectrum analysis as a monitor of anesthetic depth in horses." Veterinary Surgery 20(5): 362-371.
- Rau, G.; Becker, Kurt; Kaufmann, Ralf; Zimmermann, Hans-Jurgen (1995). "Fuzzy logic and control: principal approach and potential applications in medicine." Artificial Organs 19(1): 105-112.

- Robertson, S. A.; Johnston, S.; Beemsterboer, J. (1992). "Cardiopulmonary, anesthetic, and postanesthetic effects of intravenous infusions of propofol in Greyhounds and non-Greyhounds." American Journal of Veterinary Research 53(6): 1027-1032.
- Ross, T. J. (1995). Fuzzy Logic With Engineering Applications. New York, McGraw-Hill.
- Sebel, P. S.; Bowles, Stephen M.; Saini, Vikas; Chamoun, Nassib (1995). "EEG bispectrum predicts movement during thiopental/isoflurane anesthesia." Journal of Clinical Monitoring 11: 83-91.
- Smith, N. T.; Schwede, H. O. (1972). "The response of arterial pressure to halothane: a systems analysis." Medical and Biological Engineering 10: 207.
- Stanski, D. R. (1992). "Pharmacodynamic modeling of EEG drug effects." Annual Review of Pharmacology and Toxicology 32: 423-427.
- Suppan, P. (1972). "Feedback control monitoring in anaesthesia II: Pulse rate control of halothane administration." British Journal of Anaesthesia 44: 1263.
- Togai InfraLogic, Inc., (1995). TILShell User Manual. Irvine, California.
- Tsutsui, T.; Arita, Seizaburo (1994). "Fuzzy-logic control of blood pressure through enflurane anesthesia." Journal of Clinical Monitoring 10: 110-117.
- Watkins, S. B.; Hall, L. W.; Clarke, K. W. (1987). "Propofol as an intravenous anaesthetic agent in dogs." Veterinary Record 120: 326-329.
- Weaver, B. M. Q.; Raptopoulos, D. (1990). "Induction of anaesthesia in dogs and cats with propofol." Veterinary Record 126: 617-620.
- Yasunobu, S.; Miyamoto, Shoji (1985). Automatic train operating system by predictive fuzzy control. Industrial Applications of Fuzzy Control. M. Sugeno. Amsterdam, North-Holland: 1-18.
- Ying, H.; McEachern, Michael; Eddleman, Donald W.; Sheppard, Louis C. (1992). "Fuzzy control of mean arterial pressure in postsurgical patients with sodium nitroprusside infusion." IEEE Transactions on Biomedical Engineering 39(10): 1060-1070.
- Zadeh, L. A. (1965). "Fuzzy sets." Information and Control 8: 338-353.
- Zbinden, A. M.; Feigenwinter, Peter; Petersen-Felix, Steen; Hacısalhizade, Selim (1995). "Arterial pressure control with isoflurane using fuzzy logic." British Journal of Anaesthesia 74: 66-72.

Zoran, D. L.; Riedesel, D. H.; Dyer, D. C. (1993). "Pharmacokinetics of propofol in mixed-breed dogs and greyhounds." American Journal of Veterinary Research 54(5): 755-760.

APPENDIX A

FUZZY INFERENCE AND DEFUZZIFICATION

To illustrate the process of fuzzy inferencing and defuzzification, consider an example fuzzy optimization problem of selecting automobile tires based on cost and warranty. The cost of a tire and the duration of its warranty are both crisp inputs. The goal of this optimization is to map these crisp inputs to a crisp output, a "tire desirability index." This process consists of three steps: fuzzification, inferencing, and defuzzification.

A.1 FUZZIFICATION

Tire cost and tire warranty must both be defined in terms of fuzzy sets. This definition is accomplished with membership functions. Tire cost will be defined as either "LOW" or "HIGH" according to the membership function shown in Figure A.1. Tire warranty will be defined as either "LOW" or "HIGH" according to the membership function shown in Figure A.2.

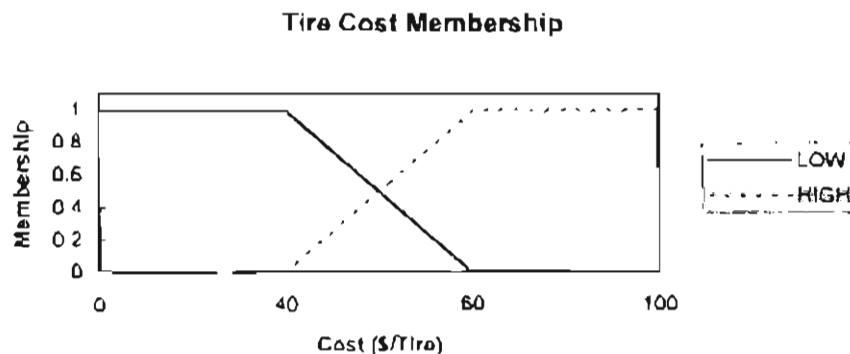


Figure A.1: Tire cost membership functions

The linguistic descriptors "LOW" and "HIGH" are actually fuzzy sets (e.g. "Tire cost is LOW" would constitute a fuzzy set). Note that a particular value for cost or

warranty may be both "LOW" and "HIGH." For example, a tire warranty of 57,500 would be "LOW" with a membership of 0.75 and "HIGH" with a membership of 0.25 (Figure A.2).

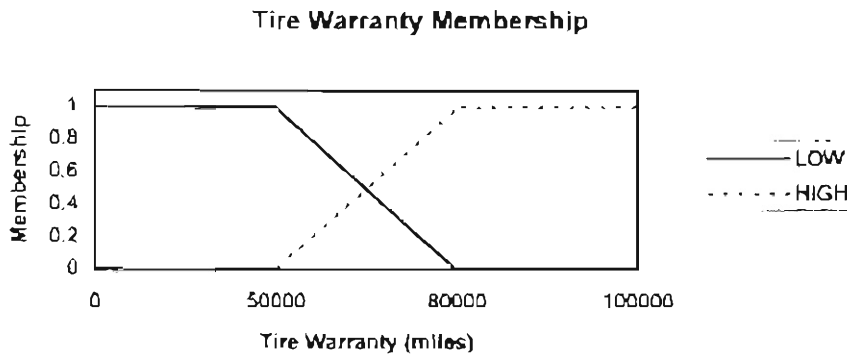


Figure A.2: Tire warranty membership functions

A.2 INFERENCE

The inputs of tire cost and tire warranty must be mapped onto an output variable, the "Tire desirability index." Before proceeding, membership functions must be defined for this output variable. For this example, "LOW," "MEDIUM," and "HIGH" will suffice (Figure A.3).

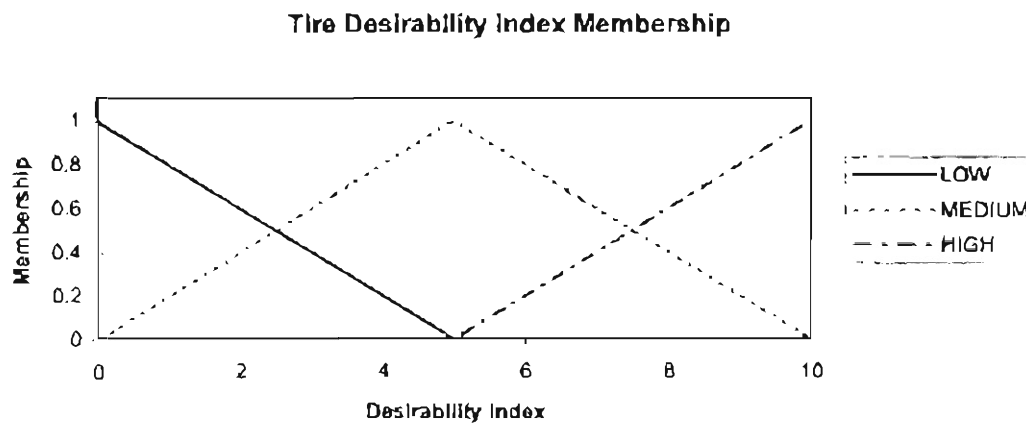


Figure A.3. Tire desirability index membership functions.

A matrix of rules relating the inputs to the outputs must be established. These rules will describe the linguistic relationship between the input variables and the output variables. For this example, four rules will be used and they are enumerated in Table A.1.

Table A.1. Rules relating tire cost and warranty to tire desirability.

Rule 1.	If tire cost is "LOW" and tire warranty is "LOW" then tire desirability is "MEDIUM."
Rule 2.	If tire cost is "HIGH" and tire warranty is "LOW" then tire desirability is "LOW."
Rule 3.	If tire cost is "LOW" and tire warranty is "HIGH" then tire desirability is "HIGH."
Rule 4.	If tire cost is "HIGH" and tire warranty is "HIGH" then tire desirability is "MEDIUM"

Now consider a specific tire costing \$43.00 with a warranty of 55,000 miles. For tire cost, this tire is "LOW" with a membership of 0.85 and "HIGH" with a membership of 0.15. For tire warranty, this tire is "LOW" with a membership of 0.8333 and "HIGH" with a membership of 0.1667. The consequence of non-zero membership in all input fuzzy sets is that all of the rules in Table A.1 will apply to some degree. To determine to what degree each rule applies, a decision must be made regarding the particular implication rule to be used. For this example, Mamdani's Rule (Mamdani 1976) will be used. This rule, also known as correlation-minimum implication (Ross 1995) is very common and easy to implement. In general, for a fuzzy relation R defined on the Cartesian product space $X \times Y$, Mamdani's rule can be expressed as $\mu_R(x, y) = \min(\mu_A(x), \mu_B(y))$ where $\mu_A(x)$ represents the membership of x in the domain X in the fuzzy set A , $\mu_B(y)$ represents the

membership of y in the domain Y in the fuzzy set B , and $\mu_R(x, y)$ represents the membership of the mapping of x, y to the fuzzy set R .

In this example, consider Rule 2. (Table A.1): If tire cost is “HIGH” and tire warranty is “LOW” then tire desirability is “LOW.” For our specific tire, the membership value of an output fuzzy set resulting from this rule is determined as follows: with tire cost “HIGH” membership of 0.15 and tire warranty “LOW” membership of 0.1667, the resulting tire desirability “LOW” membership would be the minimum of 0.15 and 0.1667, which is 0.15. A membership value in an output fuzzy set is determined for each of the four rules in this manner. These values are shown in Table A.2.

Table A.2. Membership values resulting for example tire (Cost = \$43, Warranty = 55,000) using Mamdani implication.

	Warranty is LOW $\mu_{LOW}(55,000) = 0.8333$	Warranty is HIGH $\mu_{HIGH}(55,000) = 0.1667$
Cost is LOW $\mu_{LOW}(43) = 0.85$	Desirability is MEDIUM $\mu_{MEDIUM}(43, 55,000) = 0.8333$	Desirability is HIGH $\mu_{HIGH}(43, 55,000) = 0.1667$
Cost is HIGH $\mu_{HIGH}(43) = 0.15$	Desirability is LOW $\mu_{LOW}(43, 55,000) = 0.15$	Desirability is MEDIUM $\mu_{MEDIUM}(43, 55,000) = 0.15$

Note that there are two membership values expressed for “MEDIUM” desirability. To determine the membership in the “Desirability is MEDIUM” fuzzy set, determine the logical union of the fuzzy sets defined by the two membership values. The resulting membership would be the maximum of these two values. Consequently, the degree of membership in all three output fuzzy sets is as follows: “Desirability is LOW”

membership = 0.15, “Desirability is MEDIUM” membership = 0.8333, and “Desirability is HIGH” membership is 0.1667.

A commonly used alternative to Mamdani’s rule, or maximum of minimums (max-min) inferencing is maximum of products (max-dot) inferencing. With this inference method, the composition of two membership functions is not determined by the logical intersection of the two functions, but by determining the product of the two functions. For this example, for “Warranty is HIGH” and “Cost is LOW,” $\mu_{HIGH}(55,000) = 0.1667$ and $\mu_{LOW}(43) = 0.85$, the resulting membership in the “Desirability is High” fuzzy set would be the product of the “Warranty is High” and “Cost is LOW” membership functions, i.e.,

$$\mu_{HIGH}(43, 55,000) = \mu_{LOW}(43) \cdot \mu_{HIGH}(55,000) = 0.85 \cdot 0.1667 = 0.1417.$$

As in the case with max-min inferencing, multiple instances of a rulebase consequent, such as the two cases of “Desirability is Medium” in the example above, are resolved by determining the logical union (maximum membership) of the multiple memberships within the fuzzy set. Max-dot inferencing is the method used in TILShell, the commercial fuzzy logic software used to develop the model proposed in this thesis (Togai InfraLogic, Inc. 1995). Many other methods of implication and inference exist in addition to max-min and max-dot methods, but these methods are the most common (Ross 1995).

A.3 DEFUZZIFICATION

Now that the degrees of membership for the output fuzzy sets have been determined, a method must be chosen to convert the fuzzy output to crisp output. Multiple methods can be used, but for this example the centroid method (Ross 1995) will be the method of choice. The centroid method of defuzzification is also the method used in

TILShell (Togai InfraLogic, Inc. 1995). Determination of a crisp value is accomplished by determining the logical union of the output membership functions and calculating the centroid of the area under the resultant unified membership function. The centroid is the defuzzified crisp output value.

In this example, the union of the output membership functions is presented in Figure A.4. The logical union is determined by the maximum membership value for all fuzzy sets for the domain of output. Note that the individual membership functions which can be inferred by comparison with Figure A.3 are bounded by the maximum values determined in the inferencing step.

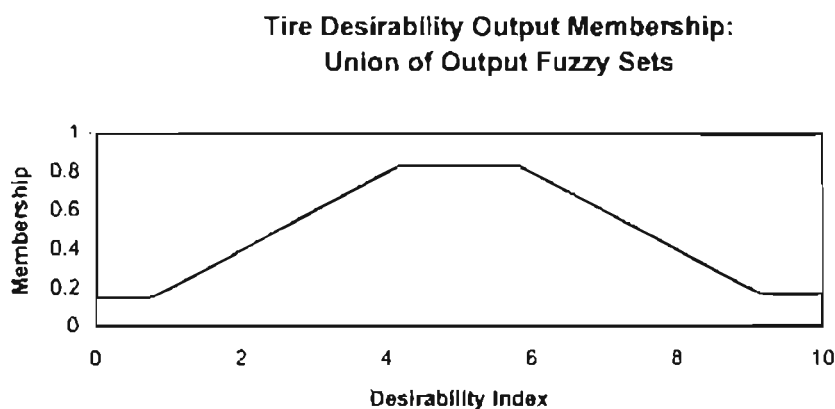


Figure A.4: Logical union of tire desirability membership functions.

In this example, the centroid of the area bounded by the function in Figure A.4 (output value) occurs at a Desirability Index of 4.9. Thus crisp inputs have been converted to crisp outputs.

APPENDIX B

EXPERIMENTAL SUBJECTS

Table B.1 Experimental subject information: experiments used for model development.

Exp. No.	Date	Dog	Weight	Notes
1	02 May 1996	#2785 "Sleepy" Heeler mix	14.4 kg	Experiments 1 - 6 are the source of data for model development.
2	08 June 1996	#2644 "Stinky" Brittany-Heeler mix	11.8 kg	
3	15 June 1996 (AM)	#2807 "Squirmy" Lab mix	12.7 kg	
4	15 June 1996 (PM)	#1090 "Timid" Rat Terrier	11.3 kg	
5	16 June 1996	#2806 "Squealy" Beagle mix	9.1 kg	
6	11 August 1996	#2858 "Stubborn" Border Collie mix	22.1 kg	
	11 September 1996	#2807(b) "Different" Generic mix	16.8 kg	Pulse experiment (bolus equivalent to induction dose administered at $t = 1$ hr)
	13 December 1996	"Elmo" German Shepherd	29.7 kg	Surgical experiment (neutering)

Table B.2. Experimental subject information: experiments used for model verification.

Exp. No.	Date	Dog	Weight	Notes
7	07 January 1997 (AM)	#2910 "Squat" Beagle	14.5 kg	Experiments 7 - 12 are the verification experiments.
8	07 January 1997 (PM)	#2912 "Stenchy" Beagle	13.4 kg	
9	08 January 1997 (AM)	#2916 "Crusty" Beagle	15.5 kg	
10	08 January 1997 (PM)	#2917 "Sniffy" Beagle	13.8 kg	Possible sibling of "Speedy"
11	09 January 1997 (AM)	#2909 "Squeaky" Beagle	11.4 kg	
12	09 January 1997 (PM)	#2911 "Speedy" Beagle	13.8 kg	Possible sibling of "Sniffy"

APPENDIX C

SAMPLE CLINICAL ASSESSMENT WORKSHEET

Pilot Project: Clinical Assessment of Anesthetic Depth

524

Date: 1/7/96 am

Dog ID: 2410

Weight: 14.5 kg

Bengle
Hind

Induction Dose (10 mg/kg) = 14.5 ml

Infusion Rate - 1st hour (1 mg/kg/min) = 14.5 mg/min
= 14.5 ml/min

2nd hour (0.5 mg/kg/min) = 7.25 mg/min
= 7.25 ml/min

Time	Alveol	Minutes	Jaw Tone (1-5)	Palp. Reflex (1-3)	Corn. Reflex (1-3)	Shivering (+/-)	Overall (1-5)	Comments
0	✓	0	1	1+	1	-	1+	
5		5	1	1	1	-	1	5:05 - 1st
10		10	1	1	1	-	1	
15	✓	15	1	1	1	-	1	
20		20	1	1	1	-	1	- muscular movement in hind legs
25		25	1	1	1	-	1	- slight head twitching
30	✓	30	1	1+	1	-	1+	- failed to rotate eyes -
35		35	1	2	1	-	2	empty
40		40	1	1+	1+	-	2	
45	✓	45	1	1+	1+	-	2	
50		50	1	1	1	-	1	
55		55	1	1+	1+	-	2	
60	✓	60	1	1+	1+	-	2	
65		65	1	1	1	-	1+	
70		70	1	1	1	-	1	
75	✓	75	1	2	2	-	2	
80		80	1	2	1+	+	2+	1st hind leg at back legs
85		85	1	2	1+	+	2+	
90	✓	90	1	2	2	+	2+	
95		95	1	1+	1+	+	2+	
100		100	1	1+	1+	+	2+	2nd hind leg at back legs
105	✓	105	1	2	1+	+	2+	2nd hind leg at back legs
110		110	1	2	2	+	3	
115		115	1	2	2	+	2+	
120	✓	120	1	2	2	+	3	
125		125	1	2+	2	+	3	1st hind leg at back legs
130		130	1	3	2	+	3	
135		135	1	3	2	+	4	2:13 still twitching, 1st hind leg
140		140	1	3	3	+	4	2:14 stretched 1st hind leg
145		145	1	3	3	+	4	2:15 stretched, 1st hind leg
150		150	2	3	3	+	4	2:20 moving hind leg
155		155						2:25 stretching
160		160						2:30 1st hind leg, 1st hind leg
165		165						2:35 1st hind leg, 1st hind leg
170		170						

APPENDIX D

SUMMARY OF SERUM PROPOFOL DATA

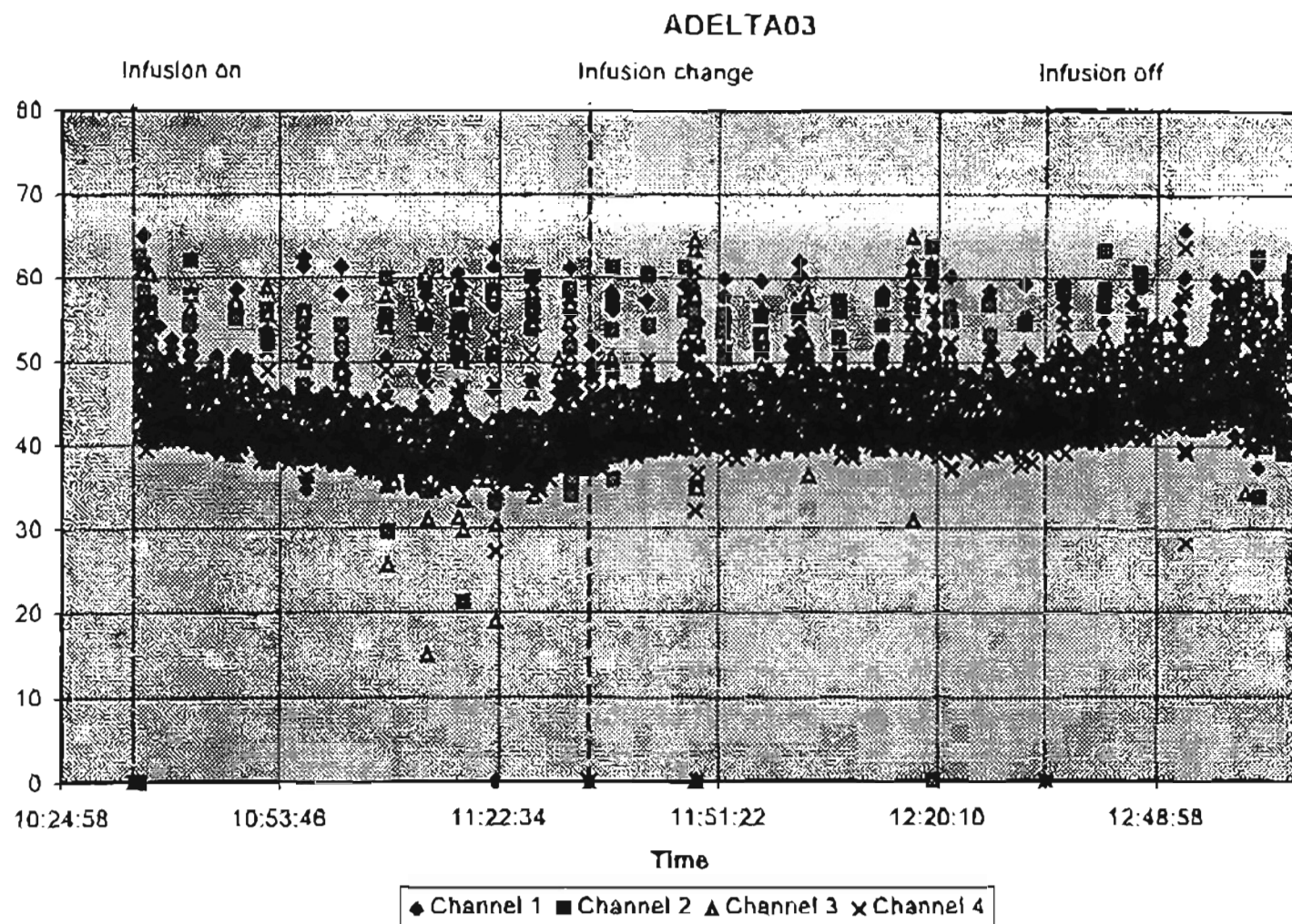
Table D.1: Serum propofol data. Concentrations expressed in $\mu\text{g} / \text{ml}$.

Time (min)	Dog#						MEAN	SD
	#2806	#1090	#2807	#2644	#2785	#2858		
Pre-admin.	0.00	0.00	0.00	0.00	0.00	0.00	0.00	0.00
15	14.1	15.78	14	14.94	18.89	27.04	17.46	5.02
30	21.24	20.33	18.02	16.05	24.44	34.70	22.46	6.64
45	19.88	22.43	19.25	26.07	23.16	38.95	24.96	7.28
60	24.09	27.28	24.02	28.07	21.78	40.13	27.56	6.58
75	15.41	11.97	15.39	17.5	16.88	26.89	17.34	5.06
90	14.43	12.38	15.84	15.09	14.11	24.75	16.10	4.39
105	14.63	12.29	11.89	9.29	12.15	23.44	13.95	4.95
120	14.06	11.75	14.15	12.81	14.09	23.52	15.06	4.25
122	9.46	7.6	10.91	9.09	13.68	14.84	10.93	2.81
124	8.06	6.56	9.12	8.31	12.12	17.19	10.23	3.88
126	6.41	5.03	7.77	7.37	9.58	13.95	8.35	3.13
128	3.14	6.39	10.76	7.58	8.63	11.75	8.04	3.11
130		5.4	7.59	6.19	7.67	13.29	8.03	3.09
132	4.49			3.51	8.67	9.04	6.43	2.84
134				3.63	8.22	9.48	7.11	3.08
136				4.52	9.47	5.01	6.33	2.73
138				4.63	4.78		4.71	0.11
140				4.62	6.12		5.37	1.06
142					4.95		4.95	
144					5.17		5.17	
146					3.64		3.64	
148					2.68		2.68	
150	4.55	2.43	4.35	4.37	5.67		4.27	1.17
152								
166						4.21	4.21	
180	1.42	2.4	3.16	2.36	3.2		2.51	0.73
182								
196						3.12	3.12	
210	0.45	1.7	2.25	1.73	3.08		1.84	0.96
212								
226						2.81	2.81	
240	0.08	1.46	1.82	0.47	1.51		1.07	0.75
242								
256						2.33	2.33	

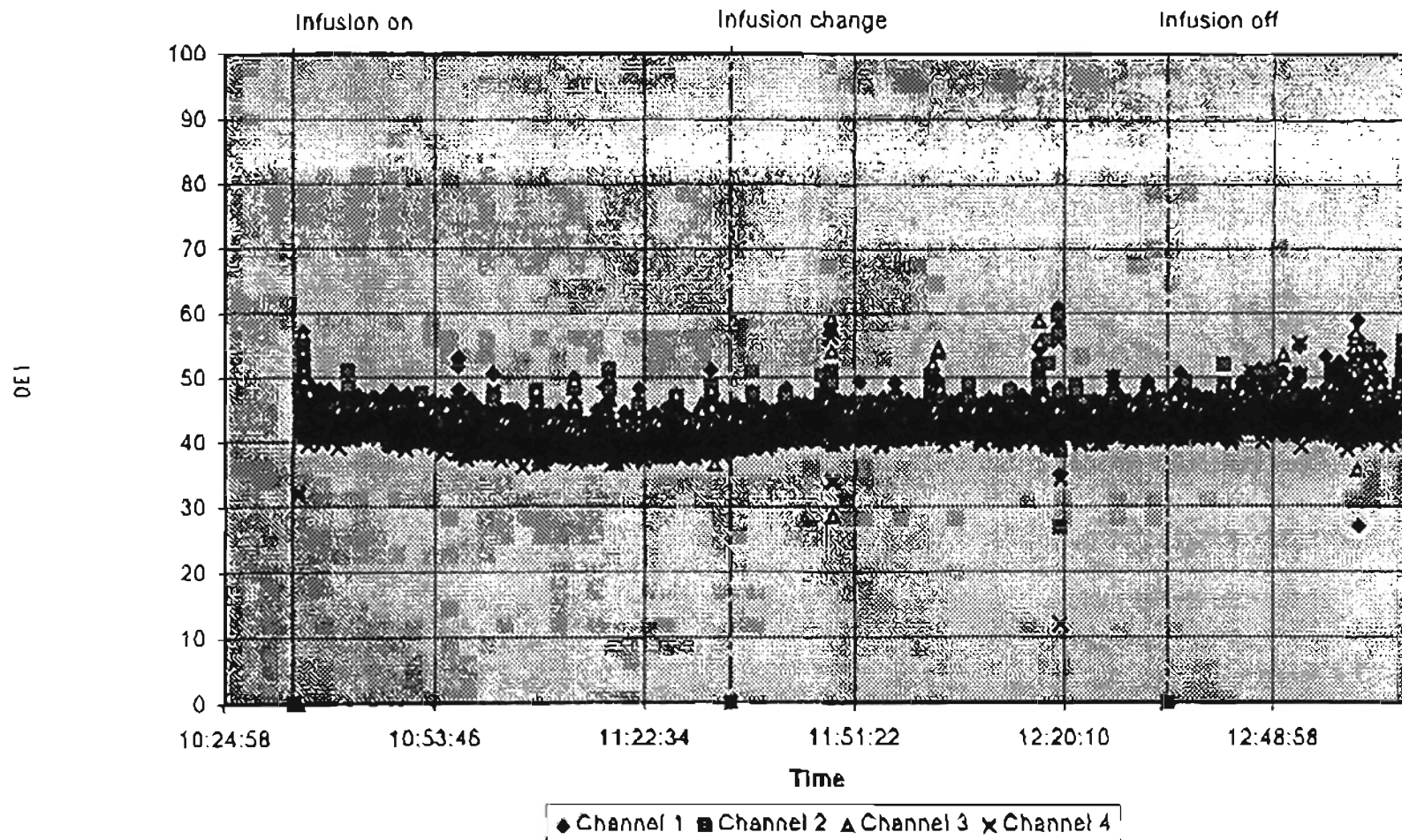
APPENDIX E

EXAMPLE EXPERIMENT PLOTS

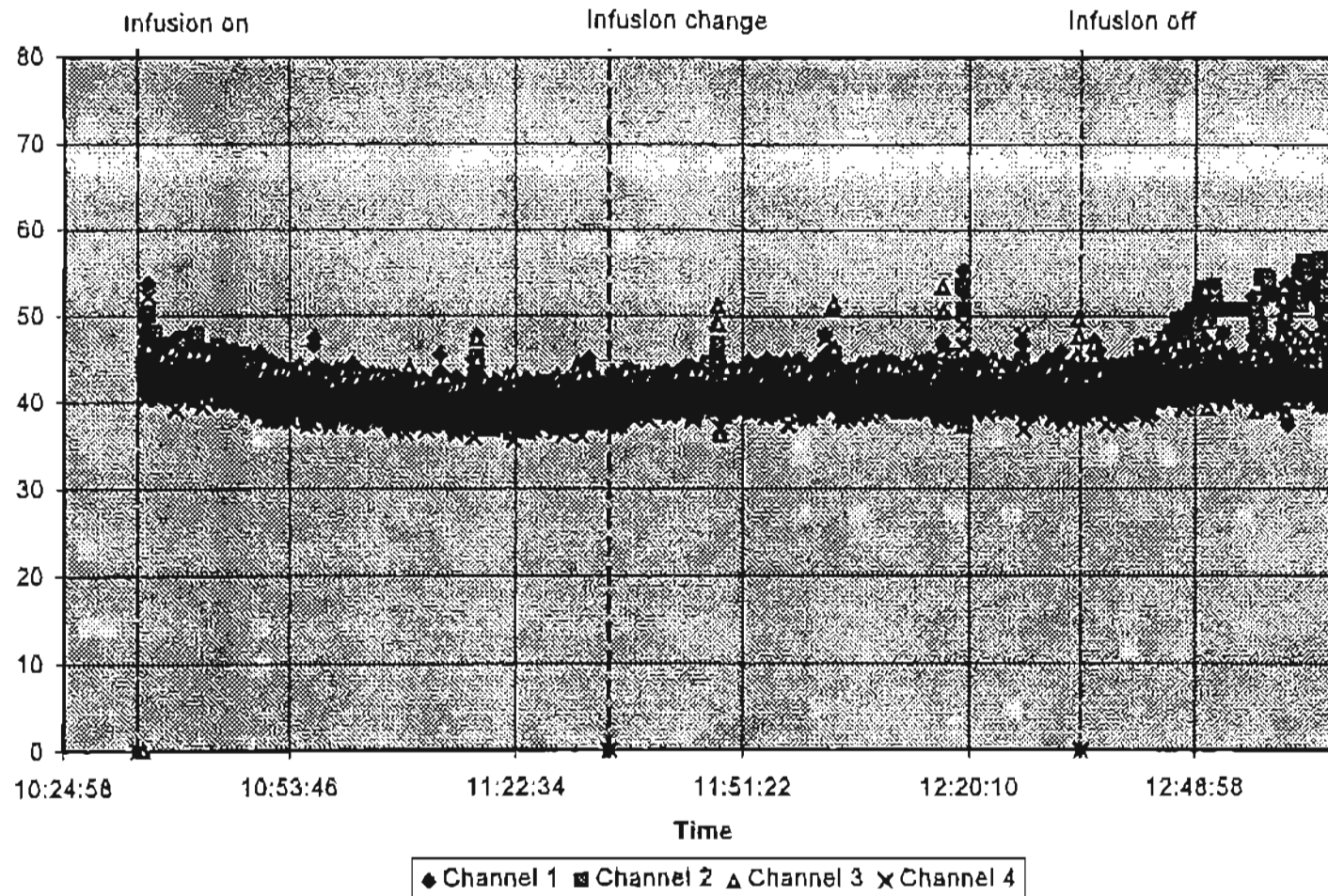
These are the experimental data obtained from Experiment 1 (02 May 1996).



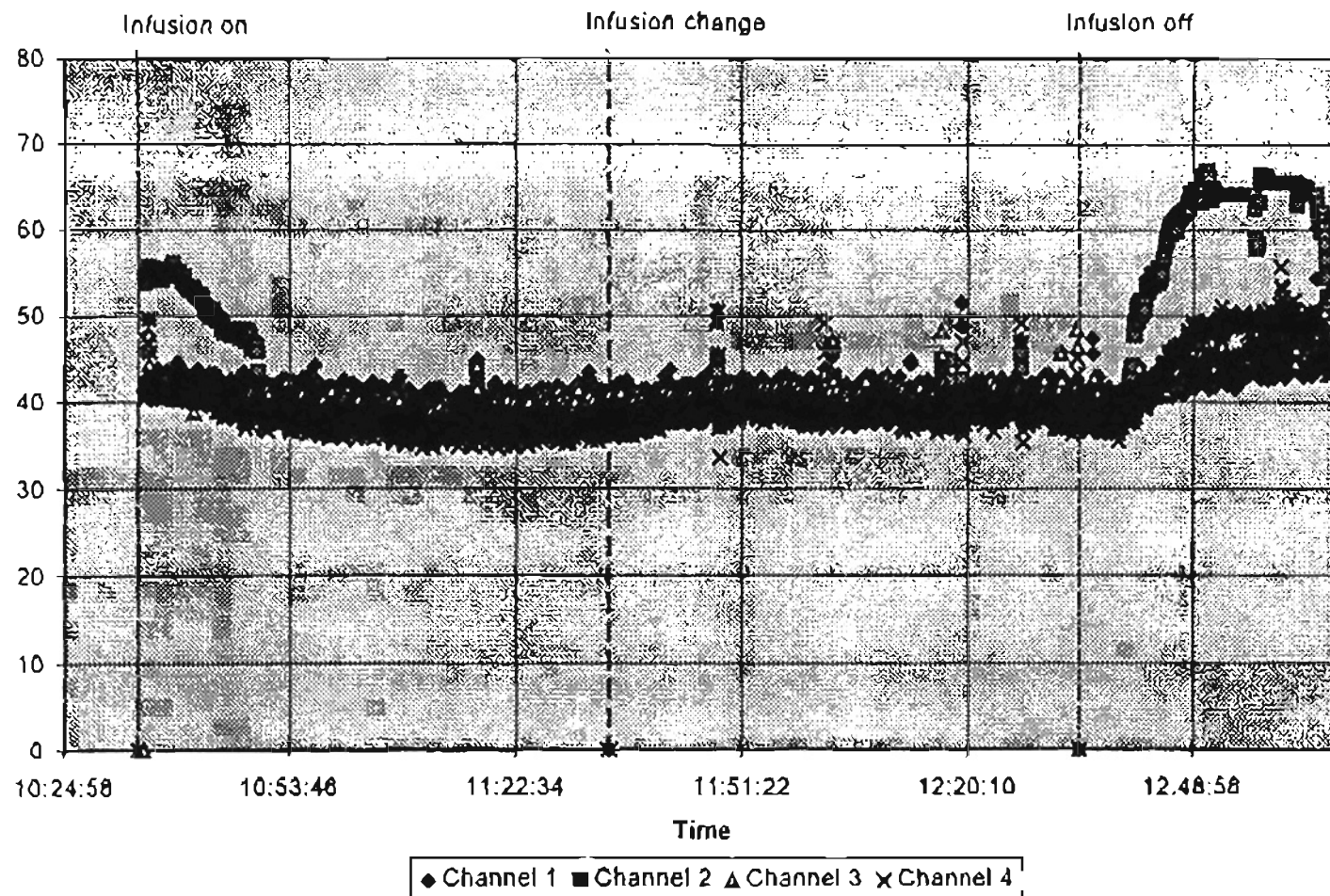
ATHETA03



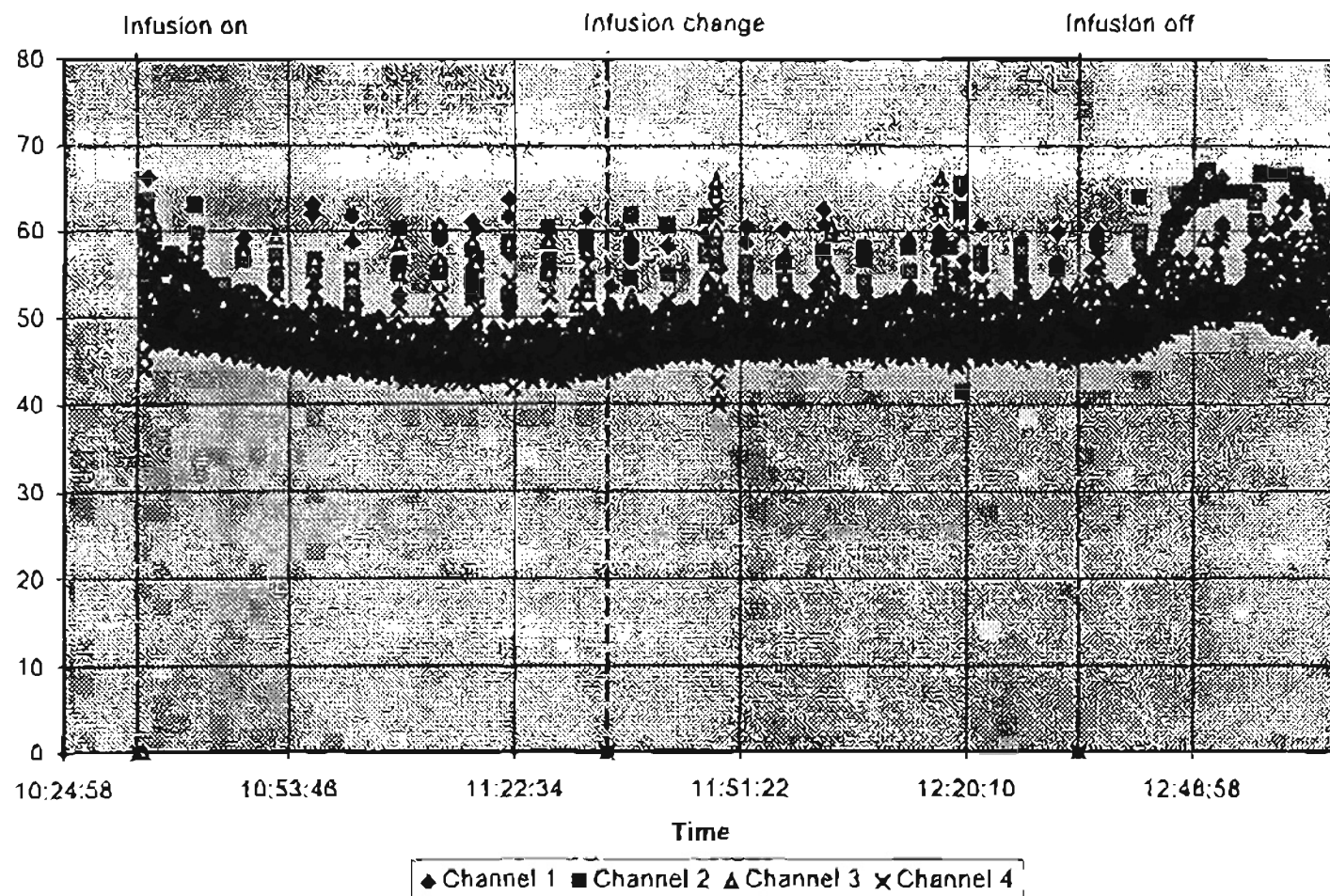
AALPHA03



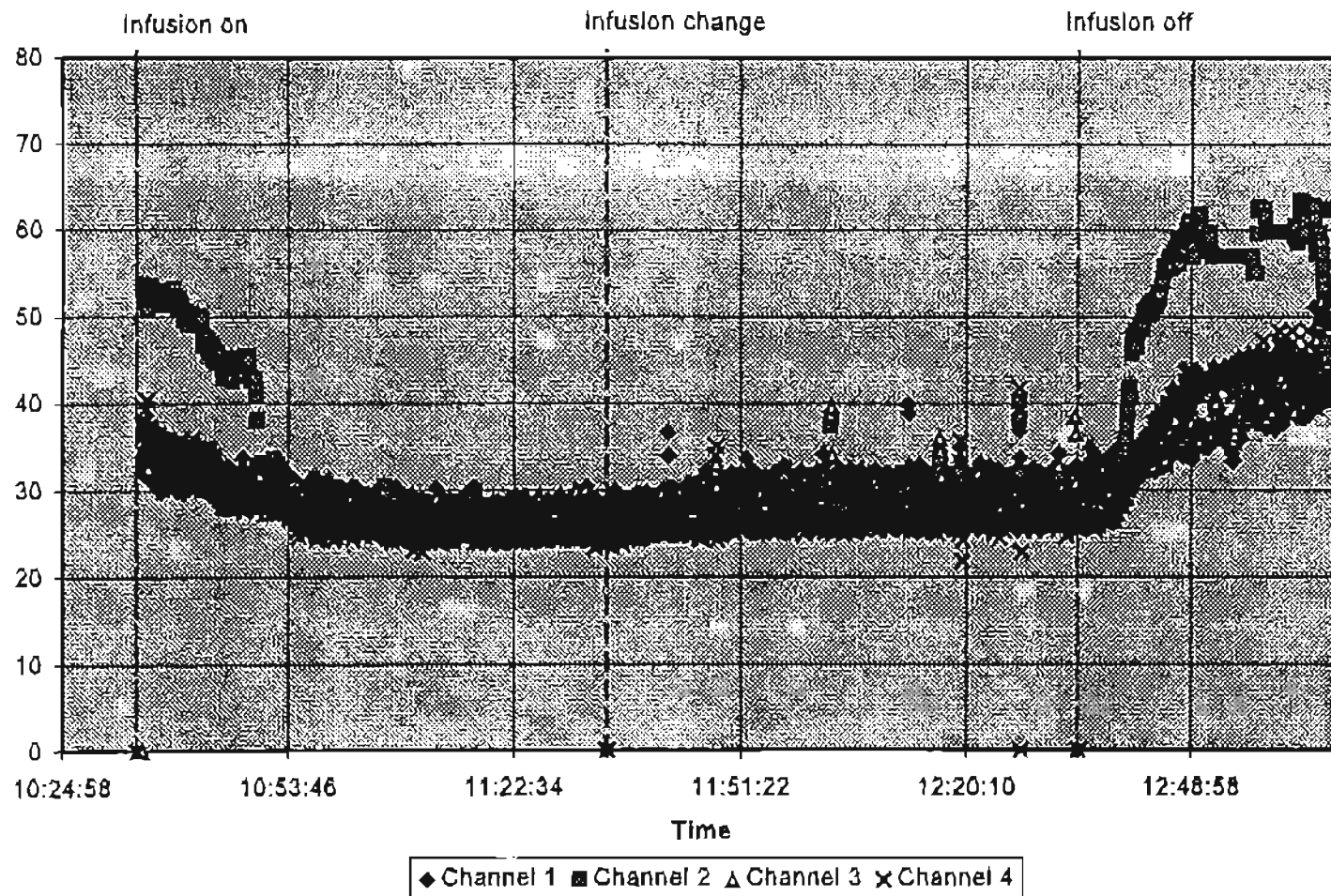
ABETA03



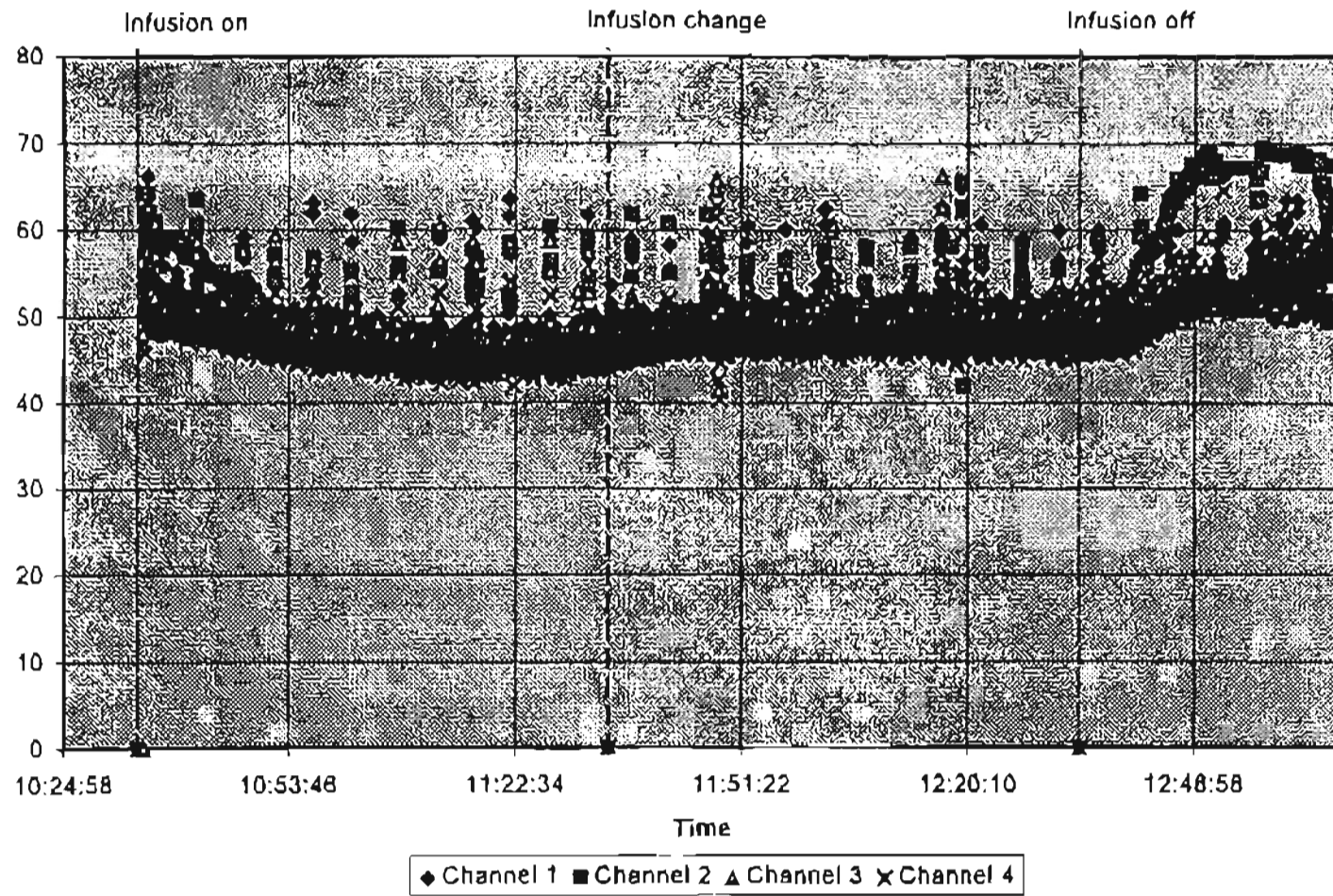
TOTPOW03



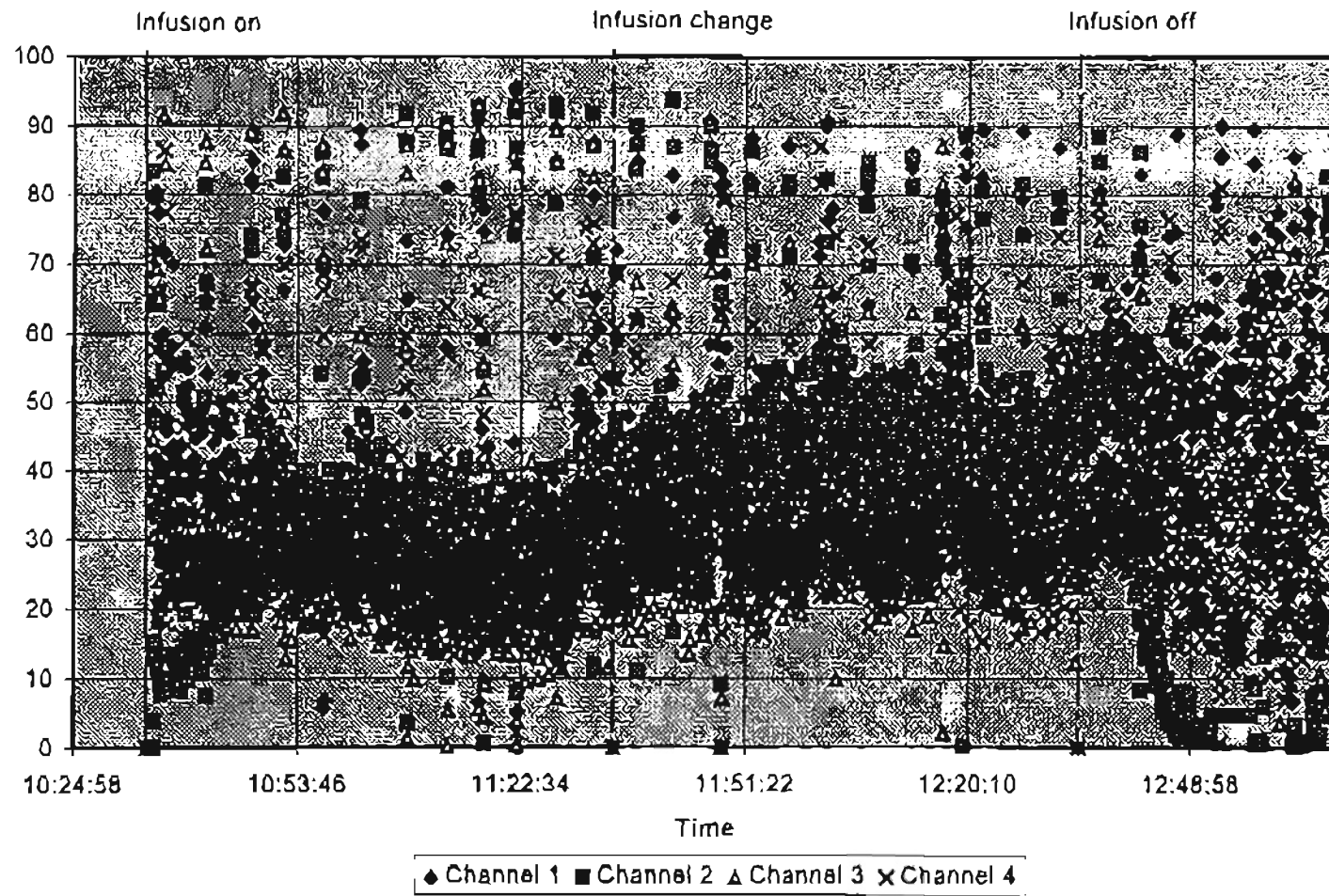
PBI03



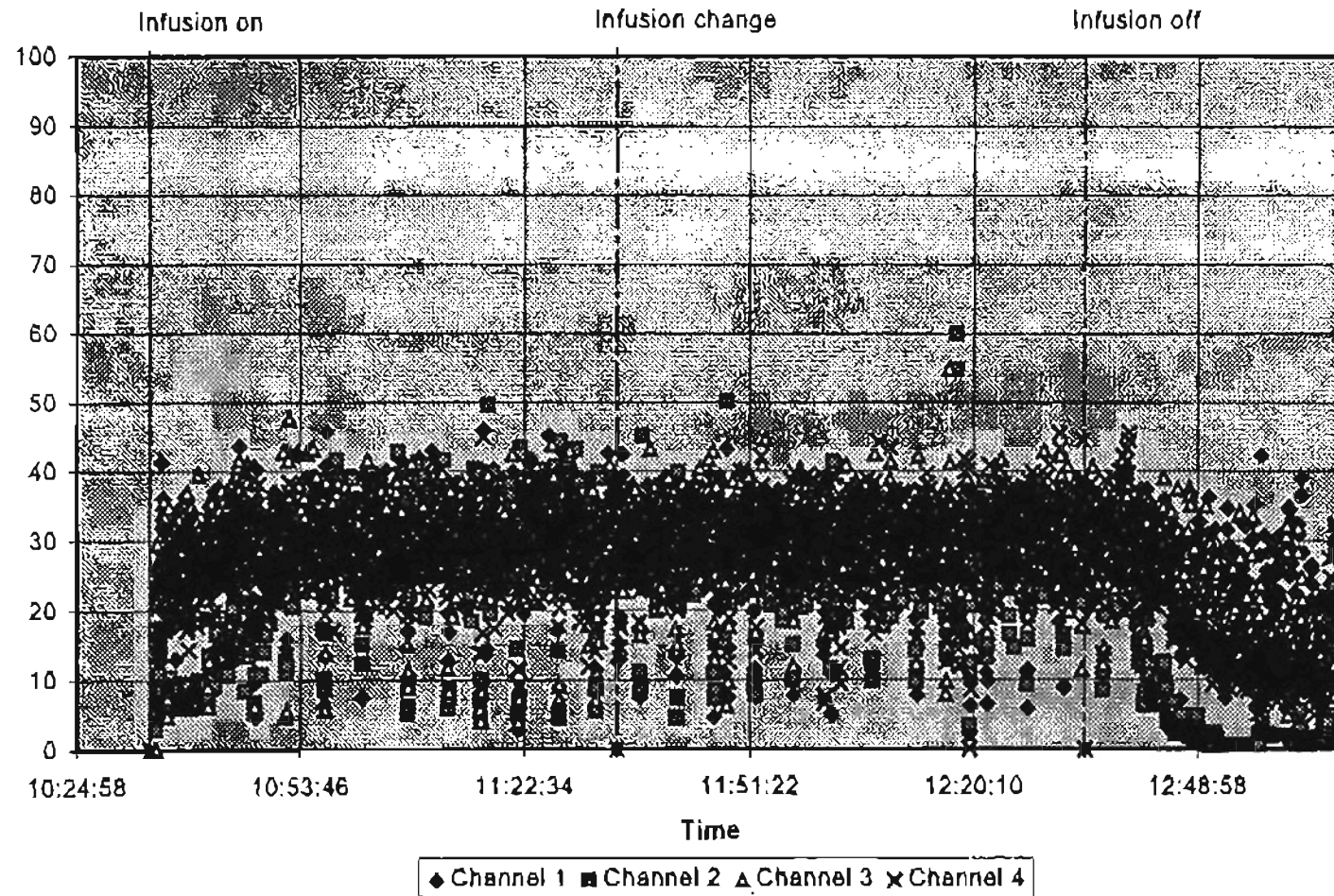
PBI03

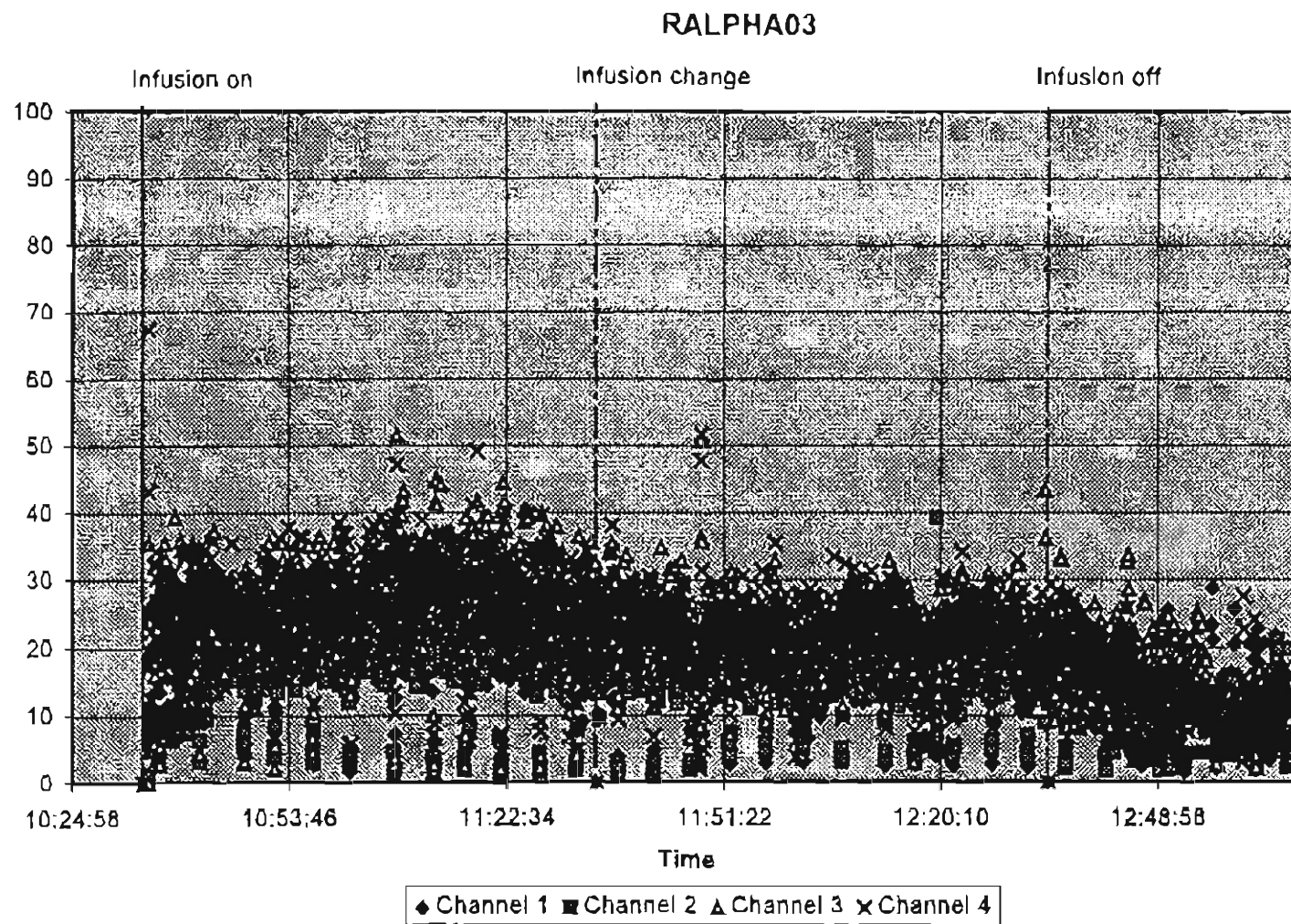


RDELTA03

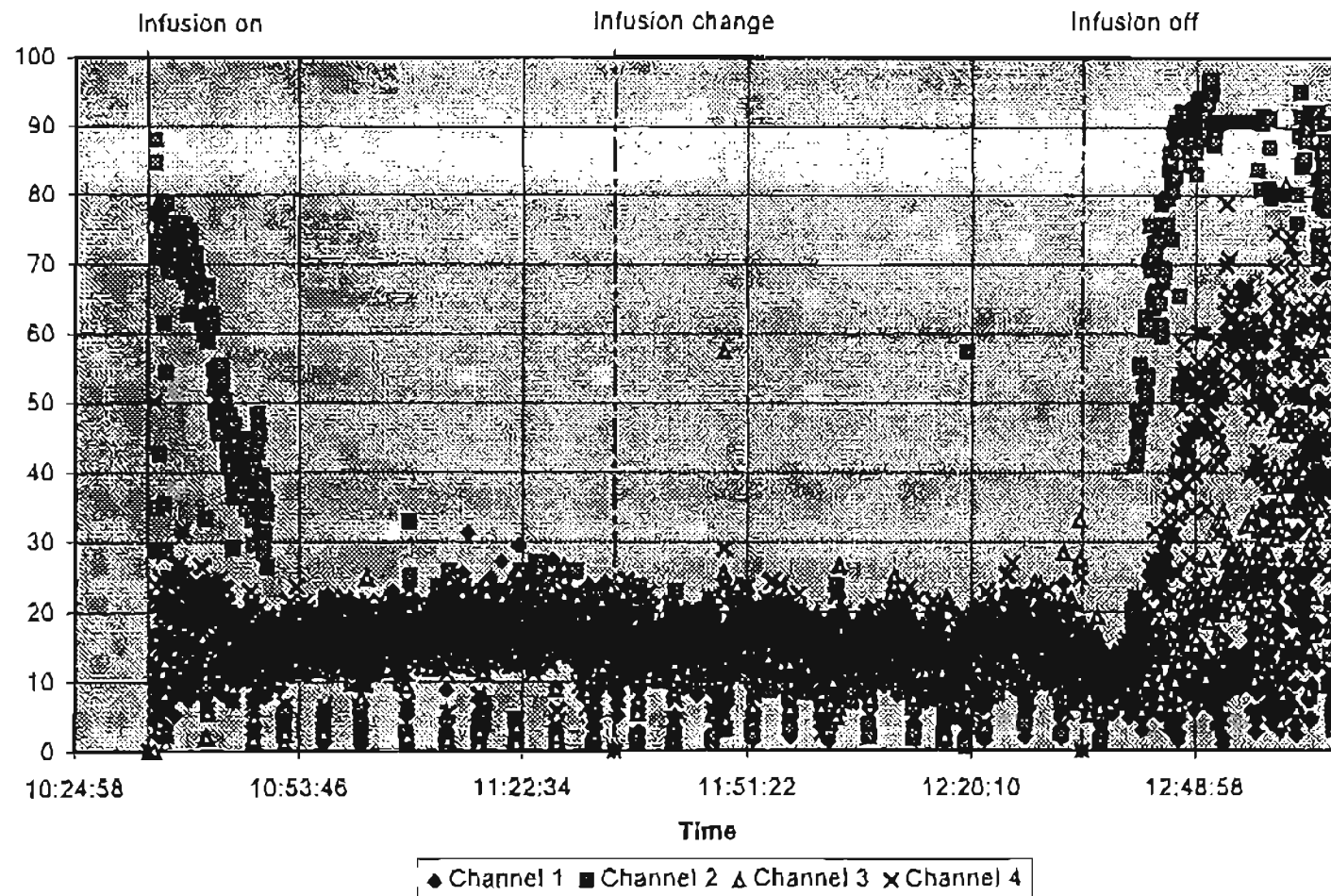


RTHETA03

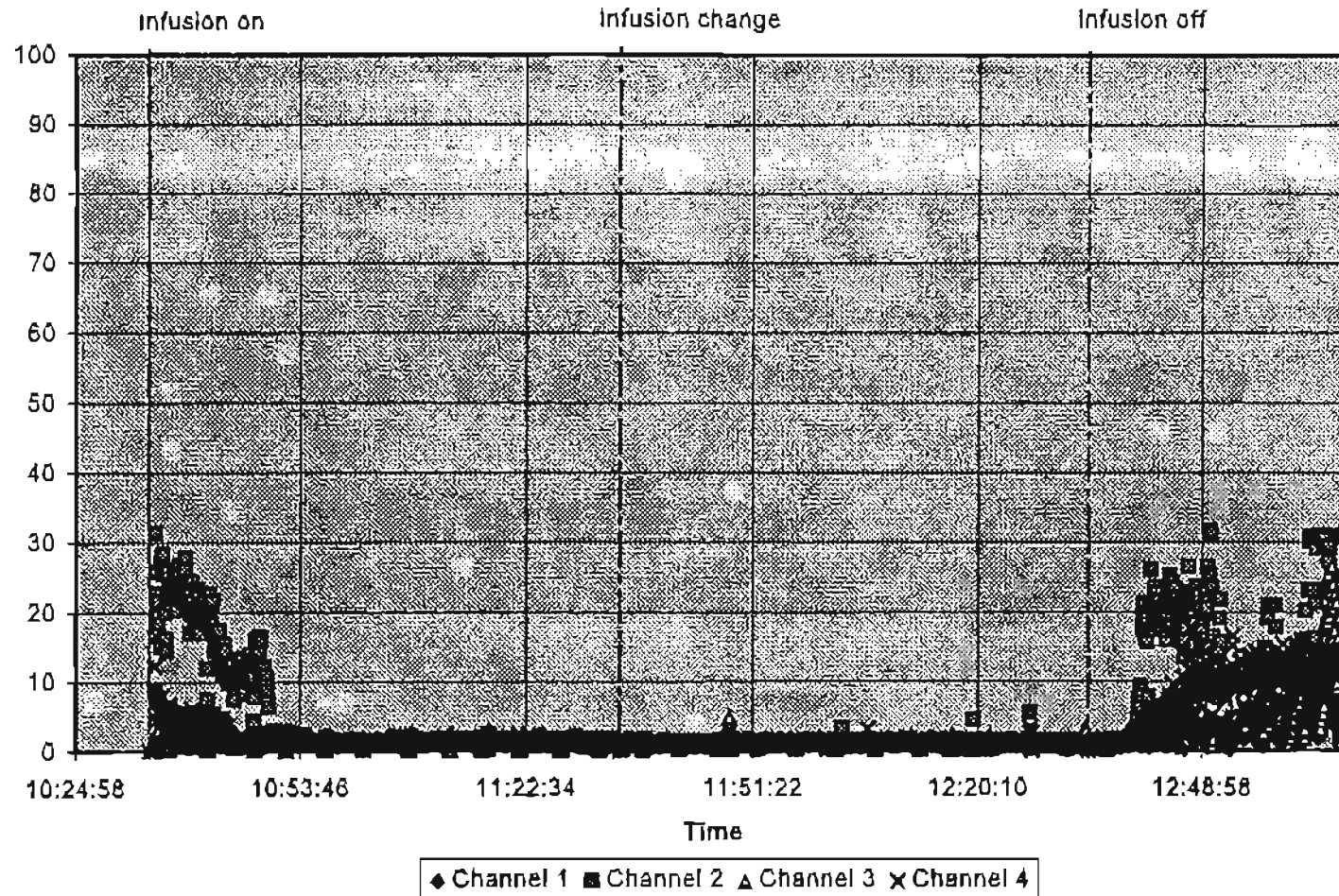


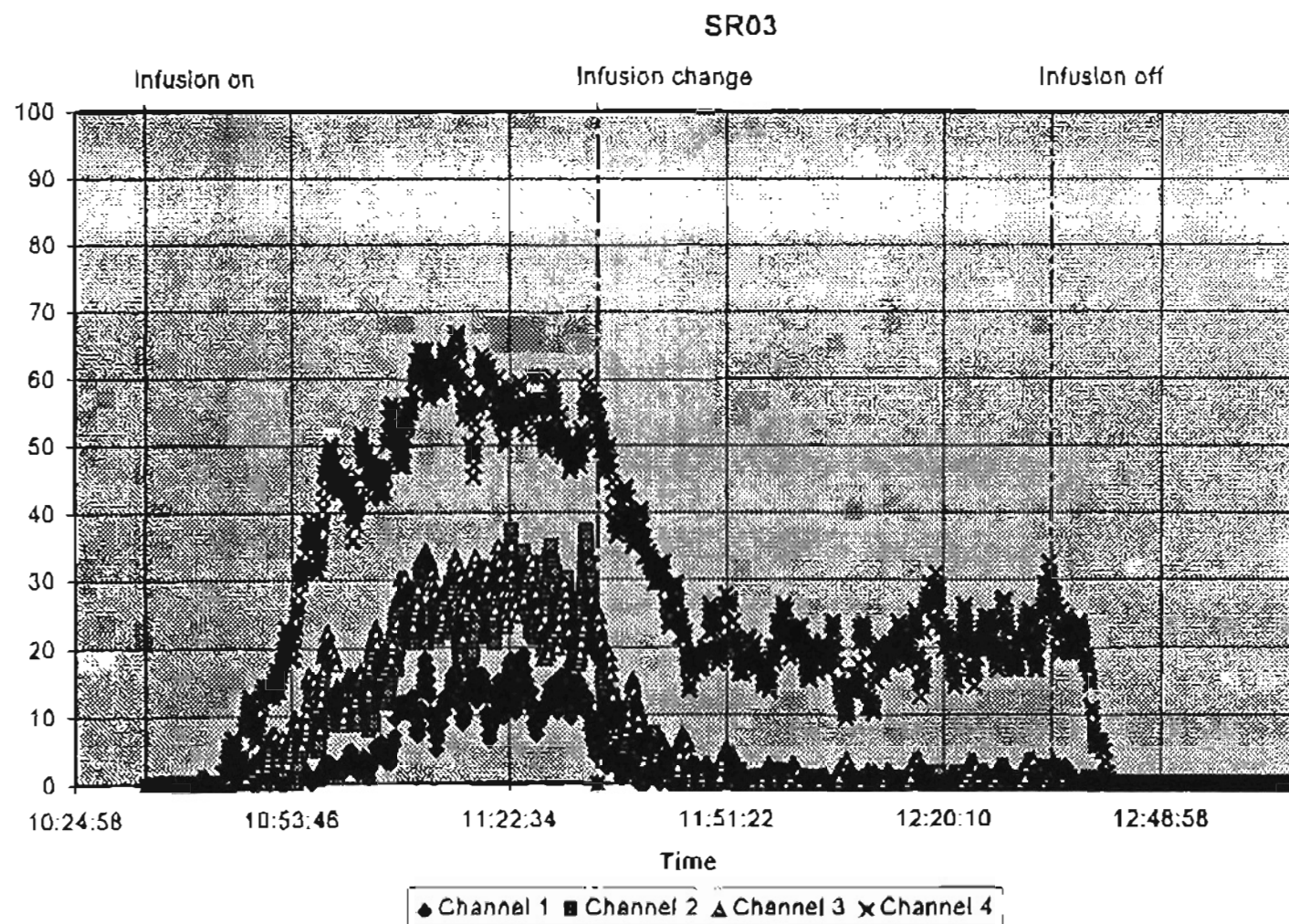


RBETA03

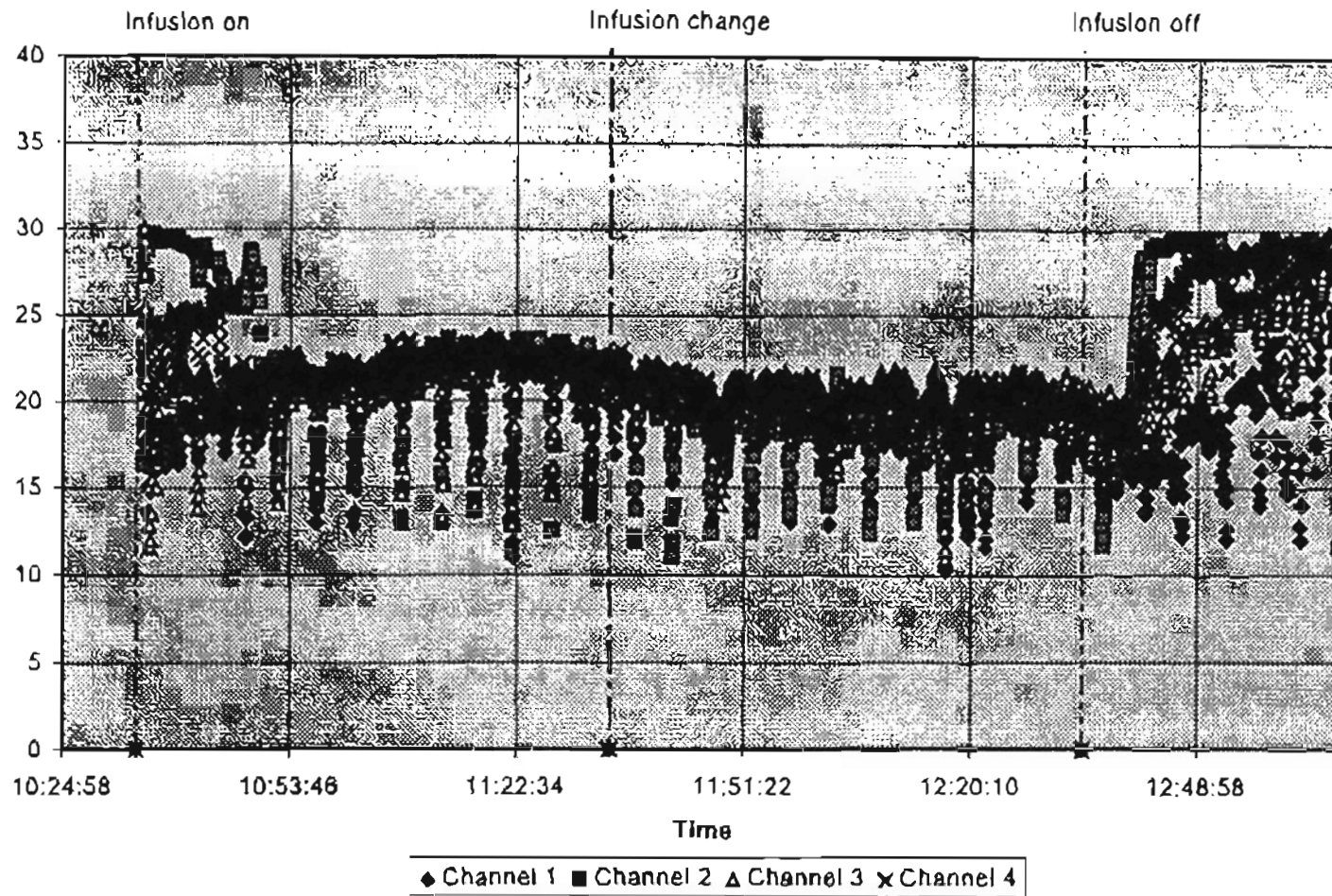


PBRAT03

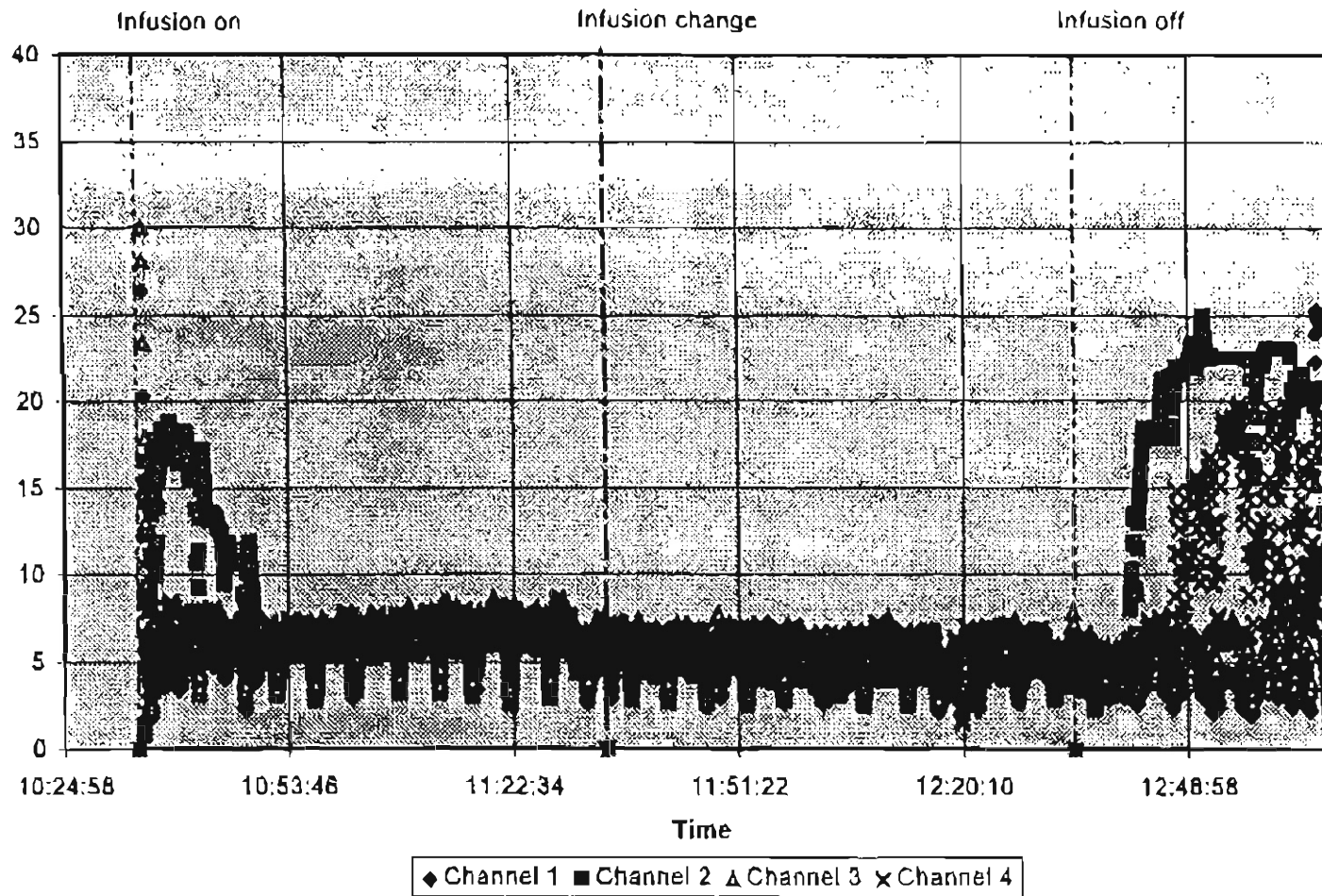




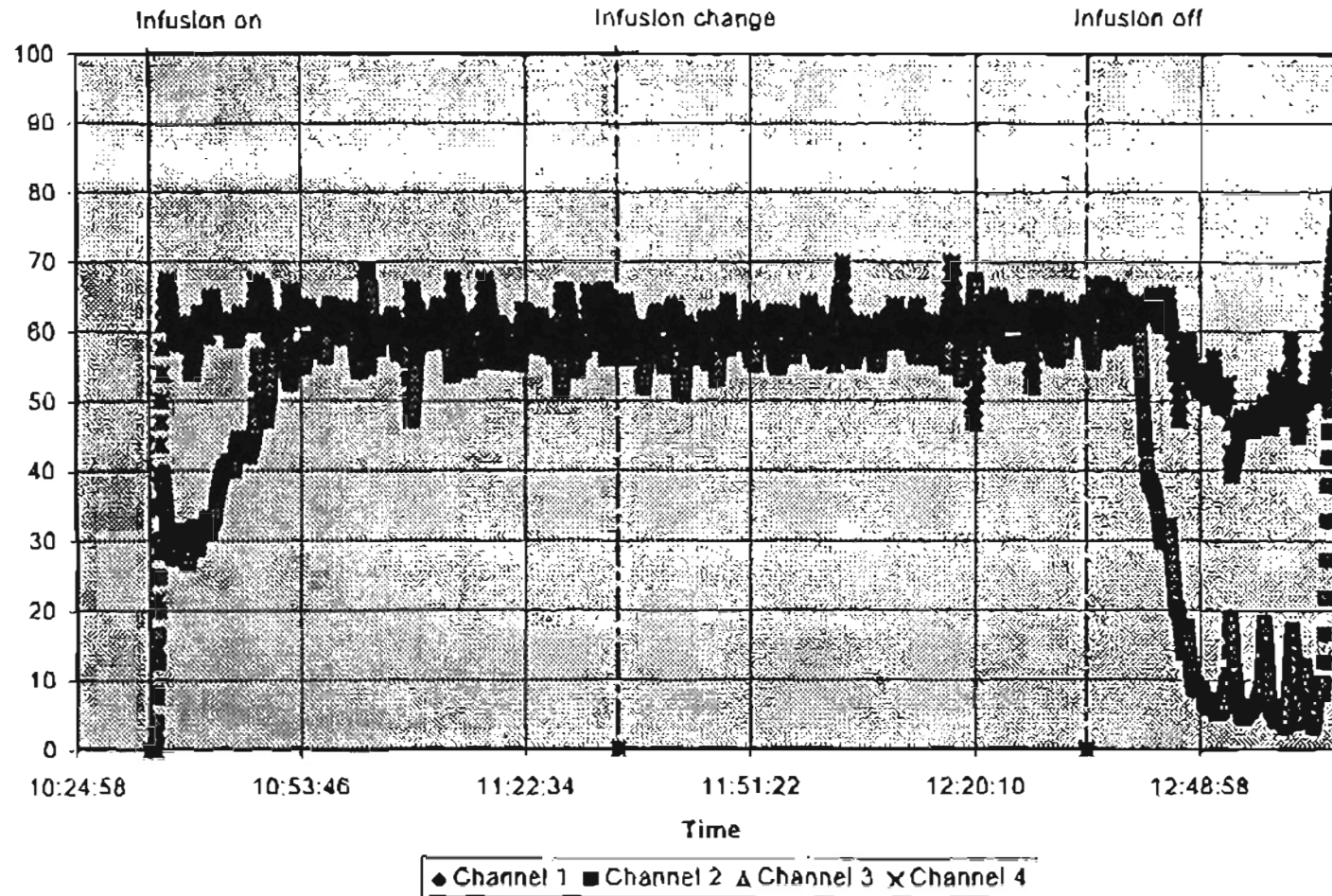
SEF03



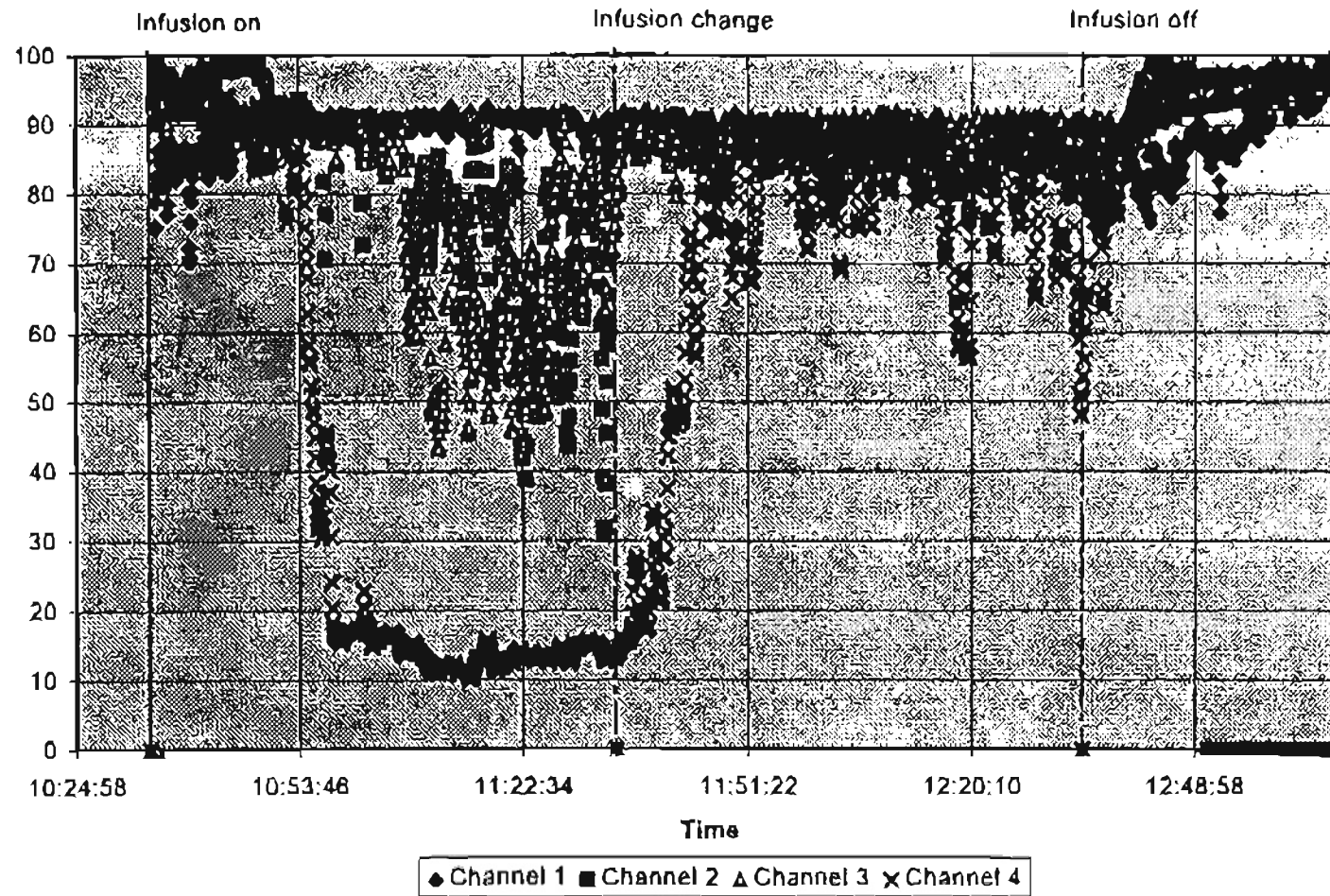
MEDFRQ03



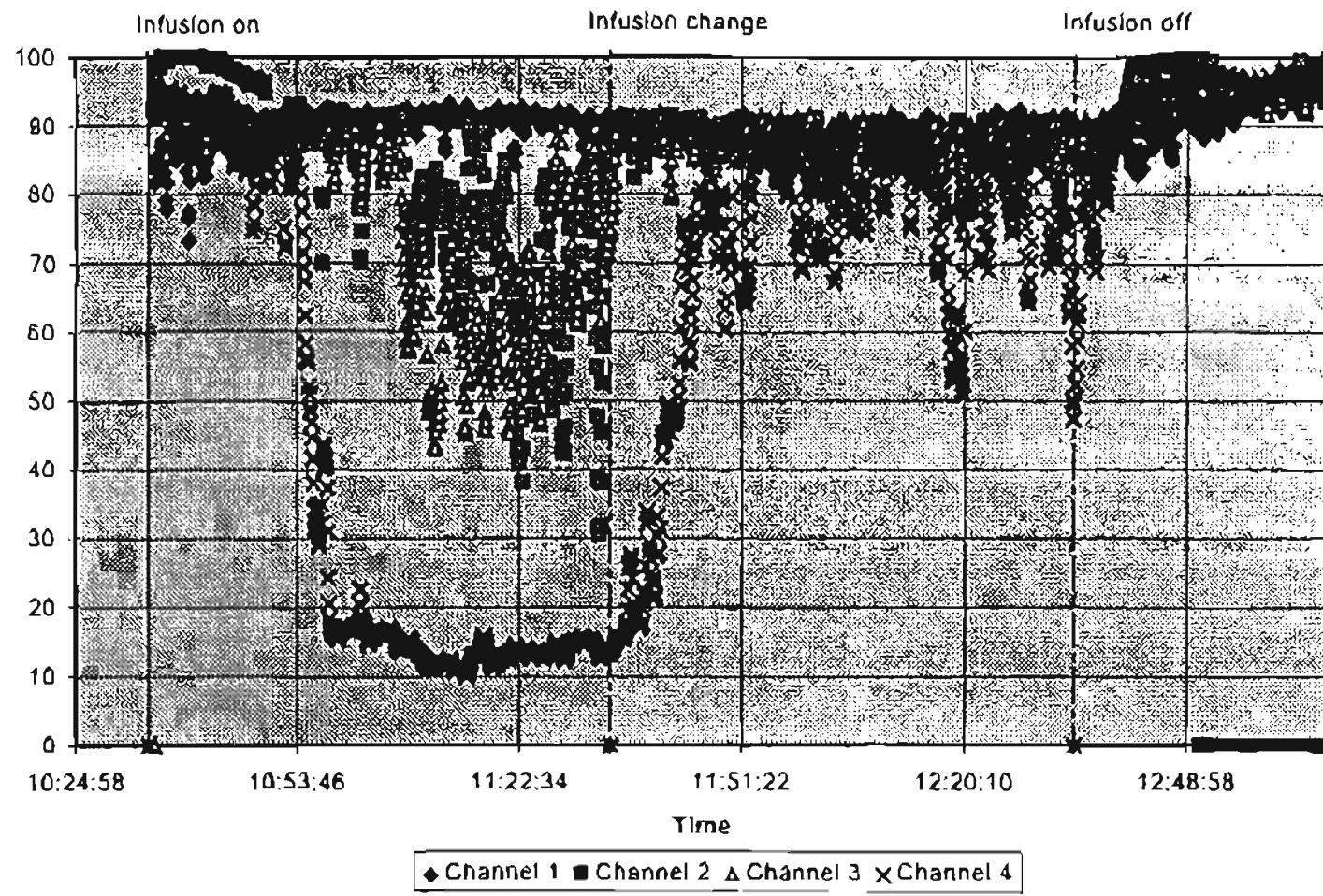
ASYM03



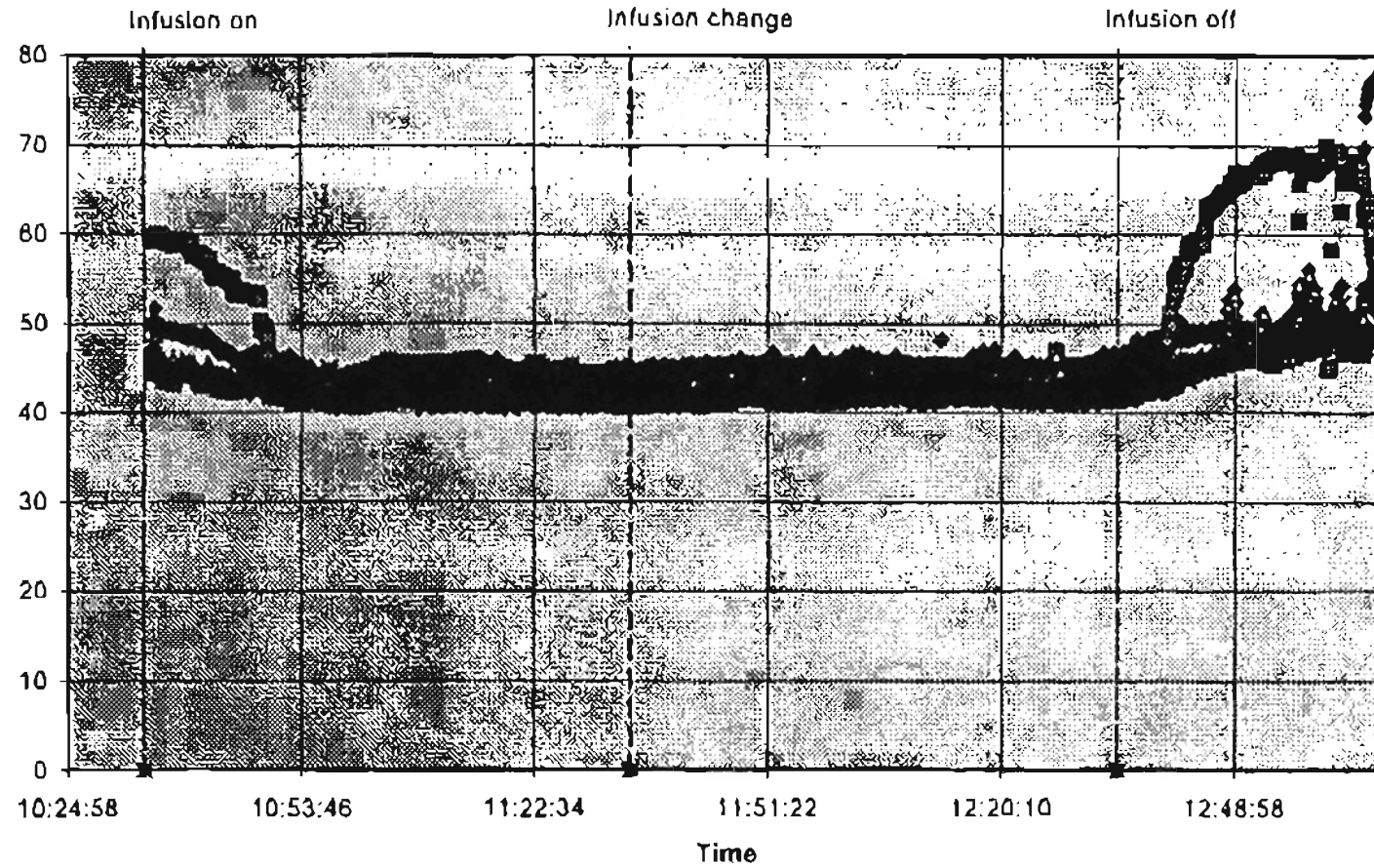
BISa04



BISALT

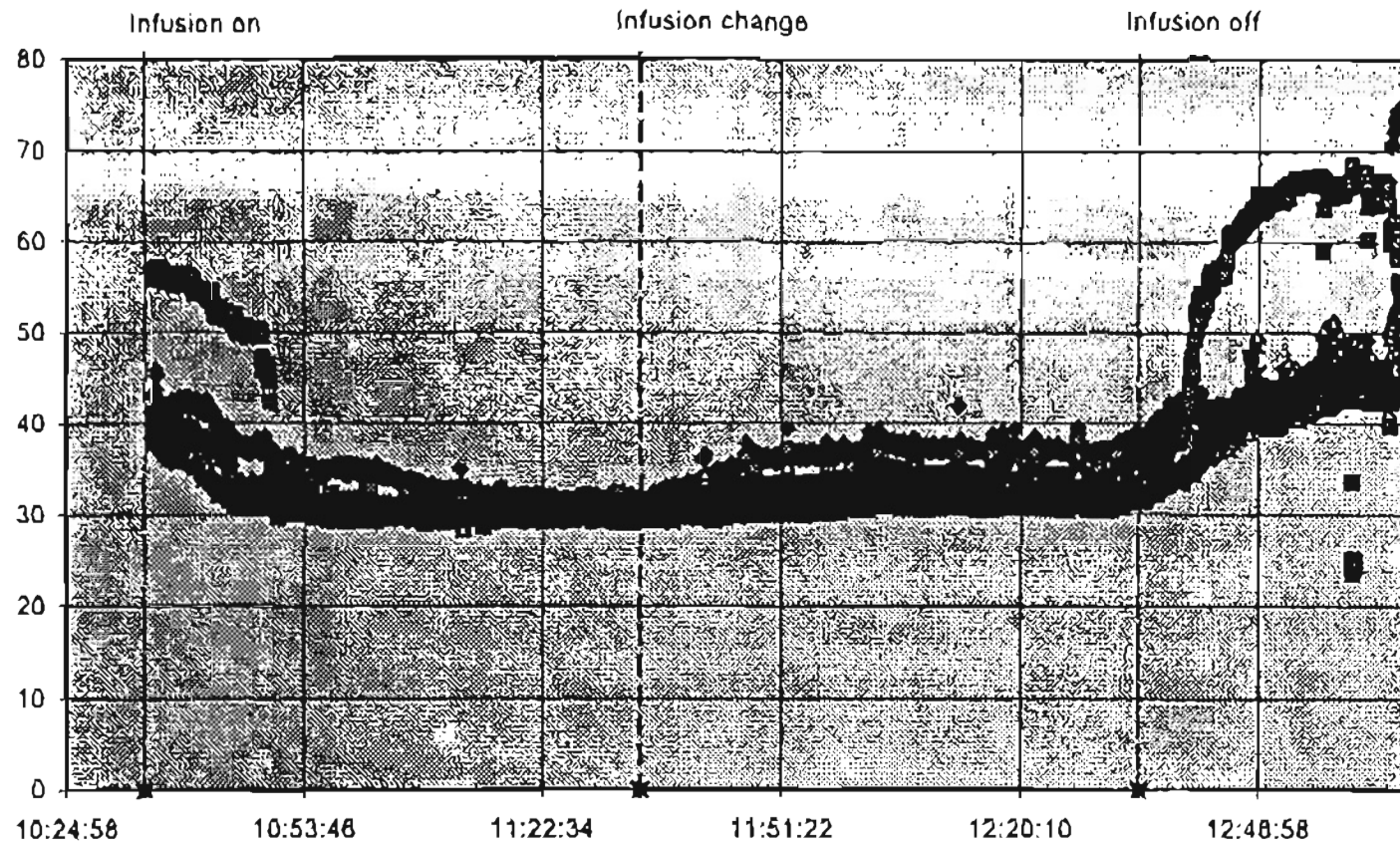


EMGH101



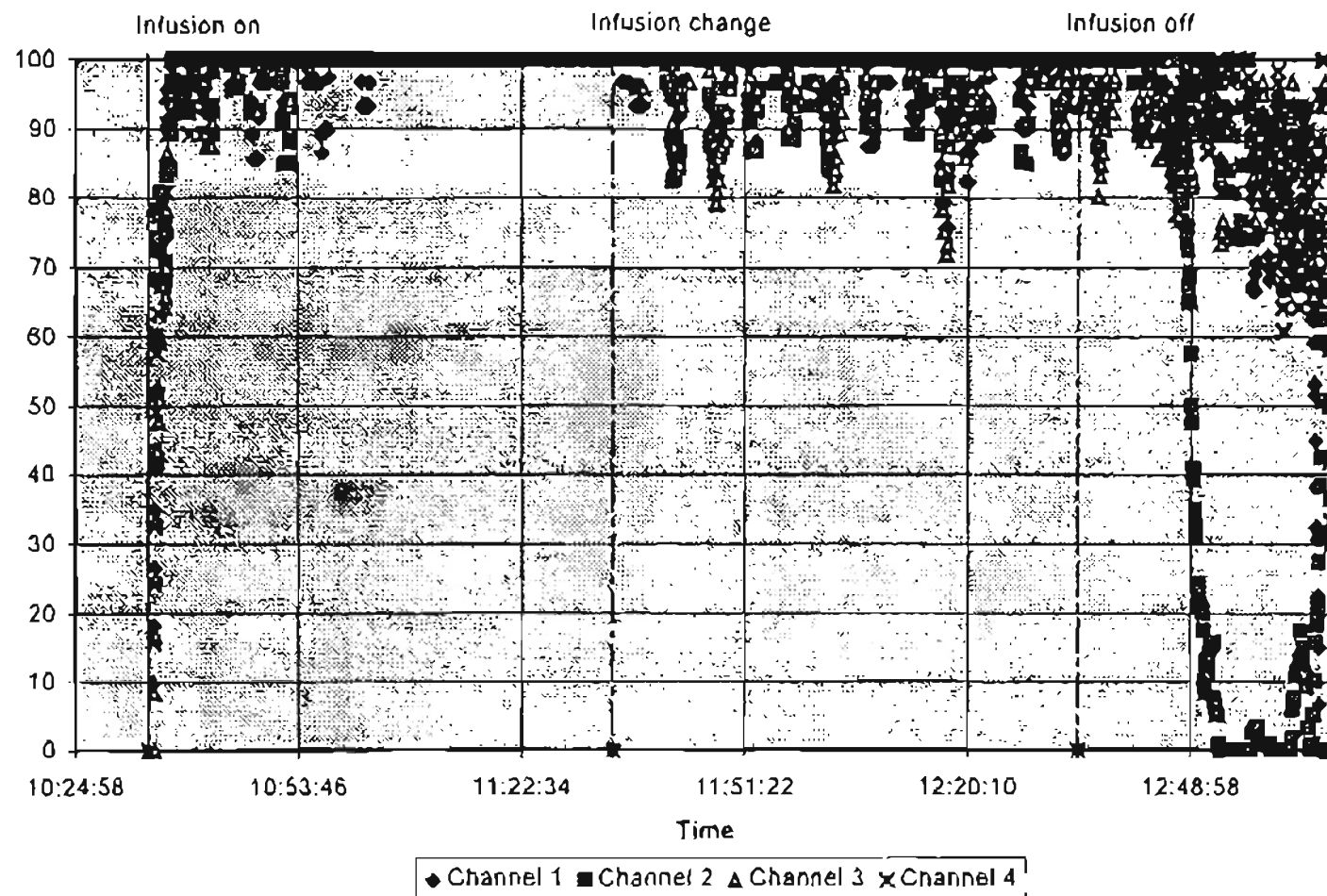
◆ Channel 1 ■ Channel 2 ▲ Channel 3 ✕ Channel 4

EMGLOW

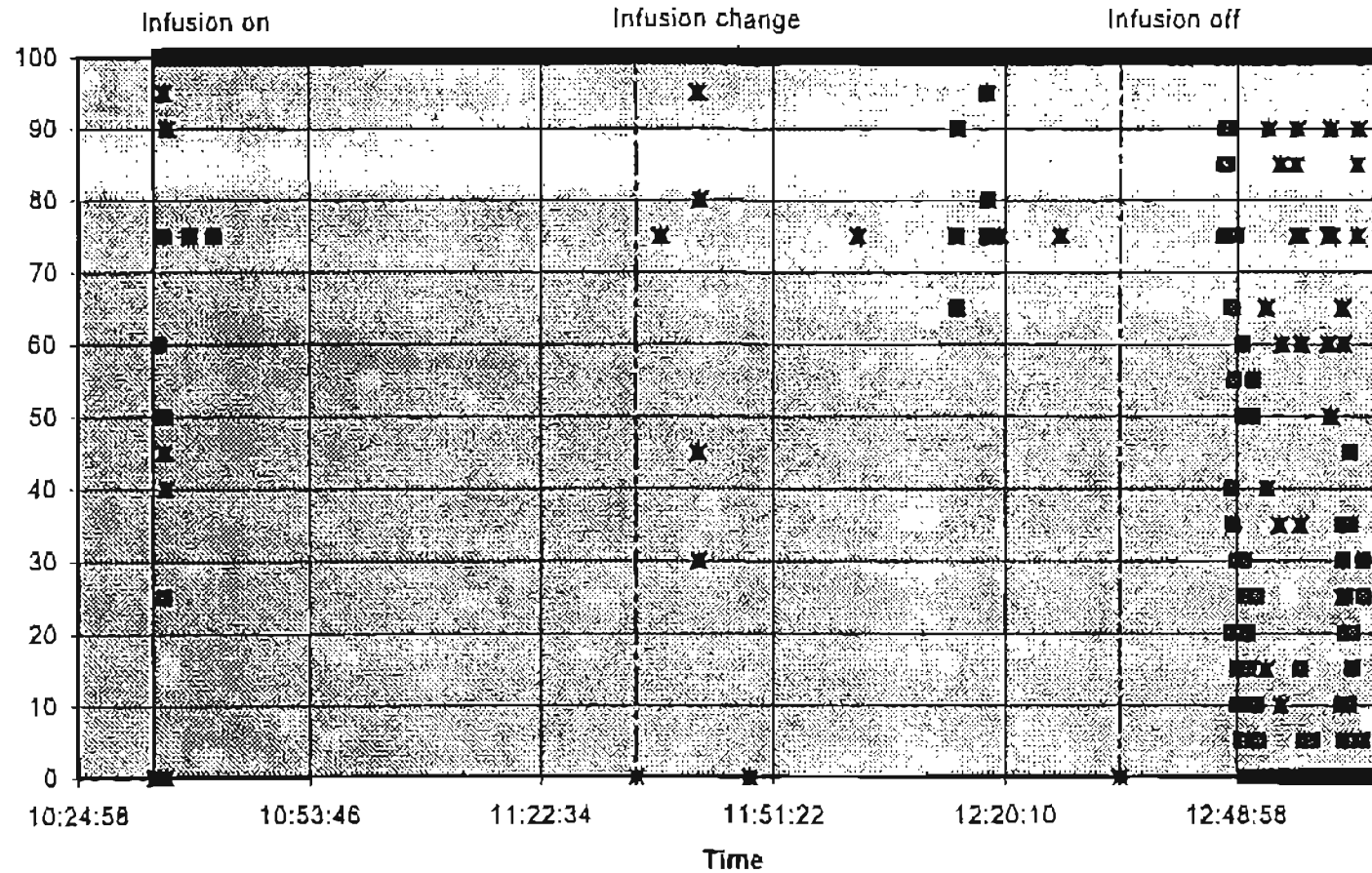


◆ Channel 1 ■ Channel 2 ▲ Channel 3 ✕ Channel 4

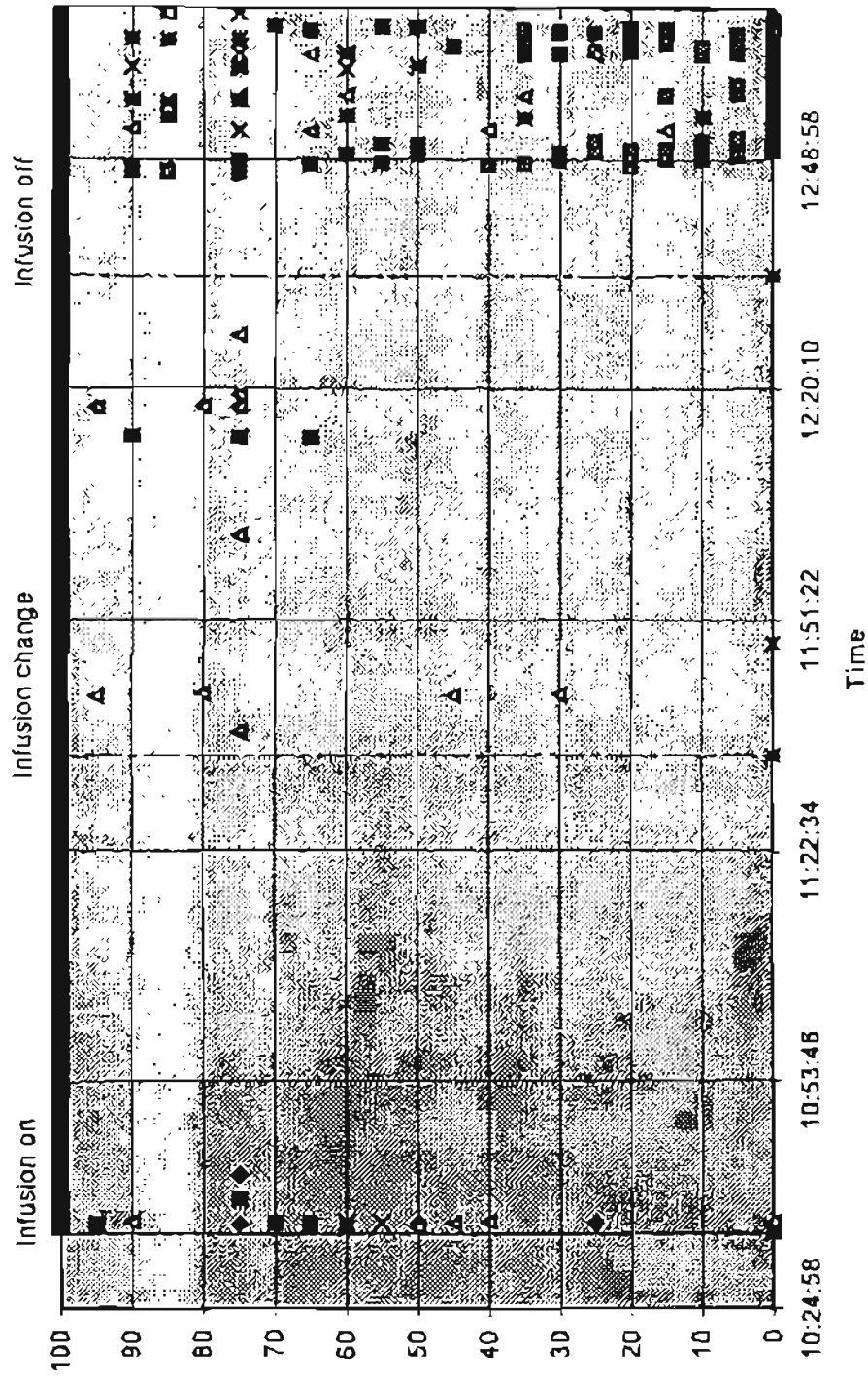
SQ103



ASYSQ103

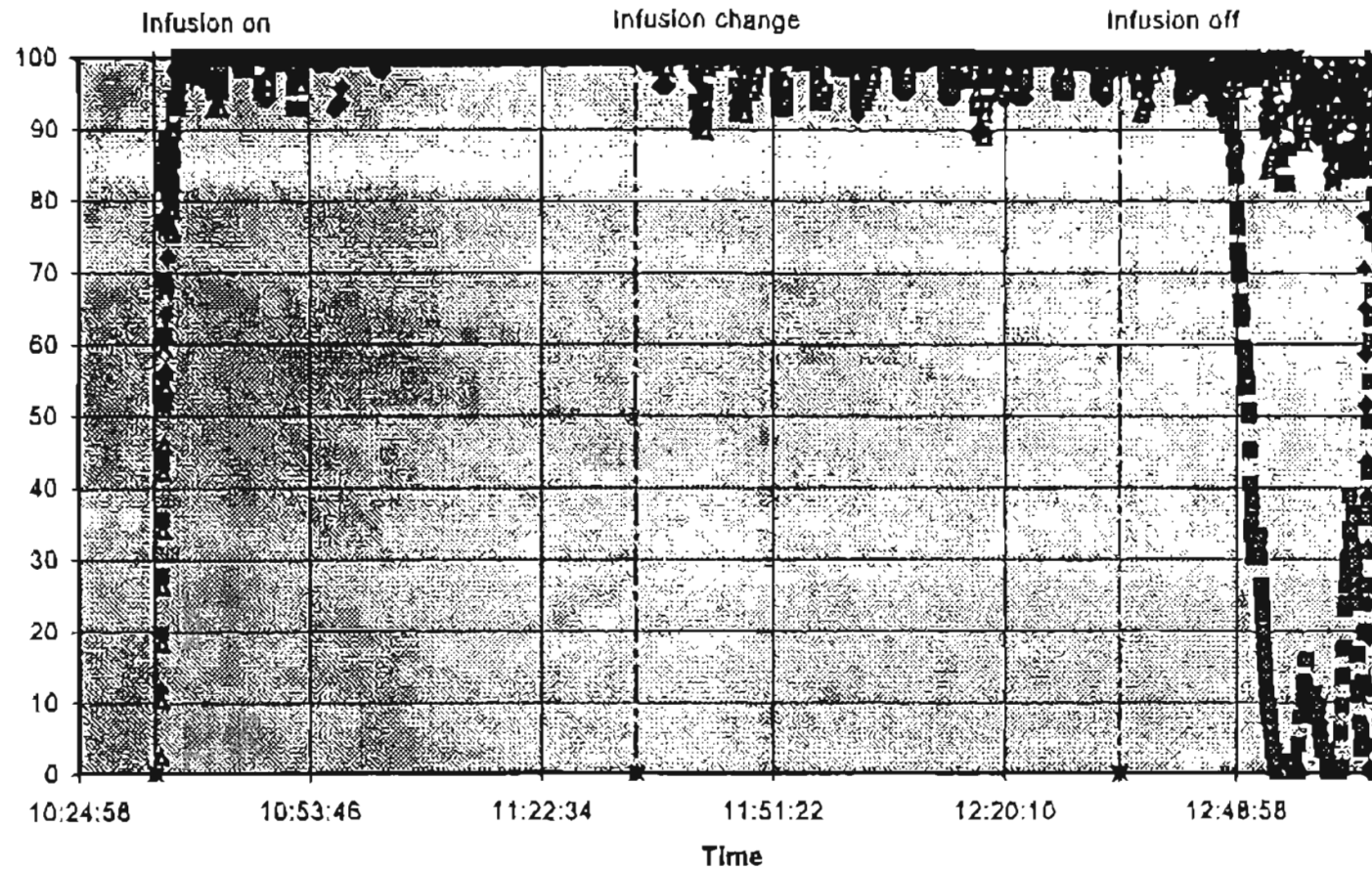


PSQID2



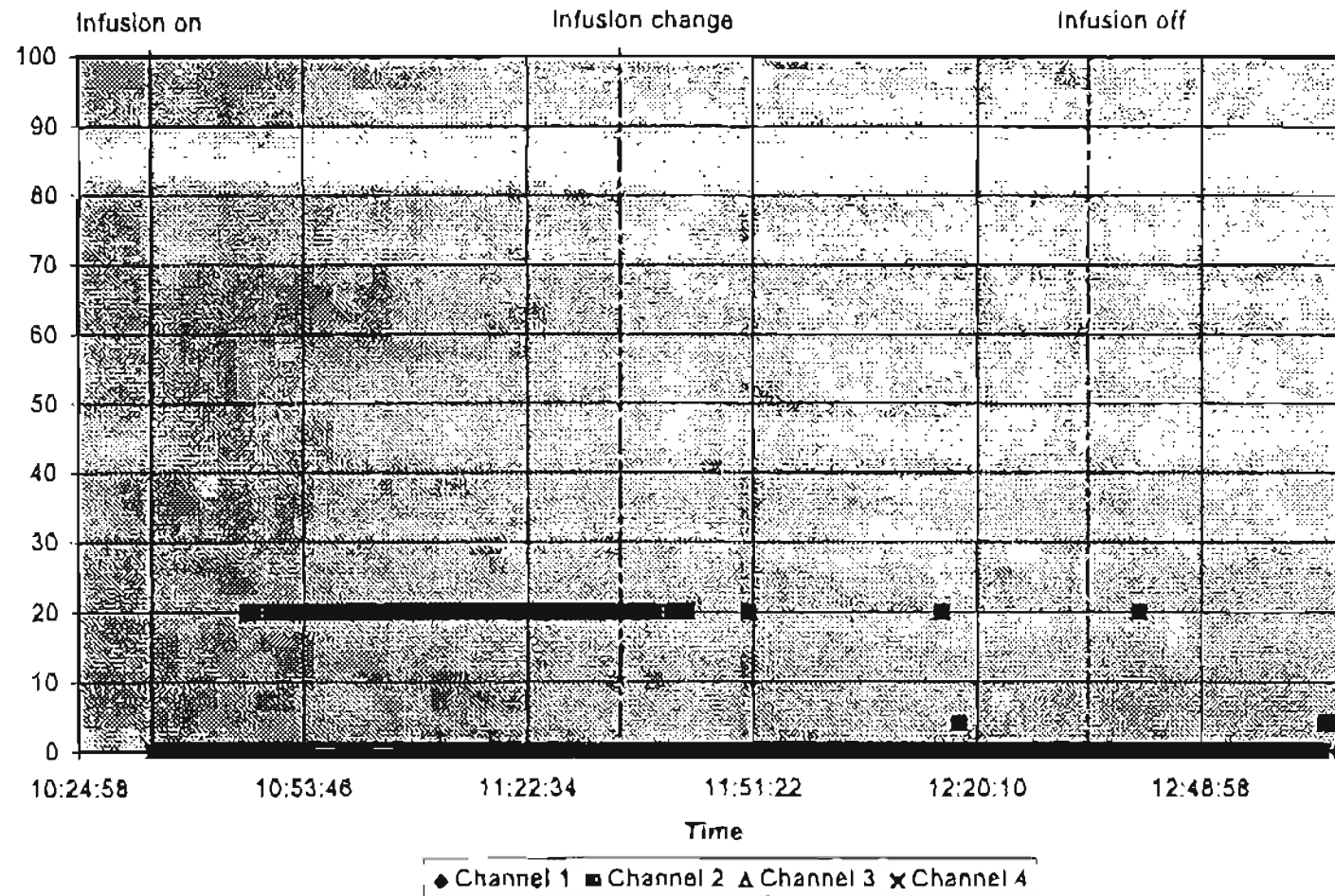
◆ Channel 1 ■ Channel 2 ▲ Channel 3 × Channel 4

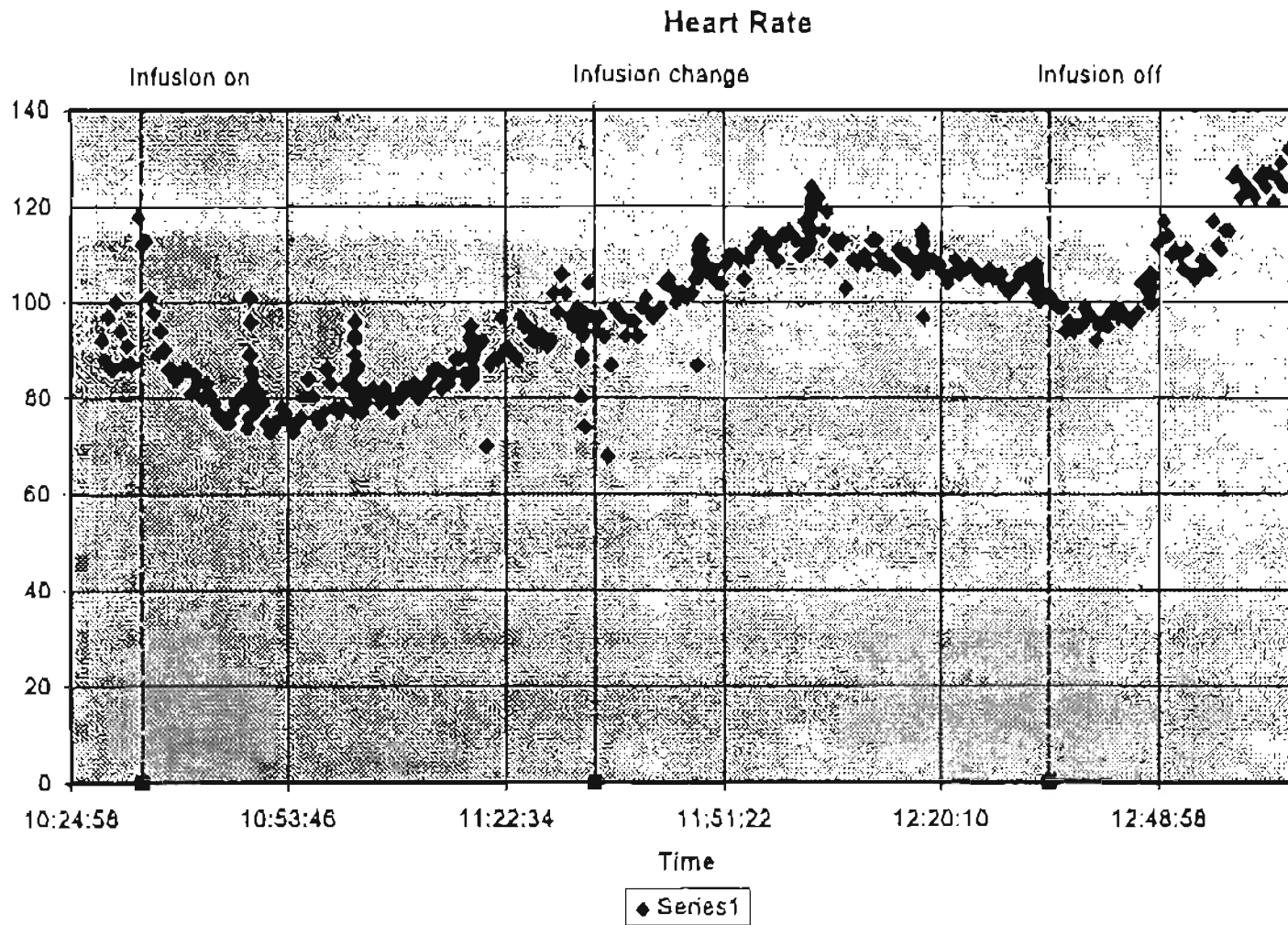
BSRSQ103



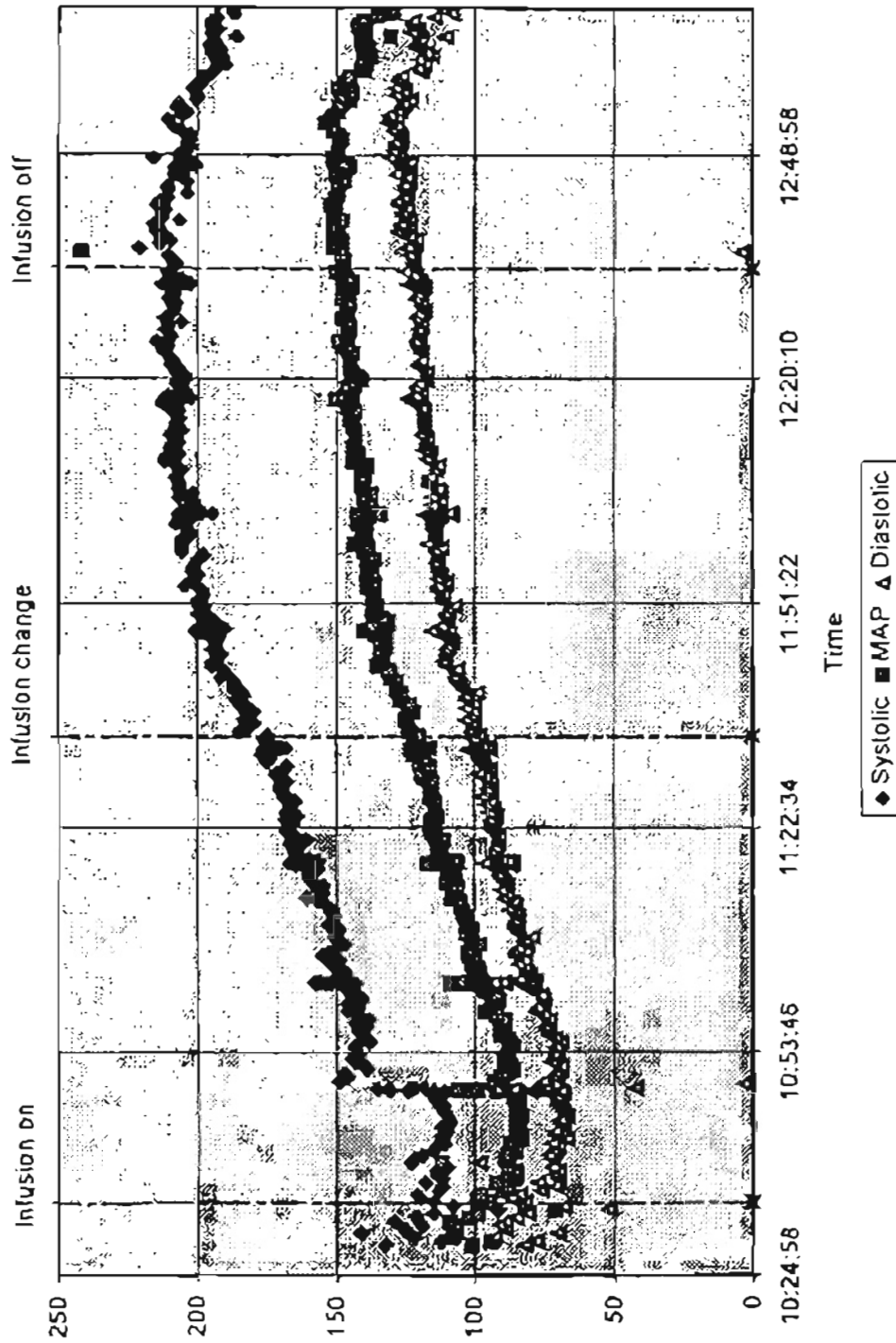
◆ Channel 1 ■ Channel 2 ▲ Channel 3 × Channel 4

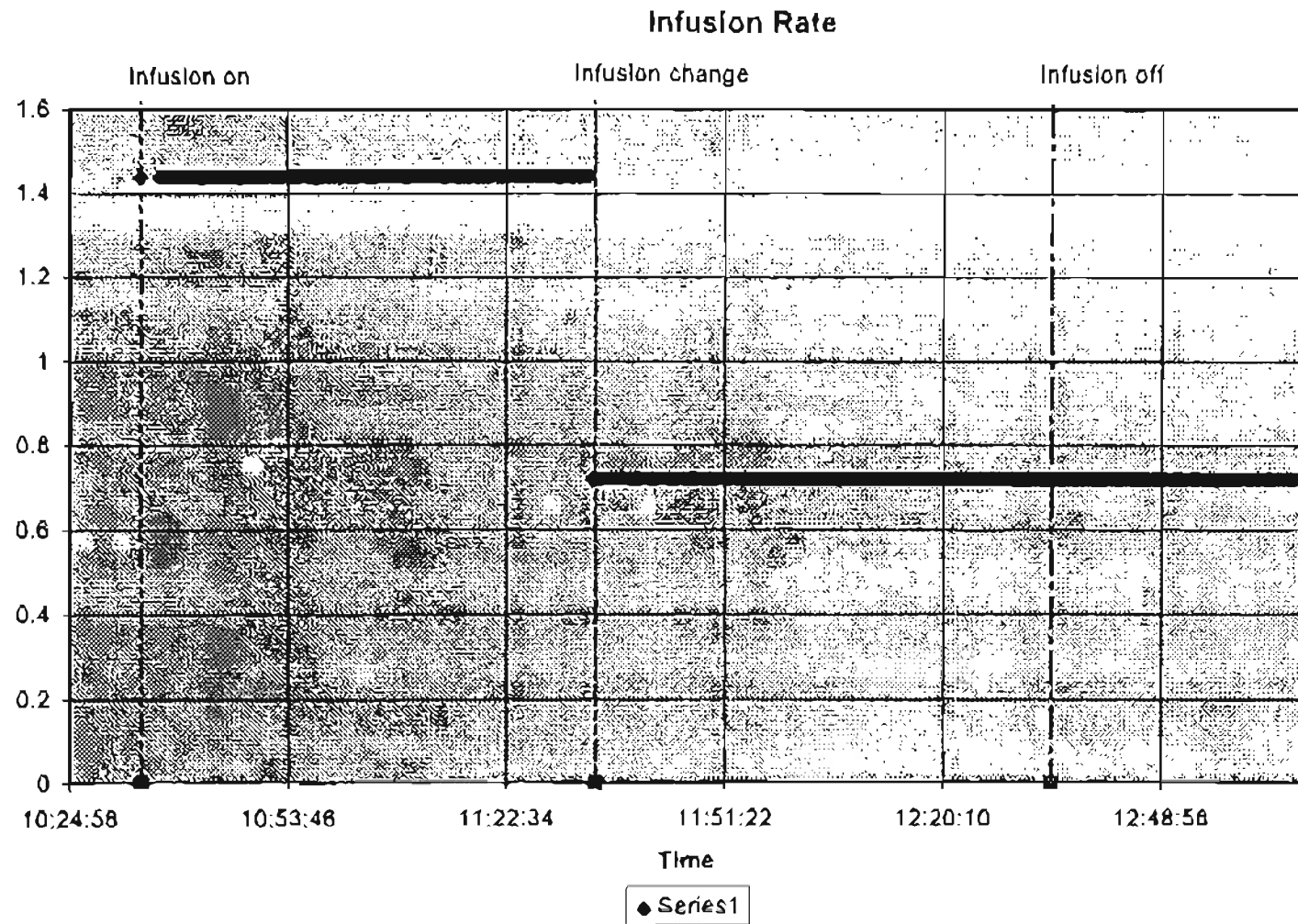
ARTF2

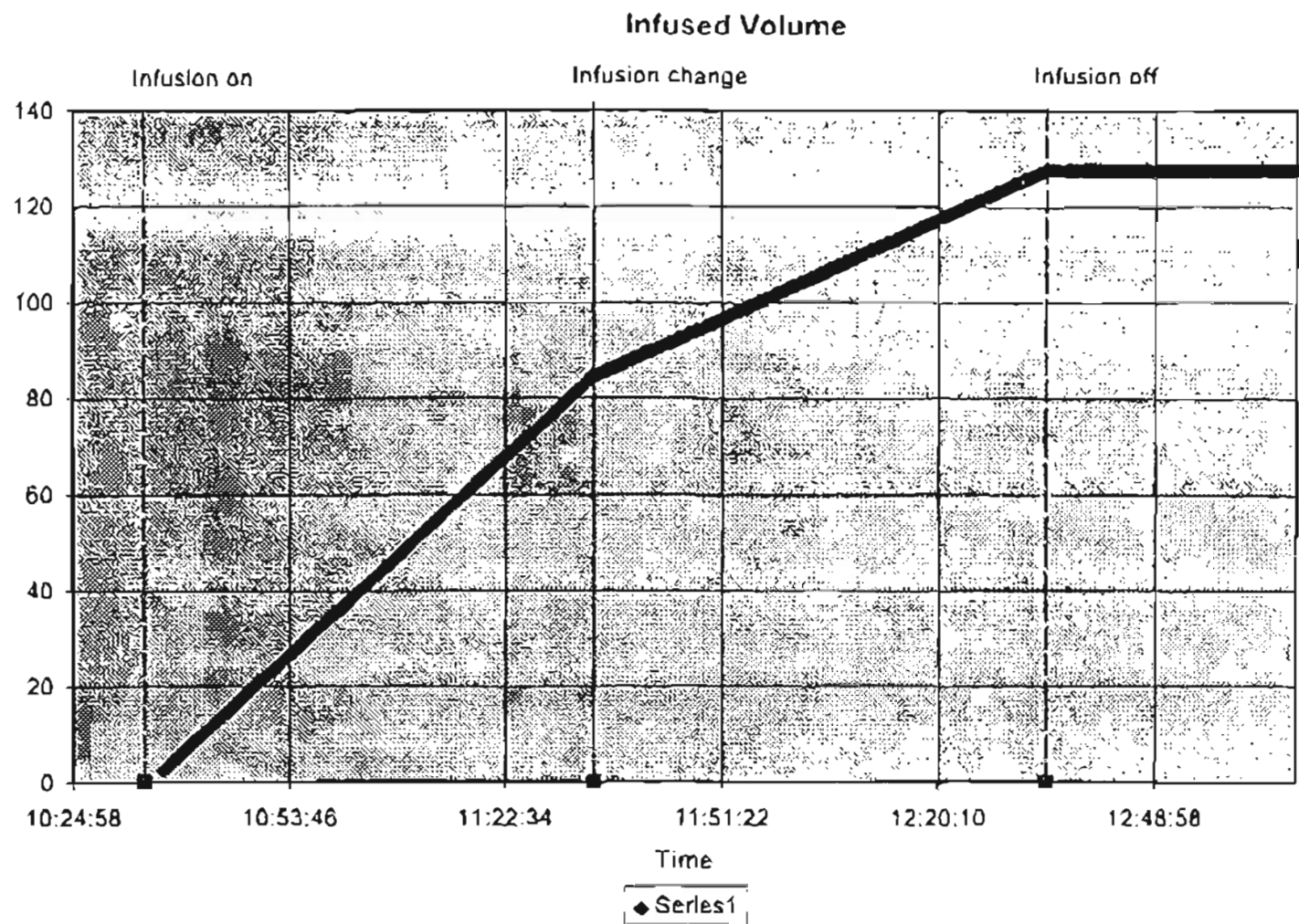




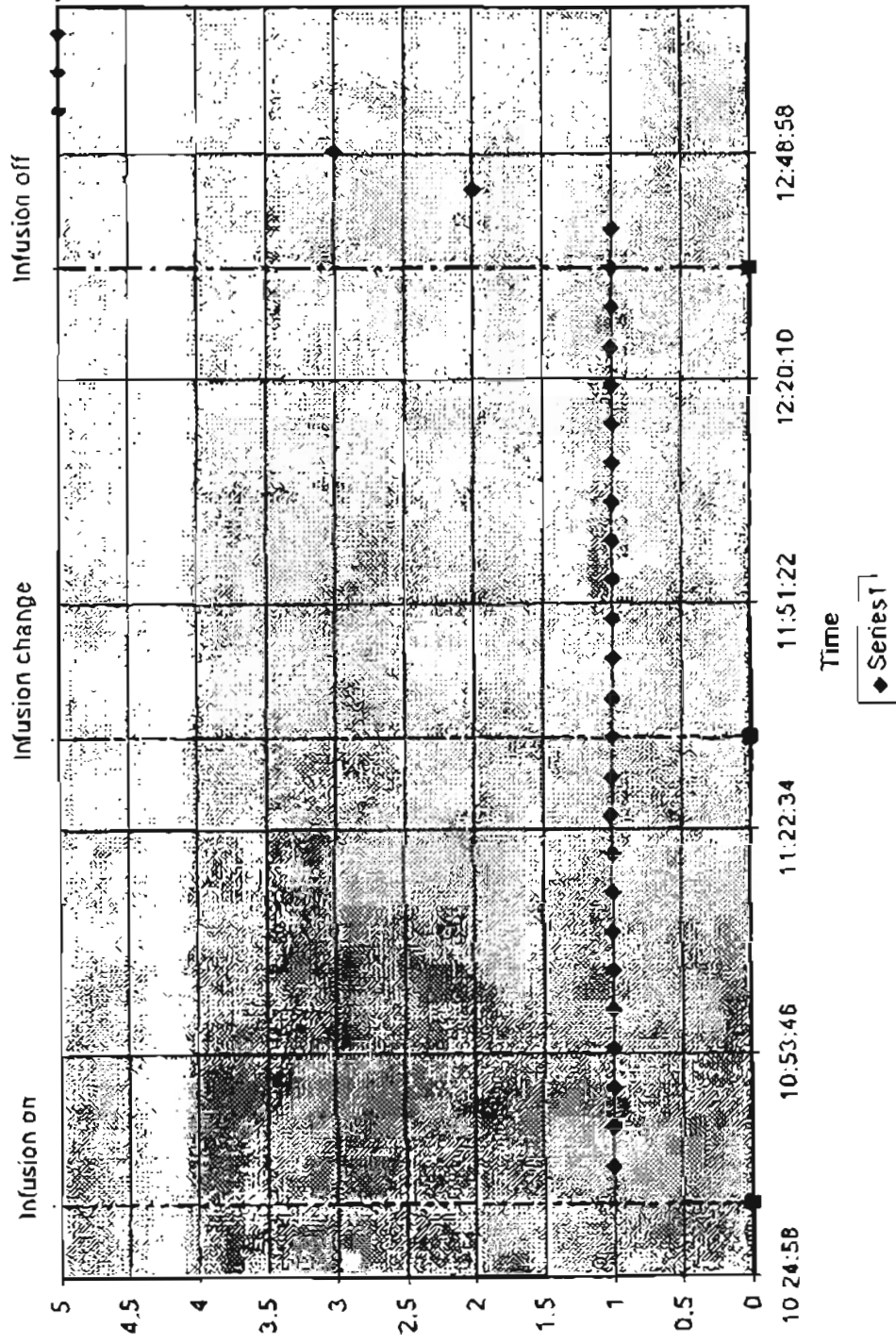
Blood Pressure

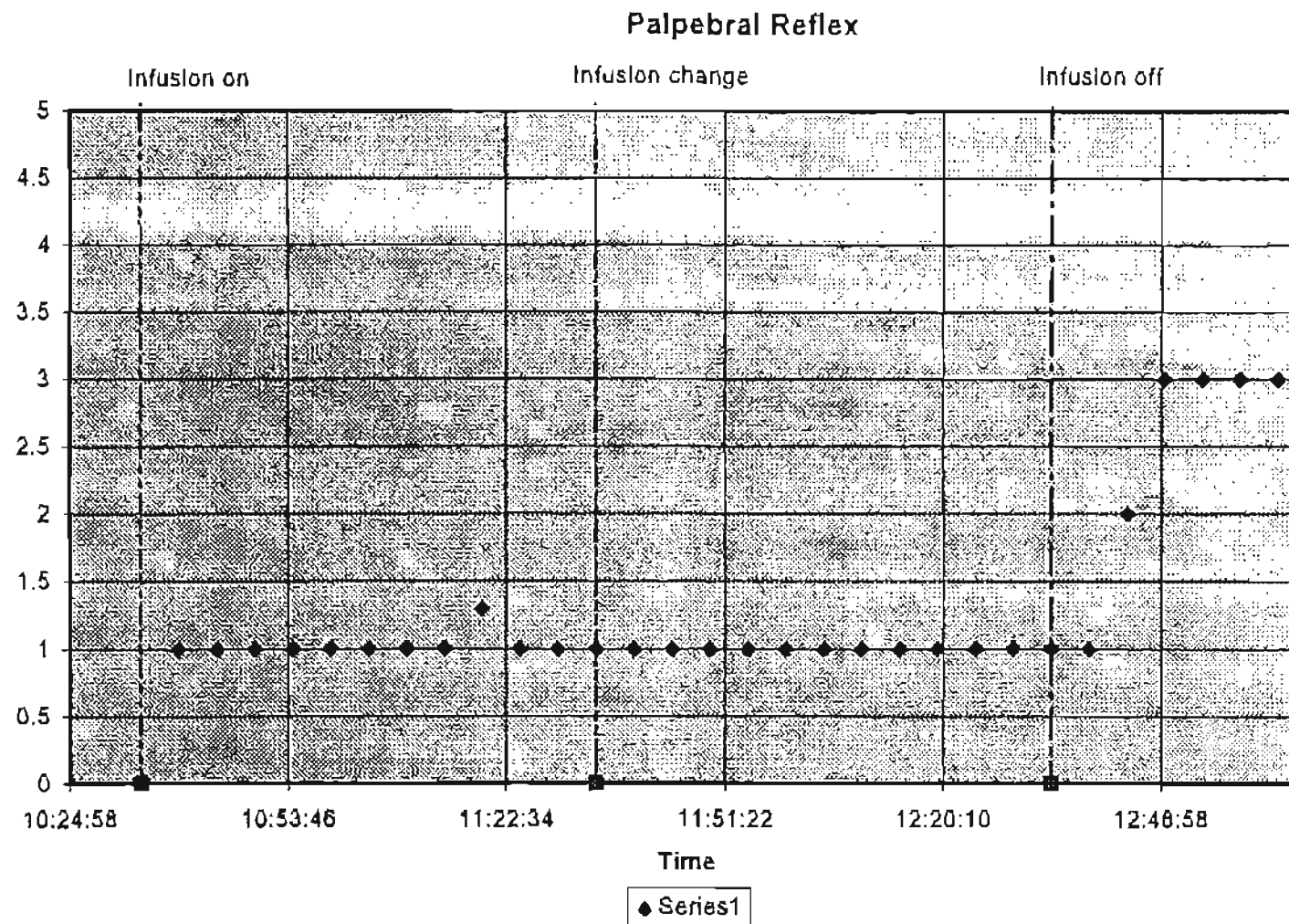




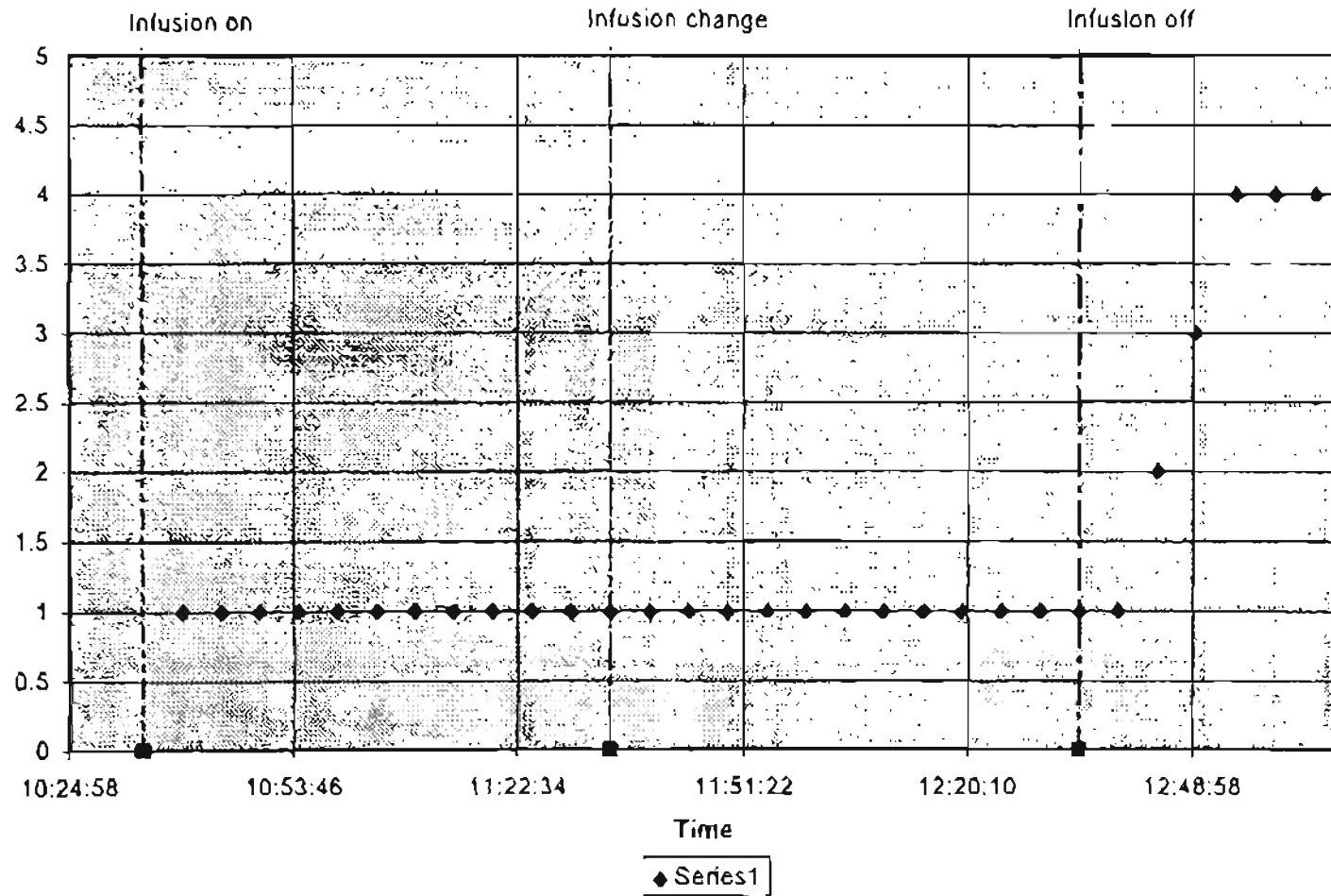


Jaw Tone





Overall Clinical Assessment



APPENDIX F

FUZZY RULEBASE

Table F.1 Rules used for fuzzy model in TILShell. Model output variable is AWARE

Rule	IF	AND	THEN
1	ABETA is HIGH	EMG is HIGH	AWARE is HIGH
2	ABETA is HIGH	TOTPOW is HIGH	AWARE is HIGH
3	ABETArate is POSITIVE	ABETA is HIGH	AWARE is HIGH
4	ABETArate is POSITIVE	ABETA is LOW	AWARE is HIGH
5	ABETArate is POSITIVE	TOTPOW is HIGH	AWARE is HIGH
6	ABETArate is ZERO	TOTPOW is HIGH	AWARE is HIGH
7	EMG is HIGH	EMGrate is POSITIVE	AWARE is HIGH
8	EMG is HIGH	TOTPOW is HIGH	AWARE is HIGH
9	EMG is LOW	EMGrate is POSITIVE	AWARE is HIGH
10	EMGrate is POSITIVE	TOTPOW is HIGH	AWARE is HIGH
11	EMGrate is ZERO	TOTPOW is HIGH	AWARE is HIGH
12	RBETA is HIGH	ABETA is HIGH	AWARE is HIGH
13	RBETA is HIGH	EMG is HIGH	AWARE is HIGH
14	TOTPOW is HIGH	RBETA is HIGH	AWARE is HIGH
15	ABETA is HIGH	SR is HIGH	AWARE is LOW
16	ABETA is LOW	ABETArate is NEGATIVE	AWARE is LOW
17	ABETA is LOW	ABETArate is ZERO	AWARE is LOW
18	ABETA is LOW	EMG is LOW	AWARE is LOW

Table F.1 (Cont'd). Rules used for fuzzy model. Model output variable is AWARE

Rule	IF	AND	THEN
19	ABETA is LOW	SR is HIGH	AWARE is LOW
20	ABETA is LOW	TOTPOW is LOW	AWARE is LOW
21	ABETArate is NEGATIVE	SR is HIGH	AWARE is LOW
22	ABETArate is POSITIVE	SR is HIGH	AWARE is LOW
23	ABETArate is ZERO	SR is HIGH	AWARE is LOW
24	EMG is HIGH	SR is HIGH	AWARE is LOW
25	EMG is LOW	EMGrate is NEGATIVE	AWARE is LOW
26	EMG is LOW	EMGrate is ZERO	AWARE is LOW
27	EMG is LOW	SR is HIGH	AWARE is LOW
28	EMG is LOW	TOTPOW is LOW	AWARE is LOW
29	EMGrate is NEGATIVE	SR is HIGH	AWARE is LOW
30	EMGrate is POSITIVE	SR is HIGH	AWARE is LOW
31	EMGrate is ZERO	SR is HIGH	AWARE is LOW
32	RBETA is LOW	ABETA is LOW	AWARE is LOW
33	RBETA is LOW	EMG is LOW	AWARE is LOW
34	SR is HIGH	RBETA is HIGH	AWARE is LOW
35	SR is HIGH	RBETA is LOW	AWARE is LOW
36	TOTPOW is HIGH	SR is HIGH	AWARE is LOW
37	TOTPOW is LOW	RBETA is LOW	AWARE is LOW
38	TOTPOW is LOW	SR is HIGH	AWARE is LOW

APPENDIX G

TILSHELL PROJECT INFORMATION

In this appendix, the code for the TILShell project is provided. The TILShell project filename is "MODEL.FPL" and requires an input file "INPUT.TXT." The parameters used for scaling the variables ABETA, EMGLO, and TOTPOW are manually entered in the code by the user. The locations of these entries within the code are identified by comments. The variable names of the scaling parameters are identified according to Table G.1. Values for scaling parameters may be found in both Table 3.4 and in comments within the TILShell project code that follows.

Table G.1: Variable names of scaling parameters for ABETA, EMGLO, and TOTPOW as found in TILShell file "MODEL.FPL."

Input Variable	Upper scaling parameter	Lower scaling parameter
ABETA	q1	p1
EMGLO	q2	p2
TOTPOW	q3	p3

The input filename must be manually entered in the code by the user. The code as written calls the file "INPUT.TXT." The variables required for input are listed in Table G.2 as well as the order of input. The input data file must be in ASCII format and may be space or tab delimited. Any input file name other than "INPUT.TXT" must be entered directly into the project code. The location of this entry within the code is identified by comment. A sample of the proper input file format is provided in Table G.3. A listing of input files containing experimental data is provided in Table G.4. The project code listing follow thereafter.

Table G.2: Variables required in input file.

Input Variable	Order (Column #)	Description
ABETA	1	Absolute beta power at current sample time
oldABETA	2	Absolute beta power 5 minutes prior to current sample time
TOTPOW	3	Absolute total power at current sample time
RBETA	4	Relative beta power at current sample time
EMGLO	5	Absolute EMG low band power at current sample time
oldEMG	6	Absolute EMG low band power 5 minutes prior to current sample time.
SR	7	Suppression ratio

Table G.3. Example input file format. From left to right, columns contain values for the variables ABETA, oldABETA, TOTPOW, RBETA, EMGLO, oldEMG, SR. Input values may be either space or tab delimited. These values excerpted from data taken during Experiment 1, 02 May 1996.

53.951313	54.059605	55.761661	66.906656	54.729064	56.018039	0
53.924129	54.071529	55.73134	66.79769	54.704548	56.004449	0
53.894915	54.083398	55.700124	66.677256	54.680287	55.989927	0
53.863527	54.095017	55.667963	66.544676	54.656117	55.974863	0
53.830044	54.10644	55.634872	66.400206	54.632289	55.959811	0
53.794668	54.117724	55.60093	66.244974	54.608855	55.944762	0
53.757403	54.128782	55.566122	66.078818	54.586062	55.930776	0
53.718339	54.13957	55.530453	65.901918	54.564309	55.919071	0
53.677462	54.15002	55.493934	65.714382	54.543389	55.908383	0
53.634655	54.160006	55.456537	65.515826	54.522984	55.8969	0
53.59004	54.169495	55.418306	65.306866	54.503215	55.884074	0
53.54373	54.17845	55.379288	65.088192	54.48405	55.86849	0
53.495535	54.186775	55.339391	64.858571	54.465659	55.850756	0
53.445236	54.194387	55.298489	64.6164	54.448432	55.832592	0
53.392709	54.201204	55.25653	64.360966	54.432391	55.813069	0
53.337723	54.207124	55.213407	64.09087	54.417614	55.791707	0
53.280344	54.212257	55.169135	63.806365	54.404259	55.769084	0
53.220765	54.216797	55.123793	63.508548	54.392379	55.745237	0

Table G.4: Input files and corresponding initial times.

Experiment	Input Filename	Time at input file start	Parent Spreadsheet File
1 (050296)	ex01.txt	10:40:04 342	050296.xls
2 (060896)	ex02.txt	9:44:54 478	060896.xls
3 (061596A)	ex03.txt	9:44:38 552	061596A.xls
4 (061596P)	ex04.txt	13:22:53 299	061596P.xls
5 (061696)	ex05.txt	9:22:18 453	061696.xls
6 (081196)	ex06.txt	9:49:39 525	081196.xls
7 (010797A)	ex07.txt	9:34:48 306	010797A.xls
8 (010797P)	ex08.txt	14:17:11 307	010797P.xls
9 (010897A)	ex09.txt	9:13:49 315	010897A.xls
10 (010897P)	ex10.txt	14:03:15 335	010897P.xls
11 (010997A)	ex11.txt	8:58:35 315	010997A.xls
12 (010997P)	ex12.txt	13:09:39 287	010997P.xls
13 (091196)	ex13.txt	9:33:47 451	091196.xls
14 (121396)	ex14.txt	9:40:20 300	121396.xls

TILSHELL PROJECT CODE

PROJECT ANESTHESIA

OPTIONS

ICONCOLOR=12632256
MODE="NORMAL"
CHANGEID=3958014928
VIEWORIGIN=3.95,0.65

END

VAR AWARE

OPTIONS

ICONPOS=10,2.5
GRIDSHOW="OFF"
GRIDSNAPE="OFF"
GRIDSPACE=0.4,0.2
NUMBER=3
SHAPE="TRAPAZOID"
TOUCHED="ON"

END

TYPE float

MIN -2

MAX 2

MEMBER LOW

OPTIONS

ICONCOLOR=65407

END

POINTS -1.25,0 -1,1 1,1 1.25,0

END

MEMBER HIGH

OPTIONS

ICONCOLOR=255

END

POINTS 1,0 1.25,1 2,1

END

END

VAR EMGLO

OPTIONS

ICONPOS=5.5,0.5
GRIDSHOW="OFF"
GRIDSNAPE="OFF"
GRIDSPACE=0.8,0.2
NUMBER=2
SHAPE="TRAPAZOID"
TOUCHED="ON"

END

TYPE float

MIN 0

MAX 8

MEMBER LOW

OPTIONS

ICONCOLOR=16711680

END

POINTS 0,1 1,1 2,0

```

END

MEMBER HIGH
  OPTION_
    ICONCOLOR=255
  END
  POINTS 1,0 2,1 8,1
END
END

VAR EMGrate
  OPTIONS
    ICONPC=3.5,0.5
    GRIDSHOW="OFF"
    GRIDSNAPE="OFF"
    GRIDSPACE=0.0016,0.2
    NUMBER=3
    SHAPE="TRAPAZOID"
    TOUCHED="ON"
  END
  TYPE float
  MIN -0.008
  MAX 0.008

  MEMBER N
    OPTIONS
      ICONCOLOR=16711680
    END
    POINTS -0.008,1 -0.001,1 0,0
  END

  MEMBER Z
    OPTIONS
      ICONCOLOR=65407
    END
    POINTS -0.001,0 0,1 0.001,0
  END

  MEMBER P
    OPTIONS
      ICONCOLOR=255
    END
    POINTS 0,0 0.001,1 0.008,1
  END
END

VAR ABETA
  OPTIONS
    ICONPOS=2,0.5
    GRIDSHOW="OFF"
    GRIDSNAPE="OFF"
    GRIDSPACE=0.8,0.2
    NUMBER=2
    SHAPE="TRAPAZOID"
    TOUCHED="ON"
  END
  TYPE float
  MIN 0
  MAX 8

```

```

MEMBER LOW
  OPTIONS
    ICONCOLOR=16711680
  END
  POINTS 0,1 1,1 2,0
END

MEMBER HIGH
  OPTIONS
    ICONCOLOR=255
  END
  POINTS 1,0 2,1 8,1
END
ENL

VAR ABETArate
  OPTIONS
    ICONPOS=0.5,2
    GRIDSHOW="OFF"
    GRIDSAP="OFF"
    GRIDSPACE=0.0016,0.2
    NUMBER=3
    SHAPE="TRAPAZOID"
    MINCLAMP=0
    MAXCLAMP=0
    TOUCHED="ON"
  END
  TYPE float
  MIN -0.008
  MAX 0.008

MEMBER N
  OPTIONS
    ICONCOLOR=16711680
  END
  POINTS -0.008,1 -0.001,1 0,0
END

MEMBER Z
  OPTIONS
    ICONCOLOR=65407
  END
  POINTS -0.001,0 0,1 0.001,0
END

MEMBER P
  OPTIONS
    ICONCOLOR=255
  END
  POINTS 0,0 0.001,1 0.008,1
END
END

VAR TOTPOW
  OPTIONS
    ICONPOS=0.5,3.5
    GRIDSHOW="OFF"
    GRIDSAP="OFF"
    GRIDSPACE=0.8,0.2
    NUMBER=2

```

```

        SHAPE="TRAPAZOID"
        TOUCHED="ON"
    END
    TYPE float
    MIN 0
    MAX 8

    MEMBER LOW
        OPTIONS
            ICONCOLOR=16711680
        END
        POINTS 0,1 1,1 2,0
    END

    MEMBER HIGH
        OPTIONS
            ICONCOLOR=255
        END
        POINTS 1,0 2,1 8,1
    END
END

VAR SR
    OPTIONS
        ICONPOS=7.5,4.5
        GRIDSHOW="OFF"
        GRIDSnap="OFF"
        GRIDSPACE=10,0.2
        NUMBER=3
        TOUCHED="ON"
    END
    TYPE float
    MIN 0
    MAX 100

    MEMBER LOW
        OPTIONS
            ICONCOLOR=16711680
        END
        POINTS 0,1 1,0
    END

    MEMBER HIGH
        OPTIONS
            ICONCOLOR=65407
        END
        POINTS 0,0 1,1 100,1
    END
END

VAR RBETA
    OPTIONS
        ICONPOS=7,0.5
        GRIDSHOW="OFF"
        GRIDSnap="OFF"
        GRIDSPACE=10,0.2
        NUMBER=2
        SHAPE="TRAPAZOID"
        TOUCHED="ON"
    END

```

```

TYPE float
MIN 0
MAX 100

MEMBER LOW
  OPTIONS
    ICONCOLOR=16711680
  END
  POINTS 0,1 30,0
END

MEMBER HIGH
  OPTIONS
    ICONCOLOR=255
  END
  POINTS 0,0 30,1 100,1
END

SIMULATE Simulatel
  OPTIONS
    WINPOS=258,83,516,166
    SAMPLETIME=300
  END

MODEL Modell

#CODE
/* Constants */
/-----*/
/* Upper scaling parameters */
/* ABETA: q1 */
/* EMGLO: q2 */
/* TOTPOW: q3 */
/* */
/-----*/
q1=65;
q2=64.3;
q3=65;
/* Initial conditions */

timestamp = 0;
timing = 0;
#END_CODE

#CODE
/-----*/
/* Lower scaling parameters */
/* ABETA: p1 */
/* EMGLO: p2 */
/* TOTPOW: p3 */
/* These parameters are presented in */
/* tabular form by experiment. */
/* */
/* */
/* Experiment */
/* 1 2 3 4 5 6 */
/* */
/* p1 38 44 52 44 47 40 */
/* p2 30 21 40 32 31 30 */

```

```

/* p3      46  53  62  57  56  48      */
/*                                     */
/*           Experiment                */
/*           7   8   9  10  11  12      */
/*                                     */
/* p1      45  46  45  45  45  47      */
/* p2      32  32  30  30  31  31      */
/* p3      52  55  54  56  56  57      */
/*                                     */
/*           Experiment                */
/*           13  14                    */
/*                                     */
/* p1           44  45                  */
/* p2           32  28                  */
/* p3           54  55                  */
/*                                     */
/.....*/

p1=45;
p2=28;
p3=55;

/* Read input data from input data file */

READ "input.txt",ABETA,oldABETA,TOTPOW,EBETA,EMGLO,oldEMG,SR;

/* Rescale ABETA and calculate ABETArate */

ABETA      = 4 * (ABETA      - p1) / (q1 - p1) + 1;
oldABETA    = 4 * (oldABETA - p1) / (q1 - p1) + 1;
ABETArate = (ABETA - oldABETA)/300;

/* Rescale EMGLO and calculate EMGrate */

EMGLO      = 4 * (EMGLO      - p2) / (q2 - p2) + 1;
oldEMG      = 4 * (oldEMG - p2) / (q2 - p2) + 1;
EMGrate     = (EMGLO-oldEMG)/300;

/* Rescale TOTPOW */

TOTPOW      = 4 * (TOTPOW      - p3) / (q3 - p3) + 1;

#END_CODE
END
END

RULEBASE Rulebase1
  OPTIONS
    ICONPOS=7,2
  END

  RULE Rule01
    IF (EMGLO IS LOW) AND (EMGrate IS N) THEN
      AWARE = LOW
    END

  RULE Rule02
    IF (EMGLO IS LOW) AND (EMGrate IS Z) THEN
      AWARE = LOW
    END

```

```

RULE Rule01
    IF (EMGLO IS LOW) AND (EMGrate IS P) THEN
        AWARE = HIGH
    END

RULE Rule04
    IF (ABETArate IS N) AND (ABETA IS LOW) THEN
        AWARE = LOW
    END

RULE Rule05
    IF (ABETArate IS Z) AND (ABETA IS LOW) THEN
        AWARE = LOW
    END

RULE Rule06
    IF (EMGLO IS LOW) AND (SR IS HIGH) THEN
        AWARE = LOW
    END

RULE Rule07
    IF (EMGLO IS HIGH) AND (SR IS HIGH) THEN
        AWARE = LOW
    END

RULE Rule08
    IF (EMGrate IS N) AND (SR IS HIGH) THEN
        AWARE = LOW
    END

RULE Rule09
    IF (EMGrate IS Z) AND (SR IS HIGH) THEN
        AWARE = LOW
    END

RULE Rule10
    IF (EMGrate IS P) AND (SR IS HIGH) THEN
        AWARE = LOW
    END

RULE Rule11
    IF (ABETA IS LOW) AND (SR IS HIGH) THEN
        AWARE = LOW
    END

RULE Rule12
    IF (ABETA IS HIGH) AND (SR IS HIGH) THEN
        AWARE = LOW
    END

RULE Rule13
    IF (TOTPOW IS LOW) AND (SR IS HIGH) THEN
        AWARE = LOW
    END

RULE Rule14
    IF (TOTPOW IS HIGH) AND (SR IS HIGH) THEN
        AWARE = LOW
    END

```

```

RULE Rule15
    IF (ABETArate IS N) AND (SR IS HIGH) THEN
        AWARE = LOW
    END

RULE Rule16
    IF (ABETArate IS Z) AND (SR IS HIGH) THEN
        AWARE = LOW
    END

RULE Rule17
    IF (ABETArate IS P) AND (SR IS HIGH) THEN
        AWARE = LOW
    END

RULE Rule18
    IF (TOTPOW IS HIGH) AND (RBETA IS HIGH) THEN
        AWARE = HIGH
    END

RULE Rule19
    IF (TOTPOW IS LOW) AND (RBETA IS LOW) THEN
        AWARE = LOW
    END

RULE Rule20
    IF (SR IS HIGH) AND (RBETA IS LOW) THEN
        AWARE = LOW
    END

RULE Rule21
    IF (SR IS HIGH) AND (RBETA IS HIGH) THEN
        AWARE = LOW
    END

RULE Rule22
    IF (ABETArate IS P) AND (ABETA IS LOW) THEN
        AWARE = HIGH
    END

RULE Rule23
    IF (ABETArate IS P) AND (ABETA IS HIGH) THEN
        AWARE = HIGH
    END

RULE Rule24
    IF (ABETA IS LOW) AND (TOTPOW IS LOW) THEN
        AWARE = LOW
    END

RULE Rule25
    IF (ABETA IS HIGH) AND (TOTPOW IS HIGH) THEN
        AWARE = HIGH
    END

RULE Rule26
    IF (EMGLO IS LOW) AND (TOTPOW IS LOW) THEN
        AWARE = LOW
    END

```

```

RULE Rule27
    IF (EMGLO IS HIGH) AND (TOTPOW IS HIGH) THEN
        AWARE = HIGH
    END

RULE Rule28
    IF (EMGrate IS P) AND (TOTPOW IS HIGH) THEN
        AWARE = HIGH
    END

RULE Rule29
    IF (EMGrate IS 2) AND (TOTPOW IS HIGH) THEN
        AWARE = HIGH
    END

RULE Rule3
    IF (ASETarate IS 2) AND (TOTPOW IS HIGH) THEN
        AWARE = HIGH
    END

RULE Rule31
    IF (ABETArate IS P) AND (TOTPOW IS HIGH) THEN
        AWARE = HIGH
    END

RULE Rule32
    IF (EMGLO IS HIGH) AND (EMGrate IS P) THEN
        AWARE = HIGH
    END

RULE Rule33
    IF (ABETA IS LOW) AND (EMGLO IS LOW) THEN
        AWARE = LOW
    END

RULE Rule34
    IF (ABETA IS HIGH) AND (EMGLO IS HIGH) THEN
        AWARE = HIGH
    END

RULE Rule35
    IF (RBETA IS LOW) AND (EMGLO IS LOW) THEN
        AWARE = LOW
    END

RULE Rule36
    IF (RBETA IS HIGH) AND (EMGLO IS HIGH) THEN
        AWARE = HIGH
    END

RULE Rule37
    IF (RBETA IS LOW) AND (ABETA IS LOW) THEN
        AWARE = LOW
    END

RULE Rule38
    IF (RBETA IS HIGH) AND (ABETA IS HIGH) THEN
        AWARE = HIGH
    END
END

```

```

DEBUG Debug1
  TXEPL AWARE
  WATCH AWARE

  CHART Chart1
    OPTIONS
      TITLE="Inputs"
      YAXIS=EMGrate
      YMINVAL=-0.008
      YMAXVAL=0.008
      YCOLOR=255
      YAXIS=ABETArate
      YMINVAL=-0.008
      YMAXVAL=0.008
      YCOLOR=65280
      YAXIS=AWARE
      YMINVAL=-2
      YMAXVAL=2
      YCOLOR=16711935
      YAXIS=TOTPOW
      YMINVAL=0
      YMAXVAL=8
      YCOLOR=0
      YAXIS=ABETA
      YMINVAL=0
      YMAXVAL=8
      YCOLOR=10485760
      YAXIS=EMGLO
      YMINVAL=0
      YMAXVAL=8
      YCOLOR=33023
      DATAPOINTS=1900
    END
  END
END

CONNECT
  FROM EMGLO
  TO Rulebase1
END

CONNECT
  FROM EMGrate
  TO Rulebase1
END

CONNECT
  FROM SR
  TO Rulebase1
END

CONNECT
  FROM Rulebase1
  TO AWARE
END

CONNECT
  FROM EMGrate
  TO Rulebase1

```

```

END

CONNECT
  FROM ABETA
  TO Rulebase1
END

CONNECT
  FROM TOTPOW
  TO Rulebase1
END

CONNECT
  FROM ABETA:rate
  TO Rulebase1
END

CONNECT
  FROM RBETA:
  TO Rulebase1
END
END

```

VITA

Brent D. Eilerts

Candidate for the Degree of

Master of Science

Thesis: FUZZY MONITORING OF INTRAVENOUS PROPOFOL INFUSION
ANESTHESIA IN DOGS

Major Field: Chemical Engineering

Biographical:

Personal Data: Born in Hutchinson, Kansas, on 27 June 1967, the son of Arless and Donald Eilerts.

Education: Graduated from Hutchinson High School, Hutchinson, Kansas in May 1985; attended Hutchinson Community College, Hutchinson, Kansas, and the University of Toronto, Toronto, Ontario, Canada; received Bachelor of Science degree in Cellular Biology and a Bachelor of Science degree in Chemical Engineering from the University of Kansas, Lawrence, Kansas in May 1989 and May 1994, respectively. Completed the requirements for the Master of Science degree with a major in Chemical Engineering at Oklahoma State University in July 1997.

Experience: Employed by Oklahoma State University School of Chemical Engineering as a graduate teaching and research assistant (1995 to present). Employed by Phillips Petroleum Company, Bartlesville, Oklahoma as summer engineering intern (1996).

Professional Memberships: American Institute of Chemical Engineers, American Chemical Society.